A Thesis for the Degree of Doctor of Philosophy

Functional and Regulatory Characteristics of IscR, a Global Regulator of *Vibrio vulnificus*

식중독 패혈증 비브리오균의 전사 조절자 IscR의 기능 및 조절 특성 연구

February, 2014

Jong Gyu Lim

Department of Agricultural Biotechnology

College of Agriculture and Life Sciences

Seoul National University

Functional and Regulatory Characteristics of IscR, a Global Regulator of *Vibrio vulnificus*

식중독 패혈증 비브리오균의 전사 조절자 IscR의 기능 및 조절 특성 연구

지도교수 최 상 호

이 논문을 농학박사학위논문으로 제출함
2013년 11월

서울대학교 대학원
농생명공학부
임 종 규

임종규의 박사학위논문을 인준함
2013년 12월

위 원 장 유 상 렬 (인)

부위원장 최 상 호 (인)

위 원 이 기 원 (인)

위 원 김 건 수 (인)

위 원 윤 상 선 (인)

Abstract

Functional and regulatory characteristics of IscR, a global regulator of *Vibrio vulnificus*

Jong Gyu Lim

Department of Agricultural Biotechnology

The Graduate School

Seoul National University

Pathogenic bacteria have evolved global regulatory mechanisms to facilitate cooperation of the numerous virulence factors during pathogenesis. In the present study, a homologue of IscR, an Fe-S cluster-containing transcriptional regulator was identified from *Vibrio vulnificus*, a causative agent of food-borne diseases, and its role and regulatory characteristics were assessed. A mutant that exhibited less cytotoxic activity toward INT-407 human intestinal epithelial cells was screened from a random transposon mutant library of *Vibrio vulnificus*, and an open reading frame encoding an Fe-S cluster regulator, IscR, was identified using a transposon-tagging method. A mutational analysis demonstrated that IscR contributes to mouse mortality as well as cytotoxicity toward the INT-407 cells, indicating that IscR is

essential for the pathogenesis of *V. vulnificus*. A whole genome microarray analysis revealed that IscR influenced the expression of 67 genes, 52 of which were up-regulated and 15 down-regulated. Among these, twelve genes most likely involved in motility and adhesion to host cells, hemolytic activity, and survival under oxidative stress of the pathogen during infection were selected and experimentally verified to be up-regulated by IscR. Accordingly, the disruption of *iscR* resulted in a significant reduction in motility and adhesion to the INT-407 cells, hemolytic activity, and resistance to reactive oxygen species (ROS) such as H_2O_2 and *t*-BOOH. Furthermore, the present study demonstrated that the *iscR* expression was induced by exposure of *V. vulnificus* to the INT-407 cells and the induction appeared to be mediated by ROS generated by the host cells during infection. Consequently, the combined results indicated that IscR is a global regulator contributing to the overall success in the pathogenesis of *V. vulnificus* by regulating the expression of various virulence and survival genes in addition to Fe-S cluster genes.

Furthermore, the regulatory mechanisms for the *iscR* expression of *V. vulnificus* were evaluated. The expression of *iscR* was found to be upregulated by a transcriptional regulator AphA, a homologue of the low cell density regulator AphA of the *Vibrio* species, in the exponential phase of growth. The promoter

activity of *iscR* appeared to be activated and repressed by AphA and IscR, respectively. EMSA and DNase I protection assay showed that both AphA and IscR bind to the *iscR* regulatory region and the binding site for AphA overlapped with part of the binding site for IscR. Mutational analysis suggested that AphA upregulates the *iscR* expression only in the presence of functional IscR. An examination of the roles of AphA and the binding sites revealed that the binding of AphA would hinder the IscR-mediated repression of the *iscR* transcription. The combined results show that *V. vulnificus* AphA upregulates *iscR* expression by antagonizing its negative autoregulation. Furthermore, the disruption of *aphA* resulted in significantly reduced virulence in tissue cultures and in mice. Accordingly, AphA contributes the pathogenesis of *V. vulnificus* possibly by promoting the production of IscR, which activates the genes required for survival and virulence.

The transcriptome analysis revealed that *Vibrio vulnificus* IscR upregulates a gene encoding a putative antioxidant, homologous to human peroxiredoxin 5. This gene was further identified as a peroxiredoxin-encoding gene of *V. vulnificus* and named as *prx3*. The *prx3* mutant was hypersusceptable to killing by hydrogen peroxide and peroxynitrite, indicating that *V. vulnificus* Prx3 is required for survival under oxidative and nitrosative stress. In addition, mouse mortality test suggested that

Prx3 is essential for the virulence of *V. vulnificus*. The expression of *prx3* was increased upon iron starvation in IscR-dependent manner, implying that IscR-dependent sensing of the cellular Fe-S cluster status involves the regulation of *prx3*. *Escherichia coli* dual plasmid system assay showed that IscR3CA mutant (apo-form of IscR) also activates the *prx3* expression, suggesting that Fe-S cluster of IscR is dispensible for the activation of *prx3*. qRT-PCR and primer extension analyses showed that the expression of *prx3* in the *iscR3CA* mutant was more increased than that in the wild type. These results might be contributed to the increased level of IscR3CA in the *iscR3CA* mutant. A direct interaction between IscR3CA and the promoter region of *prx3* was demonstrated by an EMSA, and a IscR3CA binding site, centered at 44 bp upstream of the transcription start site, was identified by a DNase I protection assay. The binding site for IscR3CA on the *prx3* promoter matched the type 2 binding motif of *Escherichia coli* IscR, reinforcing that apo-IscR also activates the *prx3* expression. Taken together, the expression of *V. vulnificus* Prx3, essential for the survival under conditions of oxidative and nitrosative stress and virulence in mice, is regulated by IscR.

Keywords : ***Vibrio vulnificus*, Fe-S cluster, IscR, AphA, Peroxiredoxin**

Student Number : 2008 − 21377

Contents

List of Figures

List of Tables

Chapter I.

Background

I-1. *Vibrio vulnificus*

Vibrio vulnificus is a species of Gram-negative, motile, and curved rod-shaped bacteria with a single flagellum of the *Vibrio* genus. The bacterium isolated from blood and wound of patients was first reported by the US Centers for Disease Control and Prevention (CDC) in 1976 (Hollis *et al*., 1976). Given name, *vulnificus* means "wound" in Greek to reflect one of its infection types. This bacterium could be differentiated from *Vibrio parahaemolyticus* by a lower tolerance for NaCl and fermentation of lactose. Like other organisms in Vibrionaceae, *V. vulnificus* is a facultative anaerobe having the ability of fermentation. The bacterium is distributed worldwide and especially found in estuarine waters and frequently contaminates oysters and other seafood (Wright *et al*., 1996; Hor *et al*., 1995). The preferred habitat of *V. vulnificus* is reported to be more selective as the water temperature rises above 18°C for proliferation and salinity ranging from 10 to 25 parts per thousand (ppt) (Hlady and Klontz, 1996; Kaspar and Tamplin, 1993). It can also be isolated from water with the temperature ranging from 9°C to 31°C (Strom and Parajpye, 2000). However, a salinity of 10 ppt at 5°C and high salinities greater than 30 ppt reduce the survival of *V. vulnificus* (Kaspar and Tamplin, 1993).

There are three biotypes of *V. vulnificus* when classified based on their biochemical

characteristics, host range, and epidemiological pettern. Biotype 1 (BT1) is predominant human pathogen while biotype 2 (BT2) is primarily eel pathogens (Amaro and Biosca, 1996; Tison *et al*., 1982). Biotype 3 (BT 3) was recently identified in Israel and shown to possess biochemical properties of both BT1 and BT2 and to cause human wound infection (Bisharat *et al*., 1999). All biotypes have been isolated from human cases, but only the BT2 strains infect the eels (Aznar *et al*., 1994). The BT2 strains possess a common plasmid, carrying the genes required for bacterial survival and virulence in the eels (Lee *et al*., 2008a). The plasmid-cured BT2 strain that loses virulence in eels remains fully virulent in mice, indicating that the virulence genes for eels in the plasmid are dispensable in mice (Lee *et al*., 2008a). The BT1 strains collected worldwide include most of the clinical and environmental isolates and are genetically heterogeneous, while the BT3 strains are genetically homogeneous (Hor *et al*., 1995; Zaidenstein *et al*., 2008). The BT3 strains exhibit different clinical characteristics when compared to those of the BT1 strains. Most of the BT3 infections were associated with percutaneous exposure to fish, typically tilapia, while people are handling the fish, and the victims had no underlying diseases (Zaidenstein *et al*., 2008). Therefore it is considered that BT3 strains are more virulent than BT1 and BT2 strains to humans.

I-2. Disease caused by *V. vulnificus*

V. vulnificus is a causative agent of foodborn diseases, such as life-threatening septicemia and possibly gastroenteritis (Gulig *et al.*, 2005; Strom and Paranjpye, 2000). Consumption of seafood containing *V. vulnificus* can result in a severe, fulminant septicemia. Characteristics of this systemic disease include fever, chills, nausea, hypotensive septic shock, and the formation of secondary lesions on the extremities of patients (Chuang *et al*., 1992; Hlady and Klontz, 1996; Klontz *et al*., 1988; Oliver, 2006; Strom and Paranjpye, 2000). In most of the cases involving *V. vulnificus* infection have underlying predisposed conditions, including liver damage, excess levels of iron, and immunocompromised conditions (Oliver, 2006). The mortality from septicemia is very high (>50%) and death can occur within one to two days after the first signs of illness (Gulig *et al.*, 2005; Jones and Oliver, 2009; Linkous and Oliver, 1999; Strom and Paranjpye, 2000). Compared with the severity of septicemia, gastroenteritis caused by *V. vulnificus* is relatively mild.

In addition to septicemia, *V. vulnificus* can produce serious wound infections that result from exposure of open wounds to water containing the bacterium (Oliver, 2005). Even healthy people are susceptible to a serious wound infection after contact with shellfish or water contaminated with the bacterium (Bisharat *et al*.,

1999; Howard *et al*., 1986). Like systemic disease, wound infections progress rapidly to cellulitis, ecchymoses and bullae which can progress to necrotizing fasciitis at the site of infection. The symptoms are pain, erythema, and edema at the infection sites (Strom and Paranjpye, 2000). Although the mortality rate for wound infections is lower than that for primary septicemia by 25% (Klontz *et al.*, 1988), amputation of the infected limbs may be done to block the aggravation of disease to life-threatening secondary septicemia. These features of *V. vulnificus* infection suggest that pathogenesis of this bacterium is a multifactorial and complex phenomenon.

Since 2010 to date (Dec 2013), total number of *V. vulnificus* infection reported in South Korea is 247, and among them 121 peoples (49%) were dead (Korea Centers for Disease Control and Prevention, KCDC; http://is.cdc.go.kr/nstat/index.jsp). In Japan, the annual estimated number of *V. vulnificus* septicemia was calculated to be approximately 400 (Osaka *et al*., 2004). According to estimates from the CDC, approximately 100 persons in the United States have been infected with *V. vulnificus*, resulting in approximately 50 deaths annually (Jones and Oliver, 2009).

I-3. Virulence factors and molecular pathogenesis of *V. vulnificus*

Molecular Koch's postulates were formulated by Stanley Falkow in 1988 based on Koch's postulates. The first postulate states that products contributing to the disease caused by a pathogen are encoded by genes found in the pathogenic organism. Genes that satisfy molecular Koch's postulates are often referred to as virulence factors (Falkow, 1988). Some of virulence factors in *V. vulnificus*, including the iron-acquisition ability, capsular polysaccharides (CPS), acid resistance, metalloprotease (VvpE), hemolysin/cytolysin (VvhA), and MARTX toxin (RtxA1) are described below.

Iron acquisition

Pathogenesis of *V. vulnificus* is highly associated with elevated serum iron concentraions in infected individuals (Wright *et al*., 1981). Iron treatment of mice prior to infection dramatically reduced the intraperitoneal LD_{50} (Stelma *et al*., 1992; Wright *et al*., 1981). Although the relationship between the serum iron levels and *V. vulnificus* infection is still unclear, there are two theories; one is that excess iron enhances growth of the pathogen (Starks *et al*., 2006), and another is that excess iron results in a compromised immune response of host (Hor *et al*., 2000). Since

most iron in human serum is bound to transferrin and other iron-binding compounds (Weinberg ED, 1978), *V. vulnificus* has developed multiple systems for iron acquisition. Primarily, the organism produces two types of siderophore, a catechol and a hydroxamate (Simpson and Oliver, 1983). The catechol siderophore (vulnibactin) is required for growth in iron-depleted medium and scavenging iron from transferrin and holotransferrin (Kim *et al*., 2006a). Several genes involved in vulnibactin-associated genes such as *vuuA, venB,* and *vvsAB* are required for virulence (Kim *et al*., 2008a; Webster and Litwin, 2000). Hydroxamate siderophore has also been shown to be involved in *V. vulnificus* infection (Alice *et al*., 2008). Non-transferrin-bound iron is uptaken through a heme receptor, HupA (Litwin and Byrne, 1998). The expressions of genes involved in iron acquisition are primarily regulated by Fur, a ferric uptake regulator. Under iron-limiting conditions, Fur increases the expression of several genes involved in vulnibactin synthesis (*venB*, *vvsAB*, and *vis*) and uptake (*vuuA*) (Alice *et al*., 2008; Kim *et al*., 2006a; Kim *et al*., 2008a; Webster and Litwin, 200). In addition, expression of *vvsAB* is also regulated differentially by Fur and SmcR, a quorum-sensing master regulator (Wen *et al*., 2012). Meanwhile, expression of *hupA* is regulated by Fur and HupR, a LysR homologue (Alice *et al*., 2008; Litwin and Quackenbush, 2001), and CRP, the cyclic AMP receptor protein (Oh *et al*., 2009).

CPS

V. vulnificus is an extracellular pathogen that uses its CPS to avoid phagocytosis by host immune cells and complement (Linkous and Oliver, 1999; Strom and Paranjpye, 2000). Capsule determines the colony morphology of *V. vulnificus*; encapsuled strain is opaque and unencapsuled strain is translucent (Yoshida *et al*., 1985; Wright *et al*., 1999). CPS allows the *V. vulnificus* cells to be more invasive in subcutaneous tissue and to be cleared from the bloodstream more slowly than unencapsulted cells (Yoshida *et al*., 1985). Encapsulated strains also showed an increased virulence than unencapsulated strains when it infects iron-loaded mice intraperitoneally (163). In contrast, unencapsulated mutants are highly susceptible to bactericidal activity of human serum (Shinoda *et al*., 1987). Inactivation of a CPS transport gene (*wza*) of *V. vulnificus* abolished capsule expression and resulted in an increase of LD_{50} (Wright *et al*., 2001). These reports reveal that CPS plays a role in *V. vulnificus* virulence. Group 1 CPS operon, which comprises highly conserved CPS transport genes followed by variable biosynthetic genes, is required for the production and expression of CPS (Chatzidaki-Livanis *et al*., 2006). In addtion, two epimerase genes, *wcvA* and *wbpP*, are also involved in capsule expression (Park *et al*., 2006; Smith and Siebeling, 2003). Recently, it has been reported that CPS plays a role in determining biofilm size and that transcription of CPS gene cluster is activated by SmcR, indicating that CPS is produced at high cell

density (Lee *et al*., 2013b).

Acid resistance

The primary route of *V. vulnificus* infection is the consumption of contaminated food, and the organism encounters a highly acidic gastric environment. To neutralize low pH, *V. vulnificus* degrades amino acids to yield amines and CO_2 like other Gram-negative bacteria (Jones and Oliver, 2009). The *cadBA* operon encoding the lysine decarboxylase is required for breakdown of lysine to form cadaverine and that its expression is increased by acid stress and regulated by CadC (Rhee *et al*., 2005; Rhee *et al*., 2002). It is known that exposure to low pH increases cellular superoxide level and that cadaverine acts as a superoxide radical scavenger (Kim *et al*., 2005a, Kang *et al*., 2007a). Consistently, *cadBA* expression is also increased upon exposure to superoxide stress (Kim *et al*., 2006b). The *sodA* gene encoding the manganese superoxide dismutase SOD is required for the survival of *V. vulnificus* at low pH and virulence in mice (Kim *et al*., 2005a). However this gene is not induced by low pH but is induced by oxidative stress (Kim *et al*., 2005a). Two other SOD genes *sodB* and *sodC* also play a role in survival under low-pH conditions and in virulence in mice (Kang *et al*., 2007b). These reports show the link between acid and oxidative stress.

VvpE

VvpE is a nonspecific extracellular protease and involves in *V. vulnificus* virulence. Purified VvpE causes tissue necrosis and cutaneous lesions and increases vascular permeability (Chang *et al*., 2005; Kothary and Kreger, 1987; Miyoshi and Shinoda, 1988). The enhanced vascular permeability caused by VvpE is occurred through the generation of bradykinin, a known vasodilator, and is known to be important for invasion of the pathogen (Miyoshi, 2006). VvpE also degrades type IV collagen, a component of the basement membrane and activates procaspase-3, an enzyme involved in cellular apoptosis, to result in local tissue damage (Kim *et al*., 2007; Miyoshi *et al*., 1987). However, inactivation of the *vvpE* gene did not show any difference in LD_{50} (Jeong *et al*., 2000; Shao and Hor, 2000), indicating VvpE is not a major virulence factor of *V. vulnificus*. Expression of *vvpE* is upregulated indirectly by CRP and directly by SmcR with activity of RpoS (Jeong *et al*., 2003; Jeong *et al*., 2001). More recently, it has been suggested that SmcR enhances the detachment of *V. vulnificus* biofilms by upregulating expression of VvpE that dissolves established biofilms directly, and thereby may promote the dispersal of the pathogen to new colonization site (Kim *et al*., 2013).

VvhA and RtxA1

VvhA, an extracellular hemolysin encoded by *vvhA*, contributes to iron release

through its hemolytic activity and is responsible for the cytotoxicity of *V. vulnificus* (Wright and Morris, 1991). The toxin acts by forming pores in host cellular membrane and leads to an increase of vascular permeability and hypotension (Kim *et al*., 1993). The toxin also causes severe tissue necrosis, fluid accumulation, intestinal irregularities, partial paralysis, and lethality (Gray and Kreger, 1987; Lee *et al*., 2005). In addition, exposure of hemolysin to host cells is known to result in the increase of vascular permeability, apoptosis of endothelial cells, and induction of inducible nitric oxide synthase (iNOS) activity (Kang *et al*., 2002; Kim and Kim, 2002; Kwon *et al*., 2001). However, mutational studies of *vvhA* suggested that hemolysin is not responsible for the lethality of *V. vulnificus* and is not solely responsible for the tissue damage (Wright and Morris, 1991). Cyclic AMP (cAMP) is known as a primary regulator of hemolysin activity, with CRP binding to the *vvhA* promoter region and activating its transcription (Choi *et al*., 2002; Kim *et al*., 2005b).

RtxA1, a multifunctional-autoprocessing RTX toxin (MARTX) encoded by *rtxA1* was also identified in *V. vulnificus* (Gulig *et al*., 2005). The amino acid sequence of RtxA1 shows a high level of identity with that of *V. cholerae* RtxA, and organization of the *rtx* gene cluster is also similar between them (Kim *et al*., 2008b; Lee *et al*., 2007). The toxin is made of multiple structural subunits and forms pores

in host cellular membranes. Inactivation of the *rtx* genes resulted in a decrease of the pathogen's ability to damage cells and to disrupt either cell monolayers or tight junctions (Kim *et al*., 2008b; Lee *et al*., 2007; Liu *et al*., 2007). RtxA1 also contributes to host cellular changes, including cytoskeleton rearrangement, bleb formation, and actin aggregation (Kim *et al*., 2008b). Such changes lead to cellular necrosis and enable *V. vulnificus* to invade the bloodstream by crossing the intestinal epithelium (Kim *et al*., 2008b). Moreover, *rtxA1* mutants showed higher LD_{50}s than those of wild type upon intragastric or intraperitoneal injection to mice (Kim *et al*., 2008b). It is also known that RtxA1 kills host cells only after contact of the pathogen with host cells (Kim *et al*., 2008b). Meanwhile, *rtxBDE* operon is likely to be involved in secretion of RtxA1. The *rtxE* mutant was unable to secrete RtxA1 and exhibited reduced virulence in tissue culture and in mice (Lee *et al*., 2008b). Expressions of *rtxHCA* and *rtxBDE* operons were induced by exposure to host epithelial cells (Park *et al*., 2012; Lee *et al*., 2008b), suggesting cell-to-cell contact is required for expression and activity of RtxA1. Furthermore, the expression of *rtxA1* is regulated by transcriptional regulator HlyU, in which HlyU binds to the upstream region of *rtxHCA* operon and acts as an H-NS antirepressor (Liu *et al*., 2007; Liu *et al*., 2009).

As mentioned above, single mutations in *vvpE* and *vvhA* did not affect either

cytotoxicity or lethality of *V. vulnificus*, and a mutant, in which both *vvhA* and *vvpE* were inactivated, remained highly cytotoxic (Fan *et al*., 2001; Kim *et al*., 2008b). An *rtxA1 vvpE* double mutant showed decreased cytotoxicity similar to that of the *rtxA1* mutant (Kim *et al*., 2008b). In addition, both of a *vvhA rtxA1* double mutant and a *vvpE vvhA rtxA1* triple mutant did not show cytotoxicity (Kim *et al*., 2008b). These results indicated that RtxA1 plays the primary role in cytotoxicity of *V. vulnificus*, while VvhA is auxiliary and VvpE is likely negligible (Kim *et al*., 2008b). More recently, it has been reported that RtxA1 and VvhA contribute to rapid *in vivo* growth of the pathogen and that the presence of these factors directly correlates with mouse mortality and suggested that these toxins seem to play an additive role for pathogenesis of *V. vulnificus* by causing intestinal tissue damage and inflammation (Jeong and Satchell, 2012).

Other virulence factors

The *flgE* gene encoding the flagellar hook protein is involved in *V. vulnifucis* adhesion to the host cells and virulence in mice (Lee *et al*., 2004). Type IV pili are related to adhesion to host cells, biofilm formation, and virulence in mice (Paranjpye *et al*., 2005). OmpU is most abundant outer membrane protein in *V. vulnificus* and is interacts with host extracellular matrix proteins, and is associated with adhesion to the host cells (Goo *et al*., 2006). The *prx*1 gene encoding a

peroxiredoxin is required not only for *V. vulnificus* survival under oxidative stress induced by hydrogen peroxide and *tert*-butyl hydroperoxide but also for virulence in tissue culture and in mice (Baek *et al*., 2009).

V. vulnificus also possesses the *nanA* gene encoding Neu5Ac lyase which is essntial for the utilization of Neu5Ac, a distal polysaccharide of glycoproteins in human intestinal mucin (Jeong *et al*., 2009; Vimr *et al*., 2004). Disruption of the *nanA* gene resulted in a reduction of *V. vulnificus* growth in the media supplemented with Neu5Ac as a sole carbon source (Jeong *et al*., 2009). The *nanA* mutant also exhibited decreased adhesion and cytotoxicity to human intestinal epithelial cells and virulence in mice (Jeong *et al*., 2009). Expression of *V. vulnificus nan* cluster including *nanA* gene is known to be regulated by the transcription factors NanR and CRP, and *N*-acetyl mannosamine 6-phosphate (Kim *et al*., 2011). The *nanA* expression is also regulated by the LysR-type transcriptional regulator AphB (Jeong and Choi, 2008). AphB is also known to play a role in acid tolerance, cytotoxicity, adhesion, motility, and lethality of *V. vulnificus* and is reported as a global regulator, which regulates genes involved in nutrient acquisition and metabolism and thus indirectly contributes to virulence by controlling growth and environmental adaptation (Rhee *et al*., 2006; Jeong and Choi, 2008).

I-4. Objective of this study

To treat the diseases developed by infection with pathogens including *V. vulnificus*, antibiotics, which aim to kill bacteria or inhibit their growth, are commonly used. As a result, clinically significant antibiotic-resistant strains have been emerged. A possible alternative approach is to target functions or mechanisms, which are essential for the infection of pathogen, such as virulence factors and global gene regulatory system (Clatworthy *et al*., 2007). For this reason, the study about the pathogen's strategies to achieve successful disease development is very important and required. However, the researches about the function and regulation of the genes encoding the virulence factors in *V. vulnificus* are still very limited. In the present study, *V. vulnificus* IscR, an Fe-S cluster-containing transcription factor, was identified as a potential virulence regulator. Several transcription factors containing the Fe-S cluster, such as IscR, Fnr, SoxR, and NsrR have been reported in bacteria (Py and Barras, 2010; Py *et al*., 2011). These regulators function as the sensors responding to O_2, iron, and oxidative and nitrosative stress and control the expression of various genes involved not only in the survival of the bacteria including biogenesis of Fe-S clusters, anaerobic respiration, and defense against oxidants but also in the virulence (Kiley and Beinert, 2003; Py and Barras, 2010). So far, however, there has been little study on function and regulatory mechanism

of IscR in pathogenic bacteria. This strongly underlines the necessity of identification and characterization of IscR as a virulence regulator and of investigating its functions in pathogenesis. Therefore, this study has made efforts to uncover the roles of *V. vulnificus* IscR during pathogensis.

Chapter II.

IscR is a global regulator essential for the pathogenesis of *Vibrio vulnificus* and induced by host cells

II-1. Introduction

It has been generally accepted that virulence factors of infecting microorganisms include all those factors contributing to survival and multiplication on or within host as well as to disease (Mekalanos, 1992). Numerous virulence factors account for the fulminating and destructive nature of *V. vulnificus* infections and contribute to survival and multiplication on or within a host as well as to disease development (for a recent review, Jones and Oliver, 2009). Most of the virulence factors of pathogenic bacteria act cooperatively to obtain maximum effectiveness during pathogenesis while their expression is coordinately regulated by common global regulators in response to environmental conditions, and this coordinated regulation facilitates the cooperation of virulence factors, and is crucial for the overall success of the pathogens during infection (Cotter and DiRita, 2000; Matson *et al*., 2007). However, studies about global regulators involved in the regulation of *V. vulnificus* virulence factors are still very limited.

Iron-sulfur proteins containing Fe-S cluster as a cofactor carry out multiple important cellular processes such as electron transfer, metabolic reaction, and gene regulation and are widely distributed (for recent reviews, Fontecave, 2006; Py and Barras, 2010). A highly conserved gene cluster *isc* operon, *iscRSUA-hscBA-fdx*,

was discovered to encode all proteins required for the biogenesis of the majority, if not all, of Fe-S cluster in *Escherichia coli* (for recent reviews, Johnson *et al*., 2005; Py and Barras, 2010). Expression of the *isc* operon is autoregulated by IscR, a [2Fe-2S] cluster-containing transcription factor (Schwartz *et al*., 2001). IscR functions as a sensor of the cellular Fe-S cluster status and homeostatically regulates the Fe-S biogenesis (Schwartz *et al*., 2001; Giel *et al*., 2013). When the cellular Fe-S cluster is sufficient to occupy IscR, the resulting [2Fe-2S]-IscR (holo-IscR) represses the *isc* operon. The repression is relieved by decreased [2Fe-2S] occupancy of IscR under iron starvation or oxidative stress conditions (Zheng *et al*., 2001; Outten *et al*., 2004; Imlay *et al*., 2006; Yeo *et al*., 2006; Giel *et al*., 2013).

IscR is proposed as a member of Rrf2 family of transcription factor, consisting of a winged helix-turn-helix (HTH) DNA-binding domain in the N-terminal region and a motif with three cysteines and one histidine (CCCH) required for Fe-S cluster ligation in the C-terminal region (Nesbit *et al*., 2009; Fleischhacker *et al*., 2012). It has been reported that IscR controls the expression of more than 40 genes including the genes encoding for additional proteins involved in Fe-S cluster biogenesis such as *suf* operon (*sufABCDSE*) and anaerobic respiratory enzymes containing Fe-S cluster (Giel *et al*., 2006). IscR also regulates genes involved in biofilm formation in response to changes in cellular Fe-S cluster levels in *E. coli*

(Wu and Outten, 2009). These findings suggested that IscR is a global regulator carrying broader roles in addition to modulating Fe-S homeostasis in bacteria.

In the present study, an open reading frame (ORF) encoding an *E. coli* IscR homologue was identified in an effort to screen for *V. vulnificus* virulence factors by a transposon-tagging method. A *V. vulnificus* null mutant, in which the *iscR* gene was inactivated, was constructed by allelic exchanges, and the possible roles of the IscR protein during infection of *V. vulnificus* were explored. As a result, it was discovered that IscR is essential for the virulence of *V. vulnificus* in mice and tissue culture. A transcriptome analysis newly identified several genes involved in motility and adhesion to host cells, hemolytic activity, and survival under oxidative stress as IscR regulon. Furthermore, IscR expression was found to be induced by exposure of the pathogen to host cells. Therefore, the results indicated that IscR is a global regulator and plays an essential role in bacterial pathogenesis, by being induced during infection.

II-2. Materials and Methods

II-2-1. Bacterial strains, plasmids and culture conditions.

The strains and plasmids used in this study are listed in Table 1. Unless otherwise noted, the *Escherichia coli* and *V. vulnificus* strains were grown in Luria-Bertani (LB) medium at 37°C and in LB medium supplemented with 2.0% (wt/vol) NaCl (LBS) at 30°C, respectively.

Table 1. Bacterial strains and plasmids used in this study

Strain or plasmid	Relevant characteristics[a]	Reference or source
Strains		
V. vulnificus		
M06-24/O	Clinical isolate; virulent	Laboratory collection
JK093	M06-24/O with Δ*iscR*	This study
JK131	M06-24/O with Δ*aphA*	This study
JK132	M06-24/O with Δ*iscR,* Δ*aphA*	This study
JK128	M06-24/O with *iscR3CA*[b]	This study
JK134	M06-24/O with Δ*prx3*	This study
E. coli		
DH5α	λ⁻ ϕ80d*lacZ*ΔM15 Δ(*lacZYA-argF*)*U169 recA1 endA1 hsdR17* (r_K^- m_K^-) *supE44 thi-1 gyrA relA1*; plasmid replication	Laboratory collection
S17-1λ*pir*	λ-*pir* lysogen; *thi pro hsdR hsdM*⁺ *recA* RP4-2 Tc::Mu-Km::Tn7;Tp^r Sm^r; host for π-requiring plasmids; conjugal donor	Simon *et al*., 1983
BL21(DE3)	F^- *ompT hsdS*$_B$ (r_B^- m_B^-) *gal dcm* (DE3)	Laboratory collection
Plasmids		
pRL27	Tn5-RL27, *ori*R6K; Km^r	Larsen *et al*., 2002
pGEM-T Easy	PCR product cloning vector; Ap^r	Promega
pDM4	R6K γ *ori sacB*; suicide vector; *oriT* of RP4; Cm^r	Milton *et al*., 1996
pJK0909	pDM4 with Δ*iscR*; Cm^r	This study
pRK415	IncP *ori*; Broad-host-range vector, *oriT* of RP4; Tc^r	Keen *et al*., 1988
pJK1016	pRK415 with *iscR*; Tc^r	This study
pET22b(+)	His_6 tag fusion expression vector; Ap^r	Novagen

pJK0928	pET22b(+) with *iscR*; Ap^r	This study
pJK1201	pGEM-T Easy with 321-bp fragment of *iscR* upstream region; Ap^r	This study
pJK1126	pDM4 with Δ*aphA*; Cm^r	This study
pET28a(+)	His_6 tag fusion expression vector; Km^r	Novagen
pJK0903	pET28a(+) with *aphA*; Km^r	This study
pBAD24	ColE1 *ori*; *ara*BAD promoter; Ap^r	Guzman *et al*., 1995
pJK1011	pBAD24 with *aphA*; Ap^r	This study
pBBR-lux	Broad host range vector with promoterless *luxCDABE*; Cm^r	Lenz *et al*., 2004
pJK1307	pBBR-*lux* with 456-bp fragment of *iscR* upstream region; Cm^r	This study
pJK1312	pBBR-*lux* with 164-bp fragment of *iscR* upstream region; Cm^r	This study
pJK1313	pBBR-*lux* with 148-bp fragment of *iscR* upstream region; Cm^r	This study
pJH0311	0.3-kb NruI fragment containing multicloning site of pUC19 cloned into pCOS5; Ap^r, Cm^r	Goo *et al*., 2006
pJK0914	pJH0311 with *aphA*; Ap^r, Cm^r	This study
pJK0915	pGEM-T Easy with *iscR*; Ap^r	This study
pJK0929	pGEM-T Easy with *iscR3CA*; Ap^r	This study
pJK0919	pGEM-T Easy with 550-bp fragment of *prx3* upstream region; Ap^r	This study
pJK1127	pDM4 with Δ*prx3*; Cm^r	This study
pJK1250	pDM4 with *iscR3CA*; Cm^r	This study
pKS1101	pBAD24 with *oriT* of RP4; Ap^r	Kim *et al*., 2012
pJK1113	pKS1101(pBAD24 with *oriT*) with *nptI*; Ap^r, Km^r	This study
pJK1303	pJK1113 with *prx3*; Ap^r, Km^r	This study
pJK0920	pBAD24 with *iscR*; Ap^r	This study
pJK1008	pBAD24 with *iscR3CA*; Ap^r	This study
pJK0924	pBBR-*lux* with 550-bp fragment of *prx3* upstream region; Cm^r	This study

pJK1001	pET22b(+) with *iscR3CA*; Ap^r	This study

[a] Tp^r, trimethoprim resistant; Sm^r, streptomycin resistant; Km^r, kanamycin resistant; Ap^r, ampicillin resistant; Cm^r, chloramphenicol resistant; Tc^r; Tetracycline resistant.

[b] The *iscR3CA* gene encodes IscR3CA mutant (IscR-C92A/C98A/C104A).

Table 2. Oligonucleotides used in this study

Oligonucleotide[a]	Sequence (5' → 3')[b]	Use
ISCR001F	TTGTGCGCTGGTTGTCGGTT	Deletion of *iscR*
ISCR001R	TAGGATCCCTCTAAGTAAGAGAGCGAAATC	
ISCR002F	AGGGATCCTATTGATCTTGCGGTAAAT	Deletion of *iscR*
ISCR002R	AGACTGCGCTGCATCGACGT	
ISCR003F	CATATGAAACTGACATCTAAAGGAAGATAT	Amplification of *iscR* ORF
ISCR003R	CTCGAGAGAGCGGAAATTTACAC	
ISCR004F	AAGCTTAGTGTGGATACGGTGTGATATG	Complementation of *iscR*
ISCR004R	TCTAGAGGCAGTTTCATTCTTCACTCC	
FLGE01F	TCTGGTTCACTTCCACGA	Amplification of the *flgE* promoter region
FLGE01R	TAACCTCTGCATTGCGTTCA	
GBPA01F	CGCCTCATCGTTATTCTCAT	Amplification of the *gbpA* promoter region
GBPA01R	GGCCAGTAAGGTTTTTTGCGGTTG	
VVHBA01F	GATAAAACAACAACGCCCACATTAATC	Amplification of the *vvhBA* promoter region
VVHBA01R	CTCGTAATGAGGAATCTATGCTTAAT	
PRX01F	CACCCAGTAAATATTGTTTGGC	Amplification of the *prx* promoter region
PRX01R	CTCAAGGCCAAACTTTACCTAA	
ISCR01F	GGTTGACGCAACTAAGTGTCAGG	Amplification of a part of the *iscR* coding

ISCR01R	TTAAGAGCGGAAATTTACACCGAT	region
APHA001F	CAACGAGAACTTGATGCAAAGCG	Deletion of *aphA*
APHA001R	TAAGGATCCATAGAAGCGGAGAATTCTTT	
APHA002F	TATGGATCCTTACGCCGTAATTTGATG	Deletion of *aphA*
APHA002R	CCCACACTTAACCTGTATTGATGCC	
APHA003F	CCATGGTTGCATCAACAAGAATGTAAA	Amplification of *aphA* ORF, purification of AphA
APHA003R	GTCGACGCCGAGGATATCCAGTT	
ISCR005F	AATAAAATGCGTCGATTGTTCAG	Amplification of *iscR* regulatory region (-194 ~ 127)[c], Primer extension, EMSA, DNase I protection assay
ISCR005R	CTCGGAAATATCAGCCAGAGG	
APHA004F	CCATGGTGTCATTACCACACGTAAT	Amplification of *aphA* ORF, *E. coli* dual plasmid system assay
APHA004R	CTGCAGCCACATTGTCTAGCGTA	
ISCR006F	GAGCTCCAACAAAGCCTATATCCA	Amplification of *iscR* regulatory region (-329 ~ 89)[c], *E. coli* dual plasmid system assay
ISCR006R	ACTAGTAATGCAGTGCCACATCCA	
ISCR007F	GAGCTCATAGGGATGAATACCTGACTAT	Amplification of *iscR* regulatory region (-75 ~ 89)[c], *E. coli* dual plasmid system assay
ISCR008F	GAGCTCGACTATTTTAGTCAAATAAATACTTG	Amplification of *iscR* regulatory region

		(-59 ~ 89)[c], *E. coli* dual plasmid system assay
APHA005F	GAGCTCTTGGATTGAAGACATGTCA	Amplification of *aphA* ORF,
APHA005R	GGTACCCTCCCTCATATAAAAACG	Complementation of *aphA*
ISCR_qRTF	GATATGCGGTAACGGCAATGCT	qRT-PCR
ISCR_qRTR	TAAGAGAGCGAAATCCCCTGACG	
APHA_qRTF	TTGGAACCGCAAGAAGGCAA	qRT-PCR
APHA_qRTR	AGTTGGGTGGGCTGTCGGTT	
PRX001F	GTGGTTGATAGACCAGCCATTCGTC	Deletion of *prx3*
PRX001R	GATGGATCCTTTTTTGCCAGCAAA	
PRX002F	AAAGGATCCATCGACAATGGCGTA	Deletion of *prx3*
PRX002R	CGCTTTCGTGACCTTAATTGGTTTG	
ISCR005F	CCATGGTGAAACTGACATCTAAAGG	Amplification of *iscR* or *iscR3CA* ORF
ISCR005R	GTCGACTCTTCACTCCAATGTAAACTT	
ISCRSDM1F	CGCAACTAAGGCGCAGGGCAAAGGAGATGCGCAAGGCGGCAC	Construction of *iscR3CA*
ISCRSDM1R	GTGCCGCCTTGCGCATCTCCTTTGCCCTGCGCCTTAGTTGCG	
ISCRSDM2F	CAAGGCGGCACTCGCGCGCTTACTCATACACTTTGGCGTGACC	Construction of *iscR3CA*
ISCRSDM2R	GGTCACGCCAAAGTGTATGAGTAAGCGCGCGAGTGCCGCCTTG	
PRX004F	GAGCTCTTGATAGACC AGCCATTC	Amplification of *prx3* regulatory region (−422 ~ 97)[d]
PRX004R	ACTAGTTGCCAGCAAACAGCTCTAA	

PRX005F	ATATTTGGACATAAAAAGACCCCC	EMSA, DNase I protection assay
PRX005R	CTAAAACAGGGTGGTGGACCA	EMSA, DNase I protection assay, Primer extension
ISCR003F	CATATGAAACTGACATCTAAAGGAAGATAT	Amplification of *iscR3CA* ORF
ISCR003R	CTCGAGAGAGCGGAAATTTACAC	
PRX_qRTF	TGAAAGCCTGGGGTGAAGCA	qRT-PCR
PRX_qRTR	ATCGCGTAGCGTTGAGAGCG	

[a] The oligonucleotides were designed using the genomic sequence of the *V. vulnificus* MO6-24/O (Park *et al.*, 2011).

[b] Regions of oligonucleotides not complementary to corresponding genes are underlined.

[c] Shown are the oligonucleotide positions, where +1 is the transcription start site of *iscR*.

[d] Shown are the oligonucleotide positions, where +1 is the transcription start site of *prx3*.

II-2-2. Identification of *V. vulnificus iscR* and generation of *iscR* mutant.

To generate a random transposon mutant library of *V. vulnificus*, *E. coli* S17-1 λ *pir, tra* strain containing pRL27, a suicide vector carrying the hypertransposable mini-Tn5 (Km^r) element (Simon *et al*., 1983), was used as a conjugal donor to *V. vulnificus* MO6-24/O. Transposon mutants of *V. vulnificus* on the LBS agar containing polymyxin B (100 U/ml, to exclude *E. coli*) (Cerdà-Cuéllar *et al*., 2000) and kanamycin (100 μg/ml) were selected and grown with 200 μl of LBS medium in 96-well culture dishes (Nunc, Roskilde, Denmark). From the transposon mutants, a mutant exhibiting decreased cytotoxic activity against the INT-407 (ATCC CCL-6) human intestinal epithelial cells was screened. A DNA segment flanking the transposon insertion was amplified by a polymerase chain reaction (PCR) as previously described (Lee *et al*., 2008b) and a search of the *V. vulnificus* MO6-24/O genome sequence (GenBank accession numbers CP002469 and CP002470, www.ncbi.nlm.nih.gov) for homology to the sequence of the resulting PCR product singled out *iscR*, which encodes a putative Fe-S cluster regulator. The *iscR* gene was inactivated *in vitro* by deletion (300-bp of 507-bp) of the *iscR* ORF using the PCR-mediated linker-scanning mutation method as described previously (Kim *et al*., 2012). Pairs of primers ISCR001F and ISCR001R (for amplification of the 5' amplicon) or ISCR002F and ISCR002R (for amplification of the 3' amplicon) were designed (Table 2). The 300-bp deleted *iscR* was amplified by PCR using the

mixture of both amplicons as the template and ISCR001F and ISCR002R as primers. The resulting 1,702-bp DNA fragment containing the deleted *iscR* was ligated with SpeI-SphI-digested pDM4 (Milton *et al*., 1996) to generate pJK0909. The *E. coli* S17-1 λ *pir, tra* strain (containing pJK0909) (Simon *et al*., 1983) was used as a conjugal donor to *V. vulnificus* MO6-24/O. The conjugation and isolation of the transconjugants were conducted as previously described (Kim *et al*., 2012), and the *V. vulnificus iscR* mutant chosen for further analysis was named JK093 (Table 1).

II-2-3. Complementation of the *iscR* mutant.

To complement the *iscR* mutation, the *iscR* coding region was amplified from the genomic DNA of *V. vulnificus* M06-24/O by PCR with a pair of primers ISCR004F and ISCR004R (Table 2) and then digested with HindIII and XbaI. The amplified *iscR* coding region was subcloned into the broad host-range vector pRK415 (Keen *et al*., 1998) linearized with the same enzymes (Table 1) to result in pJK1016. The plasmid pJK1016 was delivered into the *iscR* mutant JK093 by conjugation as described above.

II-2-4. Cytotoxicity and mouse mortality.

Cytotoxicity was evaluated by measuring the cytoplasmic lactate dehydrogenase

(LDH) activity that is released from the INT-407 cells by damage of plasma membranes (Sepp *et al*., 1996). The INT-407 cells were grown in minimum essential medium containing 1% (vol/vol) fetal bovine serum (GIBCO-BRL, Gaithersburg, MD) (MEMF) in 96-well culture dishes (Nunc, Roskilde, Denmark) as described previously (Jeong *et al*., 2009). Each well with 2×10^4 INT-407 cells were infected with the *V. vulnificus* strains at a multiplicities of infection (MOI) of 10 for various incubation times. The LDH activity released into the supernatant was determined using a Cytotoxicity Detection Kit (Roche, Mannheim, Germany).

Mouse mortalities of the wild type and *iscR* mutant were compared as described elsewhere (Hwang *et al*., 2013). Groups of (n = 20) 7-week-old ICR female mice (specific pathogen-free, Seoul National University) were starved without food and water for 12 h until infection. Then the mice, without iron-dextran pretreatment, were intragastrically administered with 50 μl of 8.5% (wt/vol) sodium bicarbonate solution, followed immediately with 50 μl of the inoculum, representing approximately 10^9 cells of either the wild type or *iscR* mutant. Mouse mortalities were recorded for 24 hr. All manipulations of mice were approved by the Animal Care and Use Committee at Seoul National University.

II-2-5. Transcriptome analysis.

A transcriptome analysis was performed using the *V. vulnificus* Whole-Genome

Twin-Chip as described previously (Jeong and Choi, 2008). Total RNAs from the *V. vulnificus* strains grown to A_{600} 0.5 were isolated with an RNeasy® Midi Kit (Qiagen, Valencia, CA), and aminoallyl-cDNA was synthesized using an Amino Allyl cDNA Labeling Kit (Ambion, Austin, TX) according to the manufacturer's procedures. The aminoallyl-cDNA from the *iscR* mutant and wild type were respectively labeled with Cy3 or Cy5, and equal amounts of the labeled cDNA were combined and used to hybridize the microarray slides at 42°C for 16 h. The arrays were washed, dried, scanned, and analyzed by GenePix Pro 3.0 software (Axon Instruments, Union City, CA), and the ORF spots that showed 2-fold or greater difference in expression with a P value of ≤ 0.05 were considered to be regulated by IscR.

II-2-6. Quantitative real-time (qRT) PCR.

Total RNAs from the *V. vulnificus* strains were isolated as described above and cDNA was synthesized using iScript™ cDNA Synthesis Kit (Bio-Rad, Hercules, CA). Real-time PCR amplification of the cDNA was performed by using the Chromo 4 real-time PCR detection system (Bio-Rad) with a pair of specific primers listed in Table 3 as described previously (Kim *et al*., 2012). Relative expression levels of the specific transcripts were calculated by using the 16S rRNA expression level as the internal reference for normalization.

Table 3. **Oligonucleotides used for real-time PCR to confirm the expression levels determined by the microarray**

Locus tag[a]	Oligonucleotide sequence (5' → 3')[b]	
	Forward	**Reverse**
VVMO6_00199	ATGGAAGCGATTGAATACCTAA	GGAACTCTTGACCGACAG
VVMO6_00216	GAGCTTGTTTGGTGCAGGTG	ATGCCACATTGGTAAGGCCA
VVMO6_00218	GGTCAACGGAGTGCCAAAAC	ATCTTCTGGTTTGCGGTCGT
VVMO6_00219	CATCAAAGACAAAGGCAAGGTA	CGTAGAATCGCAGAGTGAAC
VVMO6_00314	AGTTGTGGCGGTGGATGGTG	GTGCCCCCTGGGGTTTCATA
VVMO6_00315	TTGTGCTGACTCGTGCCCCT	CATGCTGTCGTGGGCATTGA
VVMO6_00338	GGTCAGCCATCGGTCTTTCA	TTGTCCATCTCGTGAGCACC
VVMO6_00393	GCGCGTAATAACGTCGGCAA	CGGCCACGAGTTCTTCATCG
VVMO6_00423	GAAACGTGGTTTGCCATGCT	AAAGCAAAACAATCCGCCCC
VVMO6_00532	CTCGCCTAGATGGCGTTGAT	ATGGAACGGATACGACGCTC
VVMO6_00971	TGGTATCGCTGGTCTATCTAT	TCACGGATTGGTTTCACTTT
VVMO6_00997	GGGAATGAGAGCAACCAGCG	CCGACGTGGTTTTGGCTGTT
VVMO6_01063	CCGATTACCCAGCCAATGGT	GCTTTTTGAACGCCATCGGT
VVMO6_01074	GGCAACAAAGAGTATGAGTTTC	GCACAGACCACATCACAA

VVMO6_01129	ACCAAGCGCACAATGCCAGT	CGGCTTCAATGGCAGCATTC
VVMO6_01149	CGCCATTGGGGTGGTCAGTA	GTCTTGCCGTGCTTGTTGGC
VVMO6_01150	AGCTTTTGCGAACGCTGCAC	AGCGCACAATACCAGCGGAA
VVMO6_01249	CTTTGAAACGGGCATCGCAG	AAACTCGGCGTAACGCGACA
VVMO6_01954	TGAAAGAGCAAGTCGACGCT	TTTGCCTTTTCCATTGCCCG
VVMO6_02043	CGAGCACCCAGAAACTCACT	TCGTCAGTAACAACCGCGAA
VVMO6_02138	CAAGCCTTTAGCGATGAAA	CAGCAATAATCCTCTTCCAT
VVMO6_02203	GCAACAGAAGATGAGCATATC	GTCGCCAGAGGAACATAA
VVMO6_02205	GTGGTTTACACCTCAGGCCA	ACCACTGGCTTCCAATACCG
VVMO6_02243	CTGCTGACGAAGATGGAA	AATCACGAGATACGGAACC
VVMO6_02433	TGGATCCAAAAACGGTGCGT	TCCCATTCATCCAACCAGCAA
VVMO6_02434	AGCATGGGGGCTAGAGCCTG	TCCGATGCGTGGTTTAGCGT
VVMO6_02435	CATTCCTCGCAATACCACCATTCC	ACGACAGTCATCCACCATCTCAC
VVMO6_02436	ATCAAACGCAGCCAAAGCACTC	GAAATCCGAGGTGAGCAGCAAAC
VVMO6_02437	TTAACAGAAACCGCAGCAAGTCG	TCACACCTAAACGCAAACCAACG
VVMO6_02438	GCAAATCAAAGTAACGCCAGAAGG	GCAATCGCACTACCACAACCG
VVMO6_02439	TTGTTGAAGGTGAGTCGTTACTGATG	CGAGAGCACGCAATACATAAGAAGG
VVMO6_02440	GATATGCGGTAACGGCAATGCT	TAAGAGAGCGAAATCCCCTGACG
VVMO6_02482	ACAGATGAAGTTCGAGGCCGTG	GCTCGACGTGCATCAGGCTT
VVMO6_02521	ATCGGTTCCTTTGAAGCGCC	GGCTCGAGCGACCGTTTCTT

VVMO6_02539	AAGTGGCTATCGAAGCAGCA	TCACGCTGTTGTTCTGGTGT
VVMO6_03020	AAGCGTGGATGGTGAGTA	GGAAATGAAGAAAGAGAGAAAGC
VVMO6_03043	GGCTCGTTTACGGTTTGGGG	TGGCAGATGGTGTGGGTTCC
VVMO6_03179	GGCGACAGCATCAAGATCGG	GGTGCTTCGCGCACCTCTAA
VVMO6_03472	TAAAGACGCAGCAGACAGCA	AAACCTGCATTGACGTTGCC
VVMO6_03494	TAGACAAAGACGGCACGCTGCA	CCCGCCGTGTACGAGCTCAA
VVMO6_03502	GGCAGGCCAAAACGAACAAT	CCGCGACGTCTCTTAAGTCT
VVMO6_03758	TGTTGGCGATGCCTTTGCTT	GAGCGATGCTCCCGTCACTG
VVMO6_03816	GTTTTGCCATCGCACGAACT	TCGATGCCCAACTTGTACCC
VVMO6_03848	CAACAATGCCACGAAACGCA	CCATGGCATCCACCACTCGT
VVMO6_03878	TCGACCGCTTGCATGTGATG	CTGCGTTGCCTGCAATTTCC
VVMO6_03880	CACGCTGTTTAACGGCCAGC	ATCACCACGGTGCTACCGGA
VVMO6_03881	CGCCAAGAGCTTGGGTGCTA	AGACACGGGCGCTTCGTACA
VVMO6_04018	TTTAAGGCGCGTGCAGAGTA	GTCTTGGCTCTACTGCCGTT
VVMO6_04141	TGAAAGCCTGGGGTGAAGCA	ATCGCGTAGCGTTGAGAGCG
VVMO6_04152	CGTTTGATCTCGCCGGTTTG	GCAGCCATCTCGCCTTTTGA
VVMO6_04166	GCCTTTTCGCCAATTGTGGT	CCACAACACGGAGACGGTAA
VVMO6_04170	CTGCAAAATCGGCGGCATAG	GCGAAGCGTGGCTTTGCTTA
VVMO6_04184	CGTCGCTAAAGCAGAGGCGA	AAAGCGGCGGTAGGCTCATC
VVMO6_04185	TGACGCAGCAATCTCAGCGA	GCAAATGACACGAAAGCCGC

VVMO6_04186	GGCCAACTACTGCGCTGGTG	CGCGAATGGTCTGAGAAGCG
VVMO6_04222	ATCACCCGCGAAAGCTACAA	TTTGAAGCAAAGCAGACCGC
VVMO6_04284	CTACACGCTAGAAGGCATC	CGAATTTCAAGACCCACAC
VVMO6_04286	GCGGTACTCTTCACCCTCAC	AGACGAACATCACGGCAACT
VVMO6_04436	CGTGAAATCGGAACTTGGCG	CGAGTGTTGGCAGTTTGGTG
VVMO6_04467	CCAAACATGGCGCTCGCTAC	GTTAAACCGGGGCTGATGGC
VVMO6_04468	CCCATTTTGTGCTCGCGTTC	GAGGGCTTGGCCGTCATTTT
VVMO6_04469	CCCGGCGTTTATACCGATGA	TGGAACACTGGGTGCGATAC
VVMO6_04473	GACGCGATCAAGATTGGCAC	AGCTCTTCAACGCTGCTGAT
VVMO6_04475	GCAACGGCACTTATGTCTA	GAGTAGGTCATCGCATCG
VVMO6_04488	TGTCAGTCGGTATGGTCA	GGGTATCCTGCGTGATTC
VVMO6_04555	CCGTGGTGGTGGTGCTCAAT	TGGCGGTTTGATTTCCCCTT

[a] The oligonucleotides were designed using the genomic sequence of *V. vulnificus* MO6-24/O (GenBank accession numbers CP002469.1 and CP002470.1).

[b] Locus tag numbers are based on the database of the *V. vulnificus* MO6-24/O genome sequence.

II-2-7. Purification of *V. vulnificus* IscR and electrophoretic mobility shift assay (EMSA).

The coding region of *iscR* was amplified by a PCR using the *V. vulnificus* MO6-24/O chromosomal DNA and primers, ISCR003F and ISCR003R (Table 2). The 513-bp PCR product was subcloned into a His_6 tag expression vector, pET22b(+) (Novagen, Madison, WI), to result in pJK0928 (Table 1). The His-tagged IscR was then expressed in *E. coli* BL21(DE3), purified aerobically by affinity chromatography according to the manufacturer's procedure (Qiagen).

For EMSA, four genes were randomly chosen from the pool of the 12 predicted IscR-regulated genes. The putative regulatory regions (about 300-bp) of the genes were amplified and radioactively labeled by PCR using sets of primers, FLGE01F and FLGE01R for *flgE*, GBPA01F and GBPA01R for *gbpA*, VVHBA01F and VVHBA01R for *vvhB*, or PRX01F and PRX01R for *prx* (Table 2). For negative control, a 250-bp DNA fragment of *iscR* coding region was amplified and radioactively labeled by PCR using a pair of primers ISCR01F and ISCR01R (Table 2). The labeled DNA (2.5 nM) fragment was incubated with the purified IscR at a concentration of 10 nM for 30 min at 30°C in a 20-μl reaction mixture containing 1× binding buffer (Giel *et al*., 2006) and 0.1μg of poly(dI-dC). Electrophoretic analyses of the DNA-protein complexes were performed as

described previously (Lee *et al*., 2008b).

II-2-8. Motility and adhesion assays.

For motility assays, *V. vulnificus* strains were grown to A_{600} 0.5, and subsequently stabbed into LBS semi-solid media solidified with 0.3% agar (Kim *et al*., 2012). The plates were incubated at 30°C for 24 h, and migration through the agar was photographed using a digital camera (Canon PowerShot SX220 HS, Japan).

For the adhesion assay, 2×10^5 INT-407 cells in a well of 12-well culture dishes (Nunc) were infected with the *V. vulnificus* strains at an MOI of 10 for 30 min and then washed two times to remove nonadherent bacteria as described previously (Jeong *et al*., 2009). Following the last wash, the INT-407 cells were broken with 0.1% Triton X-100 treatment for 20 min, and the recovered bacterial cells were enumerated by determining CFU per well (Jeong *et al*., 2009). Adhesion of *V. vulnificus* to INT-407 cells was also examined microscopically. For this purpose, INT-407 cells seeded onto glass coverslips were infected with the *V.vulnificus* strains at an MOI of 10 for 30 min and then were fixed in methanol and stained with 0.4% Giemsa (Jeong *et al*., 2009).

II-2-9. Hemolysis assay and survival under oxidative stresss.

For blood agar plate assays, 5 μl of the *V. vulnificus* cultures grown to A_{600} 0.5 were spotted onto blood agar containing 5% sheep blood (MB Cell, Los Angeles, CA). The plates were incubated at 37°C for 24 h and photographed as described above for motility assay. For quantitative assays, an aliquot of *V. vulnificus* culture supernatants was mixed with an equal volume of human red blood cell (hRBC) suspension (1.0% in phosphate-buffered saline; Innovative Research, Novi, MI) and incubated at 37°C for 20 min. The level of hemolysis was determined as described elsewhere (Lee *et al*., 2013a) and by expressed using the complete hemolysis by 1% Triton X-100 as 100%.

Survival of the *V. vulnificus* strains under oxidative stresses was determined by measuring the growth on the LBS agar medium containing either 250 μM H_2O_2 or 60 μM *tert*-butyl hydroperoxide (*t*-BOOH) (Baek *et al*., 2009). Equal numbers of the strains grown to A_{600} 0.5 were serially diluted and then spotted onto the agar medium, and then the growth was photographed after 16 h as described above for motility assay.

II-2-10. Western blot analysis.

The purified IscR was used to raise a rabbit anti-IscR polyclonal antibodies (AB Frontier, Seoul, South Korea). The wild type *V. vulnificus* exposed to MEMF

(control), H_2O_2, INT-407 cells, or INT-407 cells preincubated with NAC and then harvested as described above for qRT-PCR. The *V. vulnificus* cells were lysed using complete lysis-B buffer (Roche) for 1 min, and residual cell debris was removed by centrifugation (Lee *et al*., 2008b). Protein samples from the cell lysates, equivalent to 10 μg of total protein, were resolved by using SDS-PAGE and immunoblotted using the anti-IscR polyclonal antibodies as described previously (Kim *et al*., 2012).

II-2-11. Microarray data accession number.

All primary microarray data were deposited into the Gene Expression Omnibus (GEO, http://www.ncbi.nlm.nih.gov/projects/geo/) under accession number GSE44679.

II-3. Results

II-3-1. Identification of *V. vulnificus* IscR.

The amino acid sequence deduced from the putative *V. vulnifius iscR* nucleotide sequence revealed a protein, a putative IscR (*Vv*IscR), composed of 168 amino acids with a theoretical molecular mass of 18,199 Da and a pI of 6.82. *Vv*IscR exhibits a high level of identity (77% in amino acid sequences) with *E. coli* IscR (*Ec*IscR) (Schwartz *et al*., 2001). Furthermore, *Vv*IscR contains a winged HTH DNA-binding domain and the highly conserved CCCH motif at positions corresponding to those of *Ec*IscR. The predicted hydrophobicity profile (http://web.expasy.org/protscale/) was similar to that of the *Ec*IscR and consistent with the fact that IscR is a cytosolic soluble protein (data not shown). The results indicated that *Vv*IscR is also an Fe-S cluster regulator modulating Fe-S cluster biogenesis as observed in *Ec*IscR (Schwartz *et al*., 2001; Giel *et al*., 2013).

II-3-2. IscR is important for virulence.

In an effort to further understand the role of IscR in *V. vulnificus* pathogenesis, virulence of the *iscR* mutant JK093 in mice and in cell culture system was compared. For this purpose, mice were infected intragastrically with the wild type and *iscR* mutant and then numbers of dead mice were counted for 24 h. As shown

in Fig. II-1A, the deaths of mice infected with the *iscR* mutant were consistently and significantly delayed ($P = 2.88\times10^{-6}$, Log rank test), compared to those of mice infected with the parental wild type (Fig. II-1A). The result suggested that IscR is essential for pathogenesis of *V. vulnificus*. To examine the role of IscR in epithelial cell damage, the monolayers of INT-407 cells were infected with the wild type and *iscR* mutant and activities of LDH released from the INT-407 cells were compared at different incubation times (Fig. II-1B). The *iscR* mutant exhibited significantly lower LDH-releasing activities than the wild type for as long as 2 h, indicating that IscR is important for *V. vulnificus* to infect and injure host cells. (Fig. II-1B). For the complementation of the *iscR* mutant, plasmid pJK1016 was constructed by subcloning the *iscR* coding region into pRK415 and under an IPTG (isopropyl-β-D-thiogalactopyranoside)-inducible promoter (Keen *et al*., 1988) (Table 1). Complementation of the *iscR* gene in JK093 with a functional *iscR* gene (pJK1016) restored the LDH-releasing activities to levels comparable to those of the wild type (Fig. II-1B). The combined results suggested that IscR is essential for the virulence of *V. vulnificus* in mice and in tissue cultures.

Figure II-1. Mouse mortality and cytotoxicity of *V. vulnificus*. (A) Seven-week-old specific pathogen-free female ICR mice were intragastrically infected with the wild type (WT) or the *iscR* mutant at doses of 10^9 CFU. Mouse survival was monitored for 24 h. (B) INT-407 cells were infected with the wild type, the *iscR* mutant, or the complemented strain at an MOI of 10. The cytotoxicity was determined by an LDH release assay. Error bars represent the SEM. **, $P < 0.005$ relative to groups infected with the wild type at each incubation time. WT (pRK415), wild type; *iscR* (pRK415), *iscR* mutant; *iscR* (pJK1016), complemented strain.

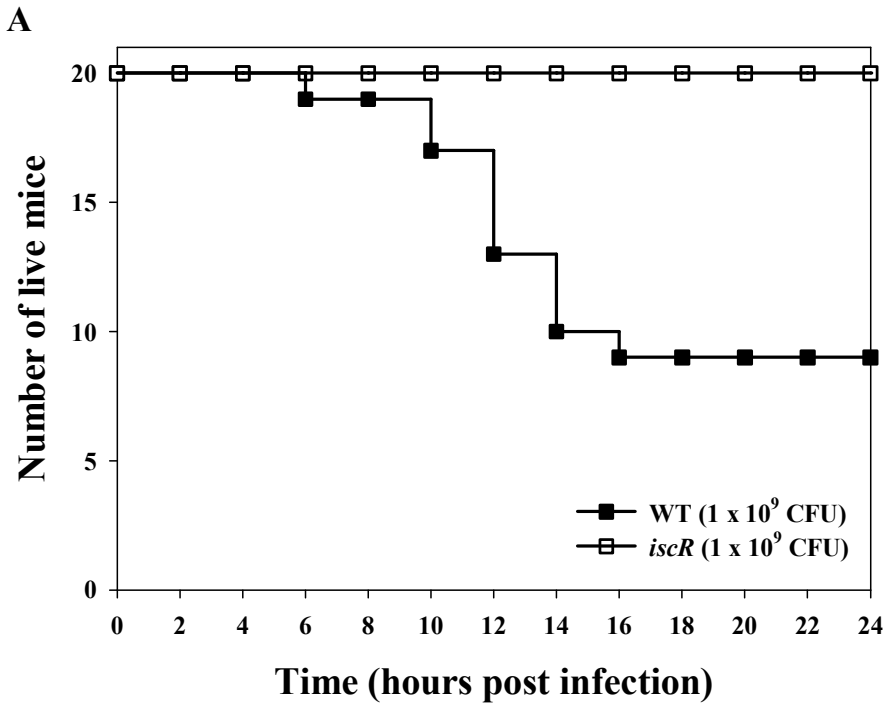
A
Number of live mice
20
15
10
5
0
0
2
4
6
8
10
12
14
16
18
20
22
24
Time (hours post infection)
WT (1 x 10^9 CFU)
iscR (1 x 10^9 CFU)

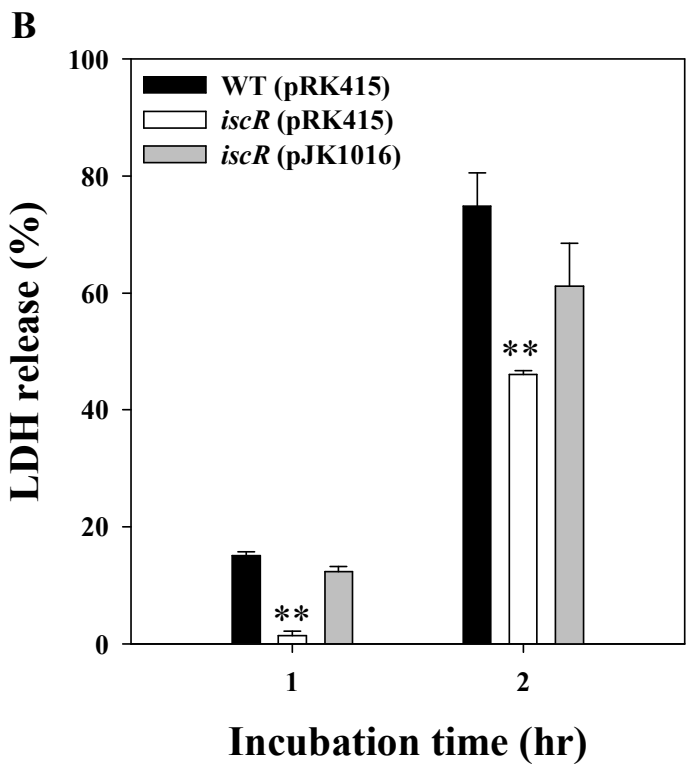
B
LDH release (%)
100
80
60
40
20
0
WT (pRK415)
iscR (pRK415)
iscR (pJK1016)
**
**
1
2
Incubation time (hr)

II-3-3. IscR-regulated genes involved in pathogenesis.

A whole-genome microarray analysis was used to compare the transcriptional profiles of the wild type and *iscR* mutant. The microarray analysis predicted 67 genes potentially regulated by IscR, 52 genes of which were up-regulated and 15 genes down-regulated (Table 4 and 5). Among them, twelve genes that most-likely participate in pathogenesis of *V. vulnificus* (Jones and Oliver, 2009) were up-regulated by IscR (Fig. II-2). Among the products of the twelve genes are a flagella protein FlgE contributing to motility (Lee *et al*., 2004) and methyl-accepting chemotaxis proteins (MCPs) and signal transduction proteins contributing to chemotaxis (Baker *et al*., 2005). A gene encoding GbpA known to participate in adhesion (Kirn *et al*., 2005), two genes involved in production of a cytolysin VvhA (Yamamoto *et al*., 1990), and two genes encoding antioxidant protein peroxiredoxin (Prx) (Seo *et al*., 2010) and glutaredoxin 2 (Grx2) (Vlamis-Gardikas *et al*., 2002) are also up-regulated by IscR (Fig. II-2).

Since many of the genes that I predicted were not previously reported to be IscR-regulated, IscR regulation of the selected twelve genes was experimentally verified. The qRT-PCR revealed that IscR indeed regulates transcription of all of the genes predicted, implying that IscR controls not only Fe-S cluster biogenesis but also survival and virulence of *V. vulnificus* (Fig. II-2). To determine whether IscR

regulates the genes directly or indirectly, four genes *flgE*, *gbpA*, *vvhB*, and *prx* were randomly chosen from the twelve genes and binding of IscR to their upstream regulatory regions was examined. EMSA revealed that IscR binds to the upstream region of all of the genes that were tested (Fig. II-3), suggesting that the genes are under direct control of IscR.

Table 4. Genes whose expression is up-regulated by IscR[a]

Locus tag	Product name	Microarray		qRT-PCR	
		Mean Log_2 ratio[b]	*P*-value	Mean Log_2 ratio[b]	*P*-value
Transport and metabolism					
VVMO6_00199	Aspartate ammonia-lyase	-1.047	7.51E-03	-1.310	2.60E-05
VVMO6_00314	Argininosuccinate synthase	-2.515	8.63E-03	-3.520	1.01E-04
VVMO6_00315	Argininosuccinate lyase	-1.622	2.64E-03	-2.373	1.68E-05
VVMO6_00338	Glucose-6-phosphate isomerase	-1.221	1.81E-03	-1.697	1.69E-04
VVMO6_00393	Ornithine carbamoyltransferase	-1.732	9.09E-03	-1.552	4.37E-05
VVMO6_01954	Cob(I)alamin adenosyltransferase	-1.184	4.83E-06	-1.007	2.96E-04
VVMO6_03020	Na+/H+ antiporter NhaD type	-1.214	5.06E-05	-1.040	2.33E-05
VVMO6_03043	Putrescine/proton symporter, Putrescine/ornithine antiporter PotE	-1.548	1.28E-02	-1.717	1.40E-04
VVMO6_03179	Argininosuccinate synthase	-1.304	5.93E-03	-2.177	1.45E-03
VVMO6_03816	Ribonucleotide reductase of class III (anaerobic) large subunit	-1.561	1.23E-02	-4.070	2.84E-06
VVMO6_04184	Aarginine ABC transporterATP-binding protein ArtP	-1.162	2.60E-02	-1.437	7.28E-05
VVMO6_04185	Arginine ABC transporter periplasmic arginine-binding protein ArtI	-3.511	4.15E-03	-3.520	1.44E-05
VVMO6_04186	Arginine ABC transporter permease ArtQ	-2.482	8.15E-03	-3.393	3.01E-05

VVMO6_04222	Tryptophanase	-1.152	2.75E-02	-2.483	1.99E-05
VVMO6_04284	Acetylornithinedeacetylase	-1.498	1.26E-02	-7.083	7.79E-07
VVMO6_04467	Dehydrogenases with different specificities (short-chain alcohol dehydrogenases)	-1.727	1.04E-07	-2.213	1.07E-04
VVMO6_04473	Ascorbate-specific PTS system, EIIA component	-1.548	1.63E-03	-3.480	8.15E-04
VVMO6_04488	Sulfate permease	-1.427	3.51E-05	-1.307	4.12E-03
Energy production and conversion					
VVMO6_00216	Fumarate reductase subunit D	-1.224	4.17E-02	-4.873	1.48E-07
VVMO6_00218	Succinate dehydrogenase flavoprotein subunit	-1.231	7.04E-03	-5.377	5.25E-06
VVMO6_00219	Succinate dehydrogenase flavoprotein subunit	-1.130	1.38E-02	-5.583	1.85E-07
VVMO6_00971	Pyruvate formate-lyase	-1.392	2.18E-03	-2.690	1.25E-04
VVMO6_01074	D-Lactate dehydrogenase	-2.245	4.53E-06	-2.380	1.54E-05
VVMO6_02043	Alcohol dehydrogenase; Acetaldehyde dehydrogenase	-1.114	1.80E-03	-3.347	3.78E-03
VVMO6_02203	Pyridine nucleotide-disulfide oxidoreductase; NADH dehydrogenase	-1.152	3.38E-02	-1.600	1.81E-04
VVMO6_03472	Alcohol dehydrogenase	-1.704	7.85E-03	-9.143	3.03E-05
VVMO6_03502	Cytochrome c553	-1.149	8.31E-05	-1.967	2.10E-05
VVMO6_04166	L-Lactate permease	-1.014	4.28E-05	-1.973	1.24E-03
VVMO6_04170	D-Lactate dehydrogenase, Fe-S protein, FAD/FMN-containing	-1.099	1.10E-03	-2.143	3.40E-05
VVMO6_04469	2,4-Dienoyl-CoA reductase	-2.133	1.75E-06	-1.758	1.82E-04
VVMO6_04475	Hydrolase	-1.548	2.21E-04	-2.810	9.34E-05

Virulence					
VVMO6_03494	*N*-acetylglucosamine-binding protein GbpA	-1.690	1.76E-05	-1.300	7.84E-04
VVMO6_03880	Cytolysin secretion protein VvhB	-2.133	3.30E-04	-2.367	5.42E-06
VVMO6_03881	Cytolysin / Hemolysin VvhA	-1.966	1.27E-03	-2.467	2.39E-06
Oxidative stress					
VVMO6_04141	Peroxiredoxin	-2.344	1.51E-08	-3.157	8.40E-05
VVMO6_04468	Glutaredoxin 2	-2.506	2.01E-07	-1.738	6.73E-05
Cell motility and chemotaxis					
VVMO6_02263	Flagellar hook protein FlgE	-1.003	2.12E-04	-1.277	5.24E-03
VVMO6_01129	Methyl-accepting chemotaxis protein II	-1.015	3.04E-05	-1.117	5.39E-04
VVMO6_01149	Signal transduction histidine kinase	-1.685	8.56E-03	-4.653	3.63E-05
VVMO6_01150	Signal transduction protein CheY	-2.184	4.58E-03	-4.697	9.51E-06
VVMO6_03848	Methyl-accepting chemotaxis protein I	-1.139	1.44E-03	-1.383	1.28E-04
VVMO6_03878	Methyl-accepting chemotaxis protein HylB	-1.377	3.63E-03	-2.440	3.41E-04
VVMO6_04555	Signal transduction protein CheW	-1.635	1.99E-04	-1.403	2.38E-03
Translation					
VVMO6_02205	Endoribonuclease L-PSP	-1.092	1.05E-03	-1.583	4.29E-05
VVMO6_02482	Ribosome hibernation protein YfiA	-1.123	3.23E-05	-5.473	3.77E-06
Replication, recombination and repair					
VVMO6_00423	A/G-specific adenine glycosylase	-1.544	1.50E-04	-1.247	6.24E-04

Function unknown					
VVMO6_00997	Hypothetical protein	-1.366	1.42E-05	-1.040	9.19E-05
VVMO6_01063	Hypothetical protein	-1.003	8.20E-04	-2.277	1.19E-05
VVMO6_02138	Hypothetical protein	-2.737	7.64E-06	-4.887	1.47E-03
VVMO6_02243	*N*-acetylglucosamine-regulated outer membrane porin	-1.308	3.70E-05	-1.340	2.19E-02
VVMO6_03758	Hypothetical protein	-1.411	8.68E-05	-4.663	6.32E-04
VVMO6_04286	Hypothetical protein	-2.184	1.67E-03	-7.127	2.88E-04

[a] Locus tag numbers, functional categories, and annotation of gene products are based on the database of the *V. vulnificus* MO6-24/O genome (Park *et al*., 2011; GenBank accession CP002469 and CP002470). Functional categories in boldface are shown above the first gene in each category.

[b] The M value represents the log2 ratio of mRNA expression of each gene in the *iscR* mutant versus the parental wild type. The values shown are the mean from three independent experiments. The genes with $M \geq 1.0$ or $M \leq -1.0$ (expression ratios of ≥ 2.0, $P \leq 0.05$) were considered as the IscR regulon. Negative numbers show up-regulation by IscR.

Table 5. Genes whose expression is down-regulated by IscR[a]

	Product name	Microarray		qRT-PCR	
		Mean Log_2 ratio[b]	*P*-value	Mean Log_2 ratio[b]	*P*-value
Fe-S cluster biogenesis					
VVMO6_02433	Hypothetical protein	2.821	1.48E-07	3.300	1.86E-05
VVMO6_02434	Ferredoxin (Fdx)	3.537	4.17E-07	3.313	3.60E-05
VVMO6_02435	Chaperone protein HscA	3.163	2.27E-07	3.037	1.81E-06
VVMO6_02436	Chaperone protein HscB	3.690	3.74E-07	3.047	3.54E-05
VVMO6_02437	Iron binding protein IscA for iron-sulfur cluster assembly	3.032	6.47E-07	2.963	1.02E-04
VVMO6_02438	Iron-sulfur cluster assembly scaffold protein IscU	3.637	8.81E-09	2.813	6.28E-04
VVMO6_02439	Cysteine desulfurase IscS subfamily	3.413	8.01E-08	3.710	1.08E-06
VVMO6_02440	Iron-sulfur cluster regulator IscR[c]	6.043	2.65E-07	4.310	1.77E-06
Energy production and conversion					
VVMO6_00532	Pyruvate dehydrogenase E1 component	1.209	3.71E-02	1.910	1.29E-03
VVMO6_02539	Pyruvate formate-lyase	1.140	1.05E-05	1.630	3.56E-06
Signal transduction mechanisms					
VVMO6_01249	Diguanylate cyclase	1.249	1.44E-04	1.087	1.49E-05
VVMO6_02521	VpsR family transcriptional regulator	1.441	3.76E-03	1.413	6.29E-05
Membrane protein					

VVMO6_04018	Outer membrane protein A	1.938	7.03E-04	3.683	3.62E-05
Function unknown					
VVMO6_04152	Hypothetical protein	2.846	3.52E-07	3.380	2.23E-05
VVMO6_04436	Hypothetical protein	1.156	5.33E-03	2.710	3.71E-03

[a] Locus tag numbers, functional categories, and annotation of gene products are based on the database of the *V. vulnificus* MO6-24/O genome (Park *et al*., 2011; GenBank accession CP002469 and CP002470). Functional categories in boldface are shown above the first gene in each category.

[b] The M value represents the log2 ratio of mRNA expression of each gene in the *iscR* mutant versus the parental wild type. The values shown are the mean from three independent experiments. The genes with $M \geq 1.0$ or $M \leq -1.0$ (expression ratios of ≥ 2.0, $P \leq 0.05$) were considered as the IscR regulon. Positive numbers show down-regulation by IscR.

[c] The probe (in microarray) and a set of primers (in qRT-PCR) used for the *iscR* gene (VVMO6_02440) expression analysis were designed to hybridize to the *iscR* coding region upstream from the deletion site of the *iscR* mutant.

Figure II-2. IscR-regulated genes possibly involved in pathogenesis of *V. vulnificus*. Twelve genes possibly involved in pathogenesis of *V. vulnificus* were chosen from the pool of the IscR regulon members predicted by microarray analysis. Regulation of their transcription by IscR was confirmed by qRT-PCR. Each column represents the mRNA expression level in the *iscR* mutant relative to that of the parental wild type. Locus tags are based on the database of the *V. vulnificus* MO6-24/O genome sequence, which was retrieved from GenBank (accession numbers CP002469 and CP002470), and the products of the twelve genes are listed on the right. Error bars represent the SEM.

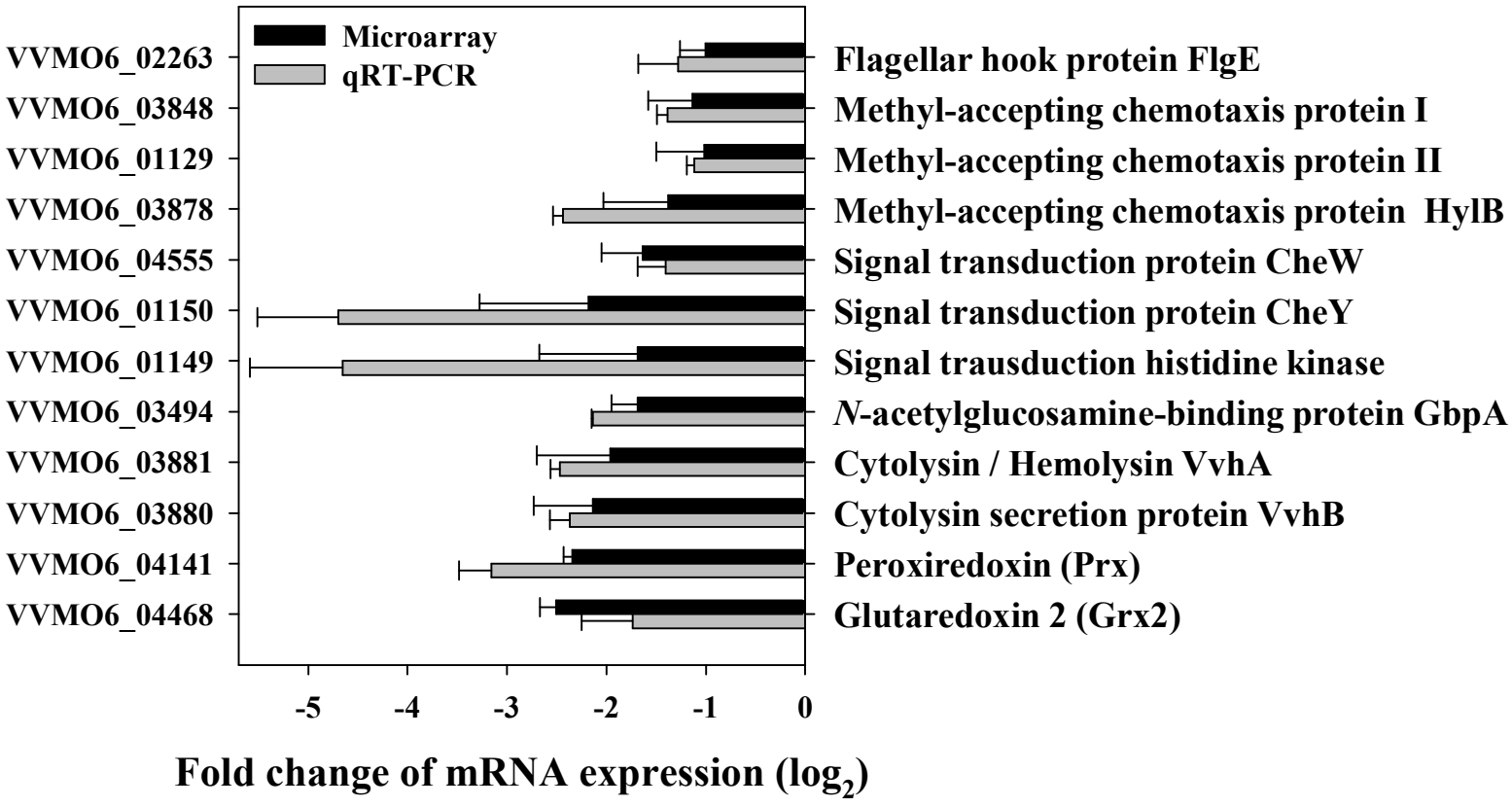
Locus tag
Gene product
Microarray
qRT-PCR
VVMO6_02263
VVMO6_03848
VVMO6_01129
VVMO6_03878
VVMO6_04555
VVMO6_01150
VVMO6_01149
VVMO6_03494
VVMO6_03881
VVMO6_03880
VVMO6_04141
VVMO6_04468
Flagellar hook protein FlgE
Methyl-accepting chemotaxis protein I
Methyl-accepting chemotaxis protein II
Methyl-accepting chemotaxis protein HylB
Signal transduction protein CheW
Signal transduction protein CheY
Signal trausduction histidine kinase
N-acetylglucosamine-binding protein GbpA
Cytolysin / Hemolysin VvhA
Cytolysin secretion protein VvhB
Peroxiredoxin (Prx)
Glutaredoxin 2 (Grx2)
-5
-4
-3
-2
-1
0
Fold change of mRNA expression (log2)

Figure II-3. Verification of IscR binding to the regulatory region of the newly identified IscR regulon. (A) The regulatory regions of VVMO6_02263 (*flgE*), VVMO6_03494 (*gbpA*), VVMO6_03880 (*vvhB*), or VVMO6_04141 (*prx*) and a part of the *iscR* coding region (negative control) were radioactively labeled and then used as probe DNAs. The same locus tag numbers that appear in Fig. II-2 are at the *top* of each *panel*. –, without IscR; +, with IscR; *B*, bound DNA; *F*, free DNA. (B) Comparison of the consensus *E. coli* IscR-binding sequence and the potential *V. vulnificus* IscR-binding sequences. The consensus *E. coli* IscR-binding sequence (type 2, see Ref. Rajahopalan *et al*., 2013) is shown on the *top*. Sequences from the regulatory region of *flgE*, *gbpA*, *vvhB*, and *prx*, retrieved from GenBank (accession numbers CP002469 and CP002470), are aligned *below*. Individual bases identical to those conserved in the consensus *E. coli* IscR-binding sequence are *highlighted*. Numbers of bases that match with those of the consensus *E. coli* IscR-binding sequence are indicated on the *right*. *R*, A or G; *Y*, C or T; *W*, A or T; *N*, any base.

A

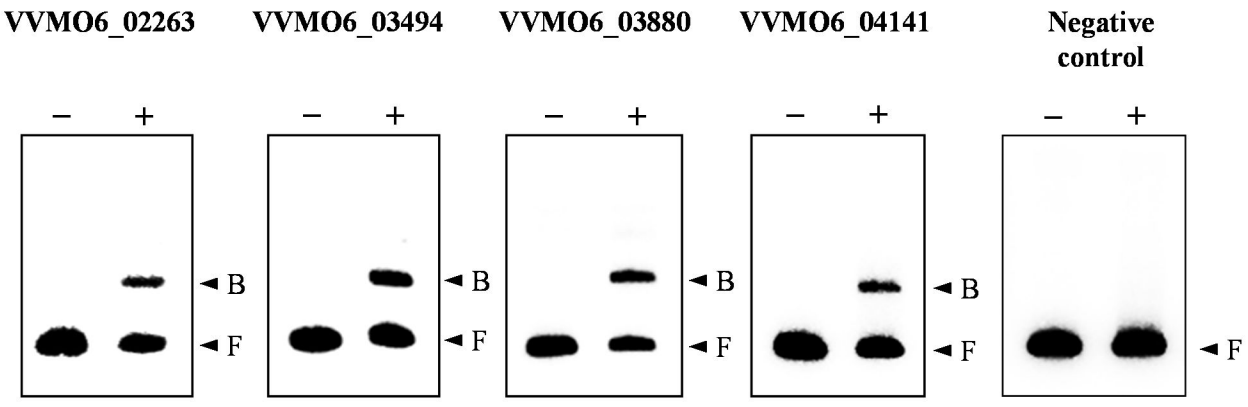

B

IscR-regulated genes	Sequence	Match out of 25-bp
	W W W W C C N Y A N N N N N N N T R N G G W W W W	
flgE	A C A T T C C C T T C A C T G A C A T G G C T T A	20
gbpA	A A T A A C A T G C G T A T G C T G T G G T T G A	22
vvhB	A A T C A C A T A A A A A C A A T A A G A T A A A	22
prx	T T A A C C C C G T T T T T C A T C C G T T T T T	22

II-3-4. Effects of the *iscR* mutation on the virulence-related phenotypes of *V. vulnificus*.

To extend my understanding of the role of IscR in the *V. vulnificus* pathogenesis, the effect of *iscR* mutation on the several phenotypes related to the virulence of many enteropathogenic bacteria were examined. The *iscR* mutant JK093 was less motile, as determined by its ability to migrate on a semisolid plate surface compared with that of the wild type (Fig. II-4A). The diameter of the swimming area of the mutant was significantly reduced (Fig. II-4B). Complementation of the *iscR* mutant by introduction of pJK1016 substantially restored the reduced motility (Fig. II-4). Since motility has been known essential for the adhesion of enteropethogens to host cells (Ottemann and Miller, 1997), INT-407 cells were infected by the *V. vulnificus* strains and the number of bacterial cells adhered to INT-407 cells was compared. The number of the *iscR* mutant adhered to INT-407 cells was about 3-fold lower than that of the wild type and the complemented strain (Fig. II-5A). The wild type and the complemented strain revealed the formation of small clusters of aggregated bacteria on the INT-407 cell surface (Fig. II-5B). In contrast, when infected with the *iscR* mutant, a much smaller area of the INT-407 cell surface was covered with the bacteria, and no clusters of aggregated bacteria were observed (Fig. II-5B). These results indicated that IscR is required for the optimum adhesion to host cells as well as motility of *V. vulnificus*. These findings

were consistent with the previous observation that IscR activates expression of the genes encoding proteins involved in motility, chemotaxis, and adhesion (Fig. II-2).

The effects of *iscR* mutation on hemolytic activity and survival under oxidative stresses were also assessed. When spotted onto the blood agar plates, the wild type and the complemented strain produced light-brown zone of hemolysis whereas the *iscR* mutant dark-brown zone of hemolysis (Fig. II-6A). The result indicated that the hemolytic activity of the *iscR* mutant is lower than that of the wild type and the complemented strain. When the hemolytic activities in the culture supernatant were quantitated, the hemolytic activity of the *iscR* mutant showed about 4-fold lower than that of the wild type and the complemented strain (Fig. II-6B). These results indicated that IscR is required for the hemolytic activity of *V. vulnificus*. The decreased expression of the *vvhBA* encoding cytolysin in the absence of IscR could be a major, if not sole, reason for the lower hemolytic activity of the *iscR* mutant (Fig. II-2).

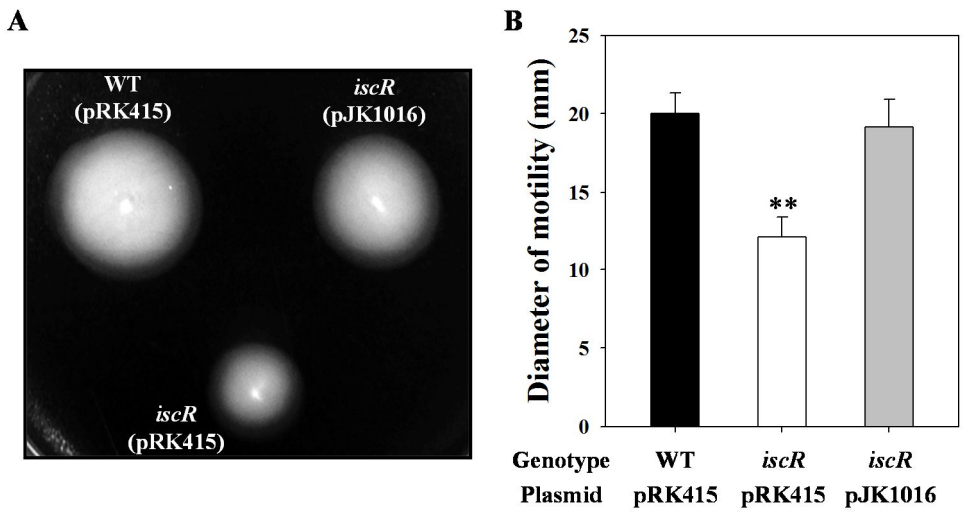

Figure II-4. Motility of the *V. vulnificus* strains. (A) The areas of motility of the strains grown at 30°C for 24 h on plates with LBS and 0.3% agar were photographed. (B) The diameters of motility areas are the means plus SEM of results from three independent experiments. **, $P < 0.005$ relative to the wild type. WT (pRK415), wild type; *iscR* (pRK415), *iscR* mutant; *iscR* (pJK1016), complemented strain.

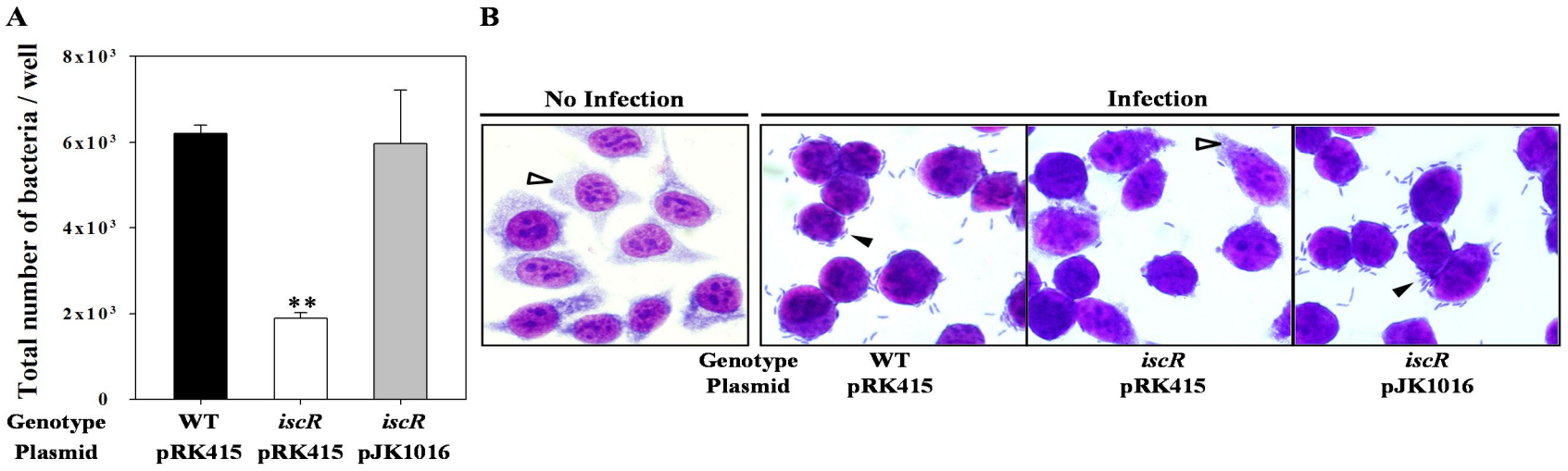

Figure II-5. Adhesion of the *V. vulnificus* strains. (A) INT-407 cells were infected at an MOI of 10 with the *V. vulnificus* strains as indicated. After 30 min, adherent bacteria were enumerated and presented as the number of bacteria per well of the tissue culture dishes. Error bars represent the SEM. **, $P < 0.005$ relative to the wild type. (B) INT-407 cells were infected with the *V. vulnificus* strains at an MOI of 10 for 30 min and morphologically observed using a light microscope after Giemsa staining (original magnification, ×1,200). The adhered *V. vulnificus* cells (closed arrowheads) and the cytoplasm of the INT-407 cells (open arrowheads) are indicated. WT (pRK415), wild type; *iscR* (pRK415), *iscR* mutant; *iscR* (pJK1016), complemented strain.

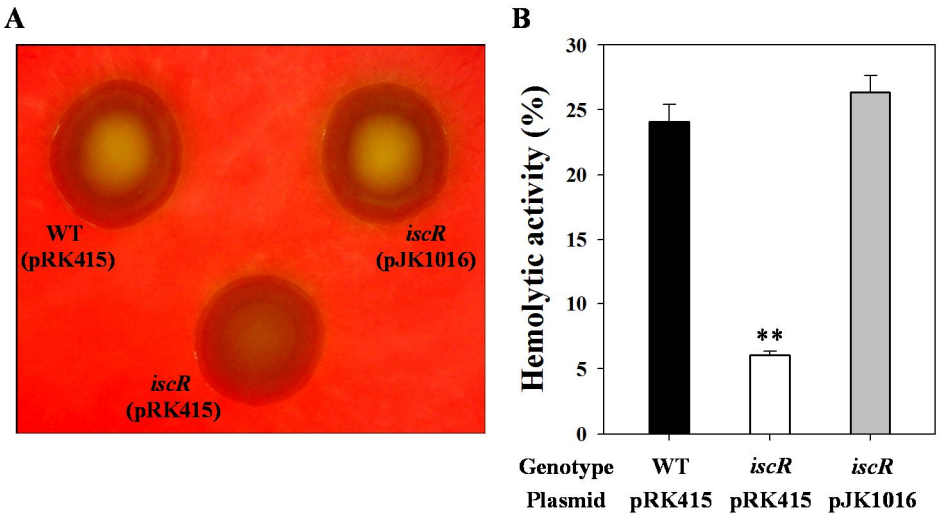

Figure II-6. Hemolytic activities of *V. vulnificus*. (A) The *V. vulnificus* strains were spotted on blood agar (5% sheep blood), then the plates were incubated at 37°C for 24 h. (B) An aliquot of the culture supernatants was mixed with an equal volume of hRBC and then incubated at 37°C for 20 min. The lysis of hRBC was determined and presented using the complete lysis of hRBC by 1% Triton X-100 as 100%. Error bars represent the SEM. **, $P < 0.005$ relative to the wild type. WT (pRK415), wild type; *iscR* (pRK415), *iscR* mutant; *iscR* (pJK1016), complemented strain.

When compared to wild type, the growth of *iscR* mutant was substantially impaired on LBS containing 250 μM H_2O_2 (Fig. II-7B) or 60 μM *t*-BOOH (Fig. II-7C). However, neither defective nor advantageous growth was observed for the strains in LBS without oxidative stresses (Fig. II-7A). These results suggested that the *iscR* mutant is more sensitive to H_2O_2- and *t*-BOOH-induced oxidative stresses than its parental wild type. The decreased growth of the *iscR* mutant under oxidative stresses was partially recovered by the reintroduction of pJK1016 (Fig. II-7B and C). These results indicated that IscR is essential for survival of *V. vulnificus* under oxidative stresses. This susceptibility of the *iscR* mutant to the oxidative stresses could be attributed to the decreased expression of antioxidant Prx and Grx2 (Fig. II-2). Taken together, the results suggested that IscR might contribute to the *V. vulnificus* pathogenesis by indeed regulating the newly identified genes of IscR regulon to assure motility and adhesion to host cells, hemolytic activity, and survival under oxidative stresses during infection.

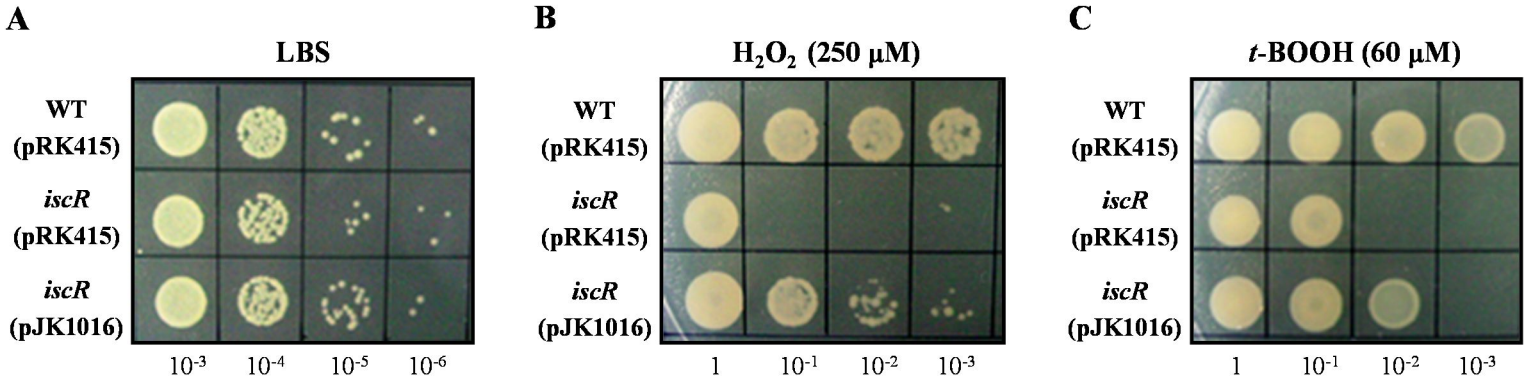

Figure II-7. Survival of *V. vulnificus* under oxidative stress. The *V. vulnificus* strains were compared for their ability to grow on LBS plates supplemented without oxidants (A) or with 250 μM H_2O_2 (B) or 60 μM *t*-BOOH (C). Serial 10-fold dilutions of each culture were spotted on the plates and photographed after 16 h growth. WT (pRK415), wild type; *iscR* (pRK415), *iscR* mutant; *iscR* (pJK1016), complemented strain.

II-3-5. Effects of host cells on IscR expression.

The *iscR* expression in the presence of INT-407 cells was analyzed by qRT-PCR and Western blot analyses (Fig. II-8). The qRT-PCR analyses were performed with RNAs isolated from the wild type *V. vulnificus* cultures exposed to different numbers of INT-407 cells. The results revealed that the *iscR* mRNA increased along with the increase of the numbers of INT-407 cells (Fig. II-8A). The *iscR* expression was almost three-fold greater in the *V. vulnificus* cells exposed to 4×10^6 cells of INT-407 compared to the cells exposed to MEMF alone (control). Cellular level of the IscR protein was also higher in the *V. vulnificus* cells exposed to INT-407 cells (Fig. II-8B). These results suggested that the *iscR* expression of *V. vulnificus* is induced by the host cells.

It has been reported that ROS induces the expression of *E. coli iscR* (Zheng *et al*., 2001; Outten *et al*., 2004; Yeo *et al*., 2006) and the host epithelial cells infected with *V. vulnficus* generates ROS (Chung *et al*., 2010). Therefore, I hypothesized that the induction of *iscR* expression upon exposure to INT-407 cells could result from the increased level of ROS generated from the host cells. To examine this hypothesis, the wild type *V. vulnificus* cultures grown anaerobically were exposed to different levels of H_2O_2. qRT-PCR and Western blot analyses were performed with the RNAs and proteins isolated from the cultures (Fig. II-9). The levels of *iscR*

mRNA and IscR protein were more than 3.5-fold greater in the *V. vulnificus* cells exposed to H_2O_2 compared to the cells unexposed to H_2O_2 (control), indicating that the *iscR* expression was induced when exposed to oxidative stress (Fig. II-9A and B). The combined results suggested that the induction of *iscR* expression by INT-407 cells is possibly mediated by the host-generated oxidative stress. To examine this possibility, the levels of *iscR* expression were determined in the *V. vulnificus* cells exposed to either INT-407 cells or INT-407 cells that were preincubated with NAC to scavenge ROS (Fig. II-10). The results revealed that the increased level of *iscR* expression by the INT-407 cells reduced to the level comparable to that of *iscR* expression observed in the *V. vulnificus* cells exposed to MEMF (control). The results implied that the *iscR* expression induced by the INT-407 cells might be mediated by the oxidative stress imposed by the host cells during infection.

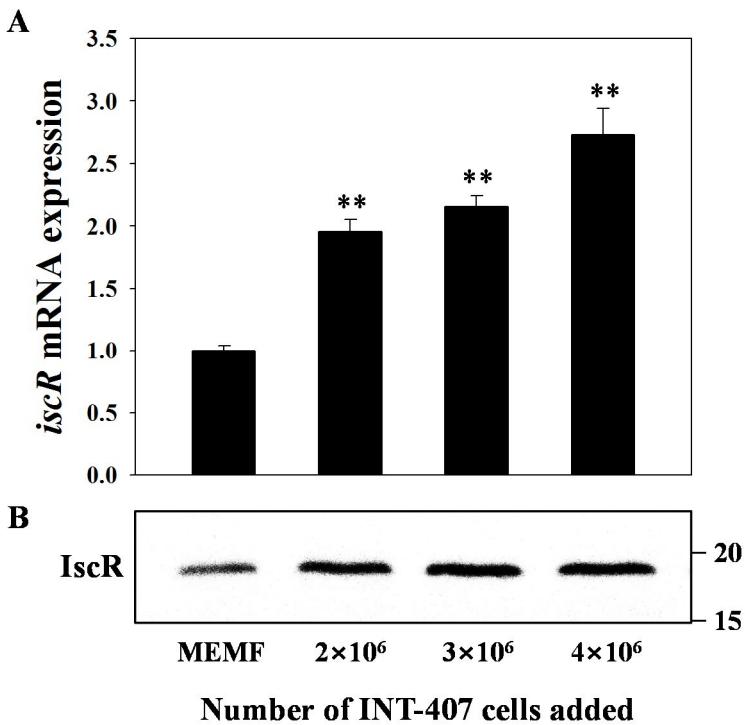

Figure II-8. Induction of *iscR* expression by INT-407 host cells. The wild type *V. vulnificus* was exposed to various numbers of INT-407 cells for 30 min as indicated, and then used to isolate total RNAs and proteins as described in Materials and Methods. (A) The *iscR* mRNA levels were determined by qRT-PCR analyses and the *iscR* mRNA level in the bacteria exposed to MEMF alone (control) was presented as 1. Error bars represent the SEM. **, $P < 0.005$ relative to the bacteria exposed to MEMF alone. (B) Protein samples were resolved by SDS-PAGE, and IscR was detected by Western blot analysis using a rabbit anti-IscR antiserum. The positions of protein size markers (in kDa, Bio-Rad) are shown on the right of the gel.

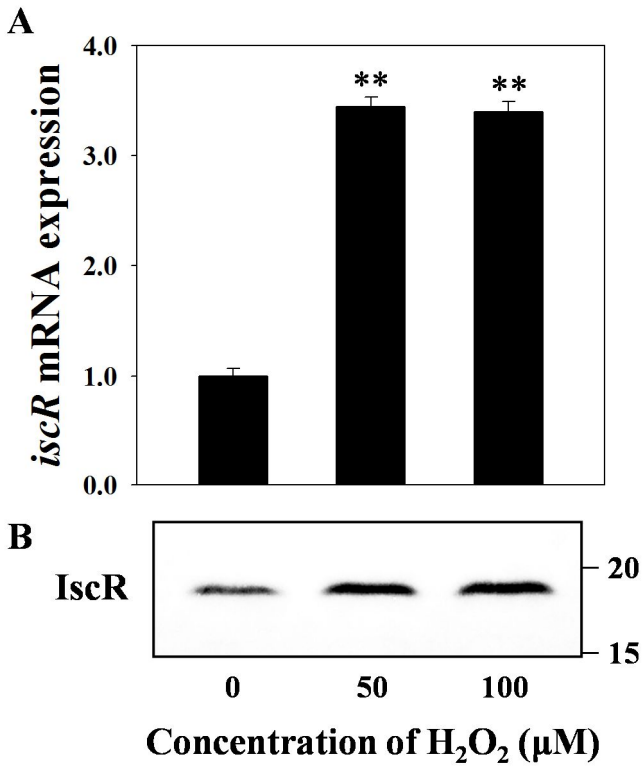

Figure II-9. Induction of *iscR* expression by H_2O_2. Total RNAs and proteins were isolated from the wild type *V. vulnificus*, grown anaerobically to A_{600} 0.5 and then exposed to various levels of H_2O_2 for 10 min as indicated. (A) The *iscR* mRNA levels were determined by qRT-PCR analyses and the *iscR* mRNA level in the bacteria unexposed to H_2O_2 (control) was presented as 1. Error bars represent the SEM. **, $P < 0.005$ relative to the bacteria unexposed to H_2O_2. (B) Protein samples were resolved by SDS-PAGE, and IscR was detected by Western blot analysis and presented as described in the legend to Fig. II-8.

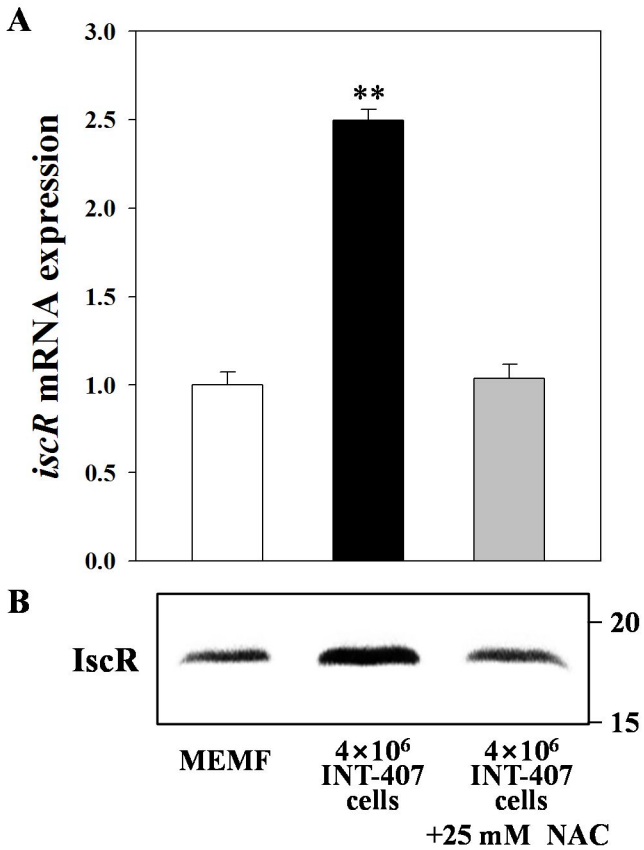

Figure II-10. Effects of scavenging ROS on the host-cell induction of *iscR* expression. (A and B) The wild type *V. vulnificus* grown to A_{600} 0.5 was exposed to MEMF (control), 4×10^6 INT-407 cells, or NAC-preincubated 4×10^6 INT-407 cells for 30 min at an MOI of 30, and then used to isolate total RNAs and proteins as described in Materials and Methods. The *iscR* mRNA and IscR protein levels in *V. vulnificus* cells were determined by qRT-PCR and Western blot analyses, respectively, and presented as described in the legend to Fig. II-8. Error bars represent the SEM. **, $P < 0.005$ relative to the bacteria exposed to MEMF alone.

II-4. Discussion

The *iscRSUA-hscBA-fdx* operon of *E. coli* is well characterized at molecular level (Johnson *et al*., 2005; Py and Barras, 2010). IscS is a cysteine desulfurase that removes the sulfur from cysteine and provides it to build a transient Fe-S cluster on the scaffold protein IscU. IscA, an A type carrier, facilitates the cluster transfer from the scaffold protein to target apoproteins. HscB and HscA interact with IscU to stabilize comformation for transfer of the cluster from IscU to a subset of apoproteins. The ferredoxin (Fdx) protein might be involved in electron transfer. The *V. vulnificus* MO6-24/O genome sequence (GenBank accession numbers CP002469 and CP002470) predicted to possess the *isc* operon (*iscRSUA-hscBA-fdx*; VVMO6_02440-02434; Table 5) as a sole Fe-S biogenesis system. The amino acid sequences of each coding region of the *isc* operon are about 47-85% identical to those of the *E. coli isc* operon (data not shown). All of this information suggested that the products of the *V. vulnificus isc* operon, are indeed involved in Fe-S cluster biogenesis as are the products of the *E. coli isc* operon and suggested that expression of the *V. vulnifius isc* operon is also regulated by IscR (as confirmed by microarray analysis, Table 5).

Iron starvation and oxidative stresses are two conditions that are highly detrimental

for maintaining Fe-S cluster homeostasis (Zheng *et al*., 2001; Outten *et al*., 2004; Yeo *et al*., 2006; Imlay *et al*., 2006; Py *et al*., 2011) and are frequently encountered by most bacterial pathogens upon infection of their host (Wilks and Burkhard, 2007; Miller and Britigan, 1997). Accordingly, Fe-S cluster biogenesis and its regulation are crucial for pathogenesis of *Erwinia chrysanthemi* and *Shigella flexeneri* by allowing adaptation to the hostile host environments (Rincon-Enriquez *et al*., 2008; Runyen-Janecky *et al*., 2008). In this study, mutation of *iscR* appeared to significantly reduce virulence of *V. vulnificus* in mice and in cell culture system, indicating that Fe-S cluster biogenesis is also essential for pathogenesis of the pathogen (Fig. II-1).

Furthermore, this study presented that *V. vulnificus* IscR regulates the twelve genes most-likely involved in pathogenesis in addition to the Fe-S cluster biogenesis (Fig. II-2 and 3, Table 4 and 5). Flagellar hook protein FlgE is required for motility, adhesion to host epithelial cells, and virulence in mice (Lee *et al*., 2004). Chemotaxis signal transduction proteins such as MCPs, CheW, CheY, and histidine kinase (Baker *et al*., 2005) are essential for the pathogenesis of many pathogenic *Vibrio* spp. (O'Toole *et al*., 1996; Kim *et al*., 2003; Butler and Camilli, 2005). GbpA is a homologue of *Vibrio cholerae N*-acetylglucosamine-binding protein A which is an adhesion factor required for initial adherence to intestinal mucin (Kirn

et al., 2005). VvhA, a secreted cytolysin/hemolysin pore-forming toxin, causes intestinal tissue damage and inflammation and promotes dissemination of the *V. vulnificus* to the bloodstream in an intragastric mouse infection (Jeong and Satchell, 2012). VvhB protein is a chaperone-like protein required for synthesis of active VvhA (Senoh *et al*., 2008). A Prx, homologous to human Prx5 (Seo *et al*., 2000), is presumably an antioxidant that protect *V. vulnificus* from oxidative stress during infection. Grx2 is homologous to *E. coli* Grx2 required for the reduction of cytosolic protein disulfides and the survival under oxidative stress (Vlamis-Gardikas *et al*., 2002). Consistent with this, the *iscR* mutant decreased motility and adhesion to host cells (Fig. II-4 and 5), hemolytic activity (Fig. II-6), and survival under oxidative stresses (Fig. II-7).

In addition to these twelve genes, a transcriptome analysis revealed that many genes primarily involved in the transport, metabolism and energy production were also regulated by IscR (Table 4 and 5). When enteropathogens invade host, increased competition for the specific nutrients imposed by the host cells and endogenous bacterial flora are faced and thereby the ability to acquire and metabolize nutrients under these adverse environments is often crucial for the bacteria to survive and multiply in the host (for a recent review, Brown *et al*., 2008). Therefore, it is also possible that mutation of *iscR* might impair the coordinated

expression of the genes involved in metabolism and energy production, leading to the reduced virulence of *V. vulnificus*. It would be not difficult to imagine that *V. vulnificus* adopted IscR, a sensor of the cellular of Fe-S cluster status, to inform that they are in the host by sensing iron bioavailability and/ or ROS levels upon infection. Consistent with this, the expression of IscR was induced upon exposure to host epithelial cells (Fig. II-8) and the induction appeared to be mediated by ROS generated by the host cells during infection (Fig. II-9 and 10).

In summary, my data presented here extended my understanding on the role of IscR in *V. vulnificus* pathogenesis by demonstrating that *iscR* expression is induced by host cells, and, in turn, the induced IscR activates expression of many genes primary required for motility, adhesion, hemolytic activity and survival under oxidative stresses. Although the exact mechanism of IscR in the regulation of these genes needs additional works, the combined results suggest that IscR is a global regulator contributing to the overall success in the pathogenesis of *V. vulnificus*.

Chapter III.

Low cell density regulator AphA upregulates the expression of *Vibrio vulnficus iscR* gene encoding Fe-S cluster regulator IscR

III-1. Introduction

IscR, an Fe-S cluster regulator controls not only the Fe-S cluster biogenesis but also 40 more genes including the genes encoding an another Fe-S cluster biogenesis system and anaerobic respiratory enzymes (Schwartz *et al*., 2001; Giel *et al*., 2006). Moreover, it has been reported that IscR proteins play an essential roles in virulence of the pathogens such as *Erwinia chrysanthemi, Shigella flexeneri*, and *Pseudomonas aeruginosa,* (Rincon-Enriquez *et al*., 2008; Runyen-Janecky *et al*., 2008; Kim *et al*., 2009). Furthermore, I have revealed in chapter II that *V. vulnificus* IscR is induced by host cells and plays an important roles in survival and virulence by upregulating the genes involved in motility and adhesion to host cells, hemolytic activity, and survival under oxidative stress.

AphA is a PadR-family transcription factor that initiates the virulence cascade in *Vibrio cholerae* by activating the transcription of *tcpPH* with the LysR-type regulator AphB, resulting in the production of cholera toxin (CT) and toxin-coregulated pilus (TCP) (Kovacikova and Skorupski, 1999; Kovacikova *et al*., 2004). It is known that AphA is required for the virulence and biofilm formation of *V. cholerae* and *Vibrio parahaemolyticus* (Kovacikova and Skorupski, 2001; Yang *et al*., 2010; Wang *et al*., 2013). In addition, AphA is known as a master regulator

of quorum sensing that operates at low cell density (LCD) in *Vibrio harveyi* and *V. cholerae*. At LCD, Qrr (quorum regulatory RNA) small noncoding RNAs activate production of AphA, and AphA and Qrrs repress production of LuxR (*V. harveyi*) or HapR (*V. cholerae*), the master regulator that operates at high cell density (HCD) (Rutherford *et al*., 2011). Conversely, at HCD, LuxR or HapR represses the production of AphA. This reciprocal regulation enables AphA to be produced abundantly at LCD, in turn, effectively control the expression of its regulon (Kovacikova *et al*., 2004; Kovacikova and Skorupski, 2005; Rutherford *et al*., 2011; van Kessel *et al*., 2013). Therefore, AphA could serve as a link between quorum sensing and virulence gene expression in *Vibrio* species (Matson *et al*., 2007).

In an effort to examine the regulatory characteristics of *iscR*, I observed that *V. vulnificus* AphA upregulates the expression of *iscR* during exponential growth. Then I demonstrated that IscR and AphA control negatively and positively the *iscR* transcription respectively by directly binding to the regulatory region of *iscR*. Mutational analysis revealed that AphA upregulates the *iscR* transcription only in the presence of functional IscR and the result was confirmed by deletion analysis of the *iscR* regulatory region, suggesting that AphA may hinder the negative autoregulation of IscR. Finally, I extended my knowledge about the role of AphA by evaluating the effect of *aphA* mutation on virulence of *V. vulnificus*. It appears

that AphA plays a role in the pathogenesis of *V. vulnificus* possibly by upregulating the expression of IscR, the global virulence regulator.

III-2. Materials and Methods

III-2-1. Bacterial strains, plasmids, and culture conditions.

The strains and plasmids used in this study are listed in Table 1. Unless noted otherwise, the *V. vulnificus* strains were grown in LB medium supplemented with 2.0% (wt/vol) NaCl (LBS) at 30°C.

III-2-2. Generation of *aphA* and *aphA iscR* mutants.

The *aphA* gene was inactivated *in vitro* by deletion of the *aphA* ORF (373-bp of 540-bp) using the PCR-mediated linker-scanning mutation method as described previously (Kim *et al*., 2011). Pairs of primers APHA001F and APHA001R (for amplification of the 5' amplicon) or APHA002F and APHA002R (for amplification of the 3' amplicon) were designed (Table 2). The 373-bp deleted *aphA* was amplified by PCR using the mixture of both amplicons as the template and APHA001F and APHA002R as primers. The resulting 1,730-bp DNA fragment containing the deleted *aphA* was ligated with SpeI-SphI-digested pDM4 (Milton *et al*., 1996) to generate pJK1126 (Table 1). The *E. coli* S17-1 λ *pir, tra* strain (containing pJK1126) (Simon *et al*., 1983) was used as a conjugal donor to *V. vulnificus* MO6-24/O and JK093 to generate the *aphA* mutant JK131 and *aphA iscR* double mutant JK132, respectively, as indicated in Table 1. The conjugation

and isolation of the transconjugants were conducted as previously described (Kim *et al*., 2011).

III-2-3. RNA purification and transcript analyses.

Total cellular RNAs were isolated from the wild type, the *iscR*, *aphA*, and *aphA iscR* double mutants grown in LBS using an RNeasy® Mini Kit (Qiagen, Valencia, CA) (Kim *et al*., 2012). For quantitative real-time PCR (qRT-PCR), cDNA was synthesized using iScript™ cDNA Synthesis Kit (Bio-Rad, Hercules, CA), and real-time PCR amplification of the cDNA was performed by using the Chromo 4 real-time PCR detection system (Bio-Rad) with the specific primer pairs for each gene listed in Table 2. Relative expression levels of the specific transcripts were calculated by using the 16 S rRNA expression level as the internal reference for normalization as described previously (Kim *et al*., 2012).

To determine the transcription start site (TSS) of the *iscR* gene, a primer extension analysis was conducted as descried previously (Park *et al*., 2012). An end-labeled 21-base primer ISCR005R (Table 2) complementary to the coding region of *iscR* was added to the RNA and then extended with SuperScript II RNase H^- reverse transcriptase (Invitrogen, Carlsbad, CA). The cDNA products were purified and resolved on a sequencing gel alongside sequencing ladders generated from

pJK1201 (Table 1) with the same primer used for the primer extension. The primer extension products were visualized using a phosphorimage analyzer (BAS1500, Fuji Photo Film Co. Ltd., Tokyo, Japan).

III-2-4. Overexpression and purification of *V. vulnificus* AphA and IscR.

The coding region of *aphA* was amplified by a PCR using the *V. vulnificus* MO6-24/O chromosomal DNA and primers, APHA003F and APHA003R (Table 2). The 621-bp PCR product was subcloned into a His_6 tag expression vector, pET28a(+) (Novagen, Madison, WI), to result in pJK0903 (Table 1). The His-tagged AphA protein was then expressed in *E. coli* BL21(DE3), and purified by affinity chromatography according to the manufacturer's procedure (Qiagen). Similarly, the expression and purification of the His-tagged IscR were carried out using pJK0928, carrying the *V. vulnificus iscR* gene (Table 1), as described in chapter II.

III-2-5. Electrophoretic mobility shift assay (EMSA) and DNase I protection assay.

For EMSA, the 321-bp *iscR* regulatory region, extending from residues −194 to +127 from the TSS of *iscR*, was amplified by a PCR using ^{32}P-labeled ISCR005F and unlabeled ISCR005R as the primers (Table 2). The labeled 321-bp DNA (5 nM) fragment was incubated with varying concentrations of purified His-tagged IscR

for 30 min at 30°C in a 20-μl reaction mixture containing 1× IscR-binding buffer (Giel *et al*., 2006) and 0.1μg of poly(dI-dC) (Sigma). The protein-DNA binding reactions with AphA were the same as those with IscR, except that the 1× AphA-binding buffer was used (Kovacikova and Skorupski, 2001). Electrophoretic analyses of the DNA-protein complexes were performed as described previously (Kim *et al*., 2011).

The same 321-bp regulatory region was labeled by PCR amplification using a combination of ^{32}P-labeled and unlabeled primers, ISCR005F and ISCR005R, and used for DNase I protection assays. The binding of IscR or AphA to the labeled DNA was performed as described above for the EMSA and DNase I digestion of the DNA-protein complexes followed the procedures previously described (Kim *et al*., 2011). After precipitation with ethanol, the digested DNA products were resolved on a sequencing gel alongside of sequencing ladders of pJK1201 generated using either ISCR005F (for the coding strand) or ISCR005R (for the noncoding strand) as the primer. The gels were visualized as described above for the primer extension analysis.

III-2-6. *E. coli* dual plasmid system.

The coding region of *aphA* was amplified by a PCR using a set of primers

APHA004F and APHA004R (Table 2). The PCR product was subcloned into the pBAD24 vector and under an arabinose-inducible promoter (Guzman *et al*., 1995), to result in pJK1011 (pBAD-*aphA*) (Table 1). A set of *iscR-luxCDABE* transcriptional fusion reporters was created by subcloning a series of DNA fragments that overlapped the *iscR* regulatory region into pBBR-*lux* carrying promoterless *luxCDABE* (Lenz *et al*., 2004). Primer sets ISCR006F and ISCR006R (for pJK1307), ISCR007F and ISCR006R (for pJK1312), and ISCR008F and ISCR006R (for pJK1313) were used in the PCR reactions (Table 1 and 2). The resulting *iscR-luxCDABE* fusion pJK reporters (Table 1; see also Fig. III-6) were confirmed by DNA sequencing. *E. coli* DH5α strains were cotransformed with pBAD24 (control) or pJK1011 and one of the pJK reporters. The cells were grown at 37°C in LB media containing 100 μg/ml (wt/vol) ampicilin, 20 μg/ml (wt/vol) chloramphenicol, and 0.2% (wt/vol) arabinose (Sigma). The luminescence in the exponential-phase cells was measured with an Infinite^{TM} M200 microplate reader (Tecan, Männedorf, Switzerland). The relative luminescence unit (RLU) was calculated by dividing the luminescence by the A_{600}, as described previously (Hwang *et al*., 2013).

III-2-7. Cytotoxicity assay.

Cytotoxicity of the *V. vulnificus* strain was evaluated by measuring the cytoplasmic

lactate dehydrogenase (LDH) activity that is released from the INT-407 (ATCC CCL-6) human intestinal epithelial cells by damage of plasma membranes (Sepp *et al*., 1996). The INT-407 cells were grown in minimum essential medium containing 1% (vol/vol) fetal bovine serum (GIBCO-BRL, Gaithersburg, MD) in 96-well culture dishes (Nunc, Roskilde, Denmark) as described previously (Jeong *et al*., 2009). Each well with 2×10^4 INT-407 cells were infected with the *V. vulnificus* strains at a multiplicities of infection (MOI) of 10 for various incubation times. The LDH activity released to the supernatant was determined using a Cytotoxicity Detection Kit (Roche, Mannheim, Germany), and expressed using the total LDH activity of the cells completely lysed by 1% Triton-X 100 as 100%.

III-2-8. LD_{50} determination.

A group of six 7-week-old ICR female mice (specific pathogen-free, Seoul National University) was injected intraperitoneally with 100-μl serial dilutions of the *V. vulnificus* suspensions as described elsewhere (Jeong *et al*., 2009). Mice were overloaded with iron immediately before injection of bacterial cells. The infected mice were observed for 24 h, and the 50% lethal doses (LD_{50}s) were calculated using a method described by Reed and Muench (1938). All manipulations of mice were approved by the Animal Care and Use Committee at Seoul National University.

III-3. Results

III-3-1. Effects of the cell growth and *aphA* mutation on the *iscR* expression.

In order to examine the effect of the *V. vulnificus* growth on the expression of *iscR*, the levels of *iscR* mRNA in the wild type were determined in exponential or stationary growth phase with qRT-PCR. The level of *iscR* mRNA in exponential-phase cells was more than 20-fold higher when compared to that in the stationary-phase cells (Fig. III-1), suggesting that *V. vulnificus iscR* is primarily expressed during exponential growth. Because it has been reported that AphA is a master quorum sensing regulator operating at low cell density (LCD) in *Vibrio* species (Rutherford *et al*., 2011), I tested whether *V. vulnificus* AphA, a homologue of the LCD regulator AphA, controls the expression of *iscR*. The level of *aphA* mRNA in the wild type, determined by qRT-PCR, was almost 15-fold higher in the exponential-phase cells than in the stationary-phase cells (Fig. III-1), implying that the high level of *iscR* mRNA in the exponential-phase cells correlates with the increased cellular level of AphA. This result suggests that AphA may act as a LCD regulator, as reported in other *Vibrio* species (Rutherford *et al*., 2011; Sun *et al*., 2012), and play a role in the growth phase-dependent variation of *iscR* expression. Consistent with this, the level of *iscR* mRNA in the *aphA* mutant was almost 10-fold less than that in the wild type during exponential growth while no significant

difference was observed between them during stationary growth (Fig. III-1). Therefore, the combined results suggest that *V. vulnificus* AphA upregulates the expression of *iscR* in a growth phase-dependent manner.

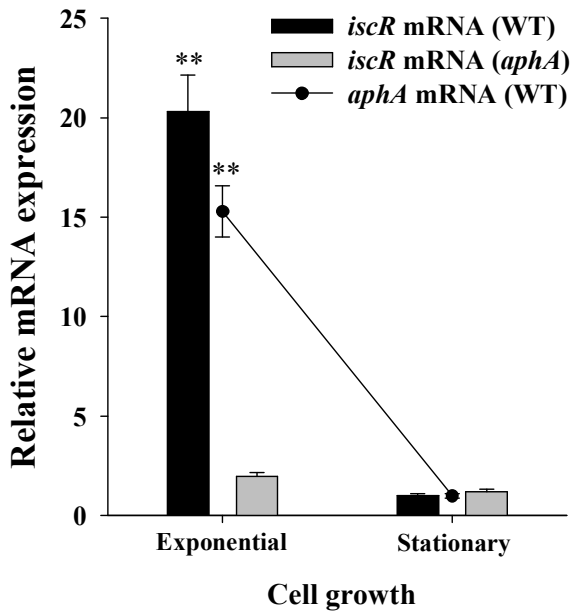

Figure III-1. Growth phase-dependent expression of *iscR* and *aphA*. Cultures of the wild type and *aphA* mutant grown with LBS were harvested at A_{600} of 0.5 (for exponential phase) or 1.5 (for stationary phase) and used to isolate total cellular RNA. The relative mRNA level of *iscR* or *aphA* was determined by qRT-PCR analyses and normalized to the 16 S rRNA expression level. The *iscR* or *aphA* mRNA level of the wild type grown to stationary phase was presented as 1. Error bars represent the SEM. **, $P < 0.005$ relative to the wild type grown to stationary phase. WT, wild type; *aphA*, *aphA* mutant JK131.

III-3-2. Effects of *iscR* or *aphA* mutation on activity of *iscR* promoter.

I have shown that the expression of *V. vulnificus isc*R is negatively autoregulated (Table 5). To confirm the effects of IscR or AphA on the transcription of *iscR*, the activities of the *iscR* promoter were compared for the wild type, the *iscR*, and *aphA* mutants grown to exponential phase by primer extension analyses. A single reverse transcript was identified from the RNAs isolated from the bacterial cells (Fig. III-2A). The 5'-end of the *iscR* transcript, located 28-bp upstream of the translational initiation codon of the *iscR* gene, was subsequently designated +1 and the putative promoter constituting this transcription start site (TSS) was named P_{iscR} (Fig. III-2B). Based on the intensity of the reverse transcripts, the P_{iscR} activity was significantly increased in the *iscR* mutant and decreased in the *aphA* mutant (Fig. III-2A). These results led us to conclude that the activity of P_{iscR} in *V. vulnificus* is under the negative control of IscR and the positive control of AphA. The sequences for the −10 and −35 regions of P_{iscR} were assigned based on similarity to the consensus sequences of the *E. coli* σ^{70} promoter (Fig. III-2B).

Figure III-2. Activities of P_{iscR} in *V. vulnificus* with different genetic backgrounds and sequence analysis of the *iscR* regulatory region. (A) The P_{iscR} activities were determined seperately by primer extension of the RNA derived from the wild type and isogenic mutants as indicated. Each total RNA was prepared from the exponential-phase cells (A_{600} 0.5). *Lanes G, A, T,* and *C* represent the nucleotide sequencing ladders of pJK1201. An *asterisk* indicates the transcription start site (TSS) of P_{iscR}. WT, wild type; *iscR*, *iscR* mutant JK093; *aphA*, *aphA* mutant JK131. (B) TSS of P_{iscR} is indicated by *bent arrow*, and the positions of putative -10 and -35 regions are *underlined*. The IscR- and AphA-binding sequences (ISCRB1, 2, 3, and 4 and APHAB) determined later in this study (from the results of both conding and noncoding strands; Fig. III-4) are represented as *open boxes* and a *gray box*, respectively. The ATG translation initiation codon and the putative ribosome-binding site (ggt) are indicated in *boldface*. The consensus sequences for the binding of IscR from *E. coli* (Rajagopalan *et al*., 2013) and AphA from *V. parahaemolyticus* (Sun *et al*., 2012) are shown above and below the *V. vulnificus* DNA sequence, respectively. *W*, A or T; *Y*, C or T; *R*, A or G; *n*, any base.

A

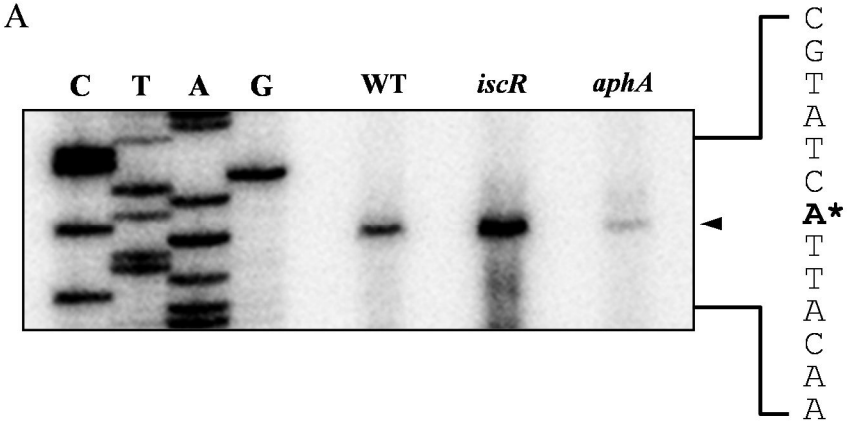

B

ISCRB1 WWWnCCGACnnnnnnnnGTCAAnWWWW

agcattaatgagcaatagtatccctgctattcatagggatgaatacctgactattttagtcaaataa

ATATGCAnnnnnnnTGCATAT

APHAB ISCRB2

WWWnTTGACnnnnnnnnGTCGGnWWW

atacttgaccattttagtcgggtatggaaaaatccgtatcAttacaaacagtgtggatacggtgtga

– 35 ISCRB3 – 10 +1 P_{iscR} ISCRB4

tATGaaactgacatctaaaggaagatatgcg

iscR

III-3-3. IscR and AphA bind specifically to the *iscR* regulatory region.

The 312-bp DNA fragment encompassing the *iscR* regulatory region was incubated with increasing amounts of IscR (Fig. III-3A) or AphA (Fig. III-3B) and then subjected to electrophoresis. As shown in Fig. 3A, the addition of IscR resulted in a concentration-dependent ladder of four retarded bands, indicating that at least two binding sites with different affinities for IscR are present within the *iscR* regulatory region. The binding of IscR was also specific because assays were performed in the presence of 100 ng poly(dI-dC), a nonspecific competitor. In a second EMSA, the same but unlabeled 321-bp DNA fragment was used as a self-competitor to confirm the specific binding of IscR. The unlabeled 321-bp DNA competed for the binding of IscR in a dose-dependent manner (Fig. III-3A, *lanes 6-9*), confirming that IscR binds specifically to the DNA. In similar DNA-binding assays, AphA also showed specific binding to the *iscR* regulatory region (Fig. III-3B). The addition of AphA resulted in a single retarded band, suggesting that a single binding site for AphA is present in the *iscR* regulatory region (Fig. III-3B).

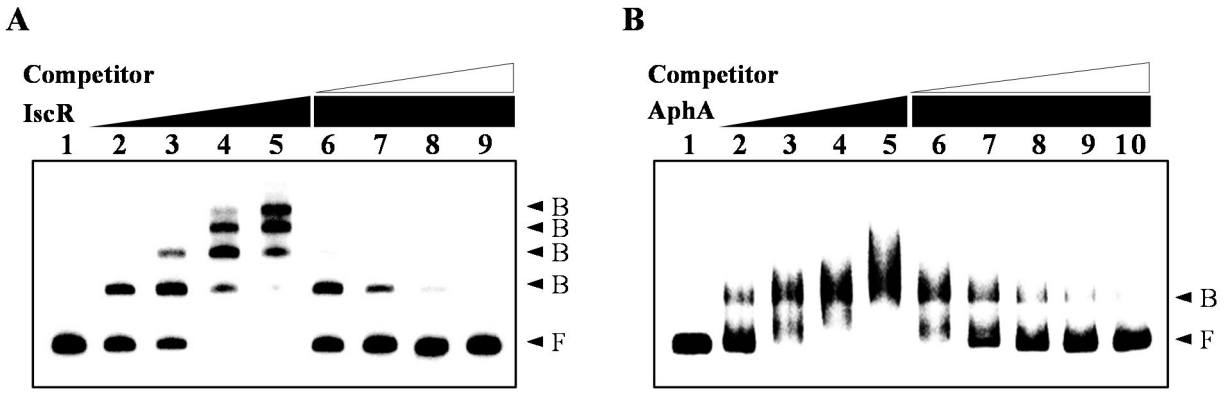

Figure III-3. EMSA for binding of IscR and AphA to the *iscR* regulatory region. A 321-bp DNA fragment of the *iscR* regulatory region was radioactively labeled and then used as a DNA probe. The radiolabeled fragments (5 nM) were mixed with increasing amounts of IscR (A) or AphA (B) and then resolved on a 5% polyacrylamide gel. For *A*, 0, 5, 10, 20, and 30 nM of IscR in the *lanes 1-5*, respectively. For *B*, 0, 20, 40, 60, and 80 nM of AphA in the *lanes 1-5*, respectively. For competition analysis, the same but unlabeled 321-bp DNA fragment was used as a self-competitor DNA. Various amounts of the self-competitor DNA were added to the reaction mixture containing the labled DNA (5 nM) prior to the addition of 30 nM IscR (A) or 80 nM AphA (B). For *A*, 25, 75, 150, and 300 nM of competitor DNA in the *lanes 6-9*, respectively. For *B*, 10, 20, 30, 50, and 100 nM of competitor DNA in the *lanes 6-10*, respectively. *B*, bound DNA; *F*, free DNA.

III-3-4. Identification of binding sites for IscR and AphA using DNase I protection analysis.

To determine the precise location of the IscR- and AphA-binding site in the *iscR* regulatory region, a DNase I protection analysis was performed with the same 321-bp DNA fragment used for the EMSA. When the sequences were mapped with 25 nM IscR, two IscR footprints extended from −95 to −66 and from −7 to +25 relative to the TSS of P_{iscR} (Fig. III-4A and 2B). When increasing the IscR, two additional regions extending from −65 to −41 and from −40 to −12 were protected from DNase I digestion (Fig. III-4A and 2B). This sequential protection with increasing IscR was consistent with the previous observation that at least two binding sites with different affinities for IscR are present in the regulatory region (Fig. III-3A). The regions extending from −95 to −66, from −65 to −41, from −40 to −12, and from −7 to +25 were named as ISCRB1, ISCRB2, ISCRB3, and ISCRB4 to represent the IscR-binding sites 1, 2, 3, and 4, respectively (Fig. III-2B). Because sequences of ISCRB3 overlap with the sequences of −10 and −35 regions of P_{iscR}, and ISCRB4 is located downstream of the −10 region comprising +1 of P_{iscR} (Fig. III-2B), bound IscR would be expected to prevent RNA polymerase (RNAP) binding and movement. This idea supported my earlier observation that IscR negatively regulates the activity of P_{iscR} (Fig. III-2A).

A similar DNase I protection analysis was performed with AphA, and the DNase I footprinting revealed a clear protection pattern in the *iscR* regulatory region extending from −87 to −59 relative to the TSS of P_{iscR} (Fig. III-4B and 2B). This position for AphA binding in the *iscR* regulatory region (APHAB) overlapped with a part of ISCRB1 and ISCRB2 (Fig. III-2B), leading us to hypothesize that AphA upregulates the *iscR* expression by hindering the IscR binding on the *iscR* regulatory region. Taken together, these observations confirm that IscR and AphA control the activity of P_{iscR} directly by binding to the *iscR* regulatory region.

Figure III-4. Identification of binding sites for IscR and AphA. DNase I protection analysis of IscR (A) and AphA (B) binding to the *iscR* regulatory region. The ^{32}P-labeled 321-bp DNA fragments were incubated with increasing amounts of IscR or AphA and then digested with DNase I. (A) *Lanes 1* and *6*, no IscR added; *lanes 2-5*, IscR at 25, 50, 100, and 200 nM, respectively. (B) *Lanes 1* and *6*, no AphA added; *lanes 2-5*, AphA at 200, 400, 600, and 800 nM, respectively. *Lanes G, A, T,* and *C* represent nucleotide sequencing ladders of pJK1201. The regions protected by IscR are indicated by the *open boxes* and the nucleotides showing enhanced cleavage are indicated by *black boxes* (A). The regions protected by AphA are indicated by *gray boxes* (B).

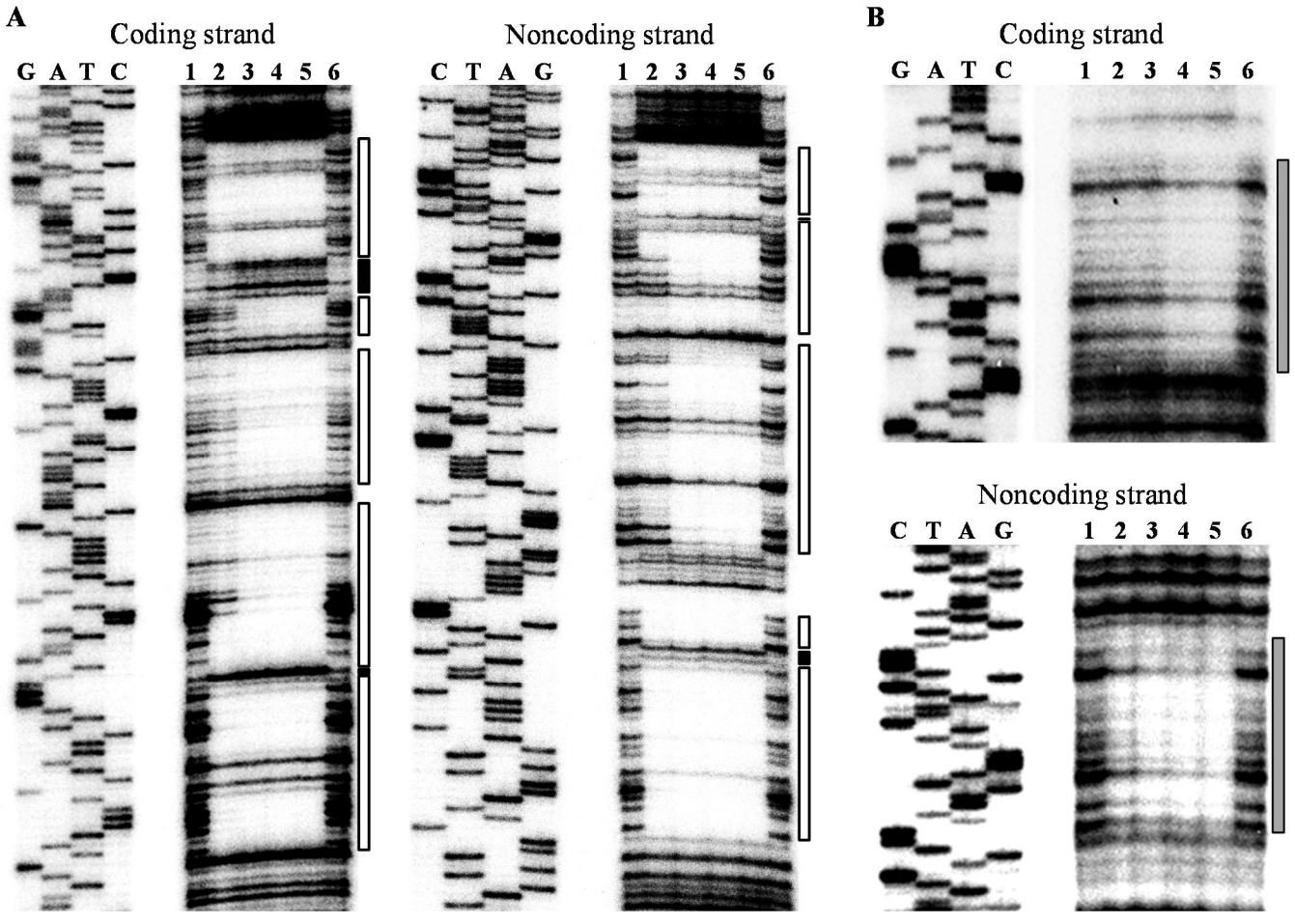
A
Coding strand
G A T C
1 2 3 4 5 6
Noncoding strand
C T A G
1 2 3 4 5 6
B
Coding strand
G A T C
1 2 3 4 5 6
Noncoding strand
C T A G
1 2 3 4 5 6

III-3-5. AphA upregulates the *iscR* expression only in the presence of functional IscR.

I further investigated the role of AphA in *iscR* regulation by comparing the levels of *iscR* mRNA in the exponential-phase cells of the wild type, the *aphA*, *iscR*, and *aphA iscR* double mutants with qRT-PCR analyses (Fig. III-5). To measure the level of *iscR* mRNA in the cells in which the *iscR* gene is disrupted, a set of primers, ISCR_qRTF and ISCR_qRTR, was designed to hybridize to the nucleotides of the *iscR* coding region upstream from the deletion site of the *iscR* mutant (Table 2). The levels of *iscR* mRNA in the *iscR* and *aphA iscR* double mutants did not show any significant difference (Fig. III-5), suggesting that the inactivation of *aphA* did not affect the *iscR* expression in the absence of functional IscR. At the same time, the difference in the *iscR* mRNA level between the *aphA* and *aphA iscR* double mutants was approximately 6-fold higher than that between the wild type and the *iscR* mutant, revealing that IscR more repressed its own expression in the absence of functional AphA than in the presence of AphA (Fig. III-5). The combined results were consistent with my hypothesis that AphA positively regulates *iscR* transcription by hindering IscR-repression on the *iscR* regulatory region (Fig. III-2B and 4).

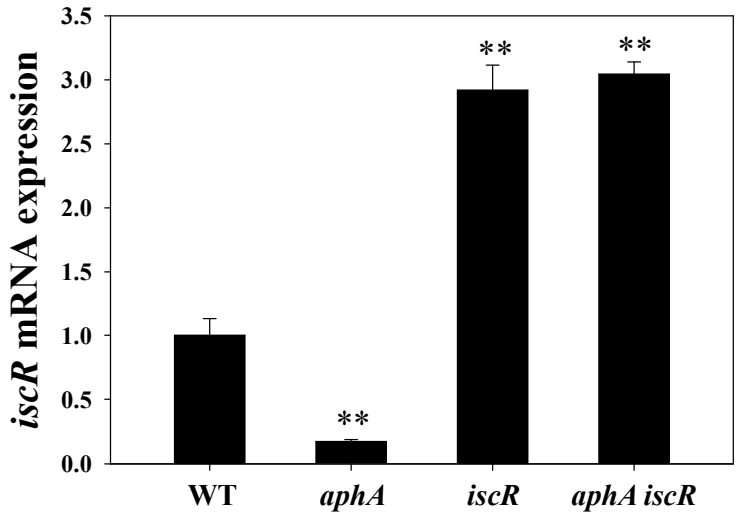

Figure III-5. Expression of *iscR* in *V. vulnificus* with different genetic backgrounds. Cultures of the wild type, the *aphA, iscR,* and *aphA iscR* double mutants grown with LBS were harvested at A_{600} of 0.5 and used to isolate total cellular RNA. The *iscR* mRNA level was determined by qRT-PCR analyses and normalized to the 16 S rRNA expression. The *iscR* mRNA level of the wild type was presented as 1. Error bars represent the SEM. **, $P < 0.005$ relative to the wild type. WT, wild type; *aphA*, *aphA* mutant JK131; *iscR*, *iscR* mutant JK093, *aphA iscR*, *aphA iscR* double mutant JK132.

III-3-6. Examination of the roles of AphA and binding sites in the control of P_{iscR} activity.

A series of *iscR-luxCDABE* transcriptional fusions carrying an intact regulatory region of *iscR* (pJK1307) or the deleted-regulatory regions of *iscR* (pJK1312 and pJK1313) was constructed as shown in Fig. III-6. The activities of P_{iscR} were evaluated by measuring the cellular luminescence of *E. coli* DH5α strains which were cotransformed with combinations of one of the pJK reporters and AphA-expressing plasmid pJK1011 (pBAD-*aphA*) or pBAD24 (control) (Fig. III-6). For pJK1307, the cellular luminescence of the AphA-expressing strain was about 3-fold higher when compared to the control strain (Fig. III-6, *upper* panel), indicating that the activity of P_{iscR} was positively controlled by AphA *in vivo*, consistent with the previous transcript analyses (Fig. III-1 and 2A). When the chromosomal *iscR* gene of *E. coli* was deleted (Yeo *et al*., 2006), the activity of P_{iscR} highly increased and the induction of AphA no longer affected the activity of P_{iscR} (data not shown), suggesting that *E. coli* IscR could repress the activity of P_{iscR} in *V. vulnificus* and the overexpressed-*V. vulnificus* AphA hindered the binding of *E. coli* IscR on P_{iscR}.

When the region of ISCRB1 and APHAB were deleted (pJK1312), there was no

difference in the luminescence between the AphA-expressing and control strains (Fig. III-6, *middle* panel). These results show that AphA and the APHAB region are essential for the upregulation of P_{iscR} activity. When the regulatory region was further deleted to ISCRB2 (pJK1313), the luminescences of both strains were increased to about 3.7×10^5 RLU (Fig. III-6, *lower* panel) corresponding to the luminescence of the strain containing pJK1307 and pBAD-*aphA*. The combined results led us to conclude that bound AphA on the APHAB region would hinder IscR-binding to the ISCRB2 region which is essential for negative autoregulation, resulting in the AphA-mediated upregulation of P_{iscR} activity.

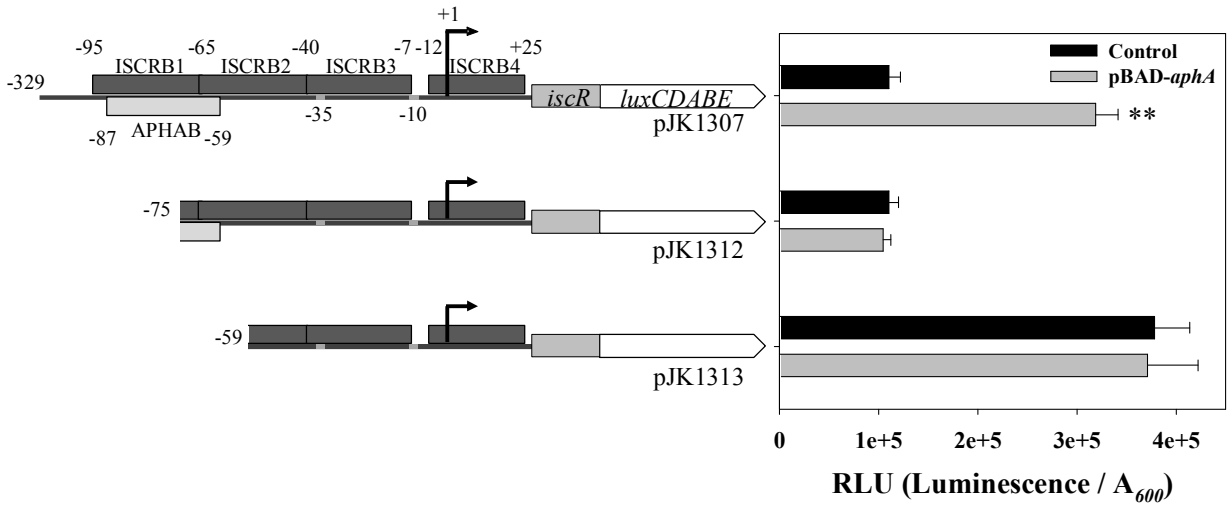

Figure III-6. Deletion analysis of the *iscR* regulatory region. A series of PCR fragments carrying the intact- or deleted-regulatory region of *iscR* was subcloned into pBBR-*lux* to create pJK1307, pJK1312 or pJK1313 (pJK reporters) as shown on the *left*. The proposed -10 and -35 regions and the binding sites for IscR (ISCRB1, 2, 3 and 4) and AphA (APHAB) were indicated as shown in Fig. 2B. Activities of each promoter were determined by using an *E. coli* dual plasmid system assay, as described in Materials and Methods. The relative luminescence unit (RLU) was measured in exponential-phase cells and calculated by dividing the luminescence by the A_{600} of each strain. Error bars represent the SEM. **, $P < 0.005$ relative to the each control vector-containing cell.

III-3-7. AphA is important for virulence.

Since it has been suggested that *V. vulnificus* IscR contributes to cytotoxicity toward the INT-407 cells and virulence in mice (Lim and Choi, manuscript in revision), I tested whether the disruption of *aphA* affects the virulence of *V. vulnificus* toward the INT-407 cells and in mice. To examine the role of AphA in epithelial cell damage, the LDH activities from monolayers of INT-407 cells infected with the wild type and *aphA* mutant JK131 at different MOIs and incubated for 1.5 h were determined (Fig. III-7). The *aphA* mutant exhibited significantly less LDH activity when the MOI was up to 10. The level of LDH activity from the INT-407 cells infected with the *aphA* mutant was almost 2-fold less than that from the cells infected with the wild type. For the complementation of the *aphA* mutant, plasmid pJK0914 was constructed by subcloning the *aphA* amplified by a PCR using the primers APHA005F and APHA005R (Table 2) into the broad host-range vector pJH0311 (Goo *et al*., 2006; Table 1). Complementation of the *aphA* gene in JK131 with a functional *aphA* gene (pJK0914) restored the LDH-releasing activity to levels comparable to that of the wild type (Fig. III-7).

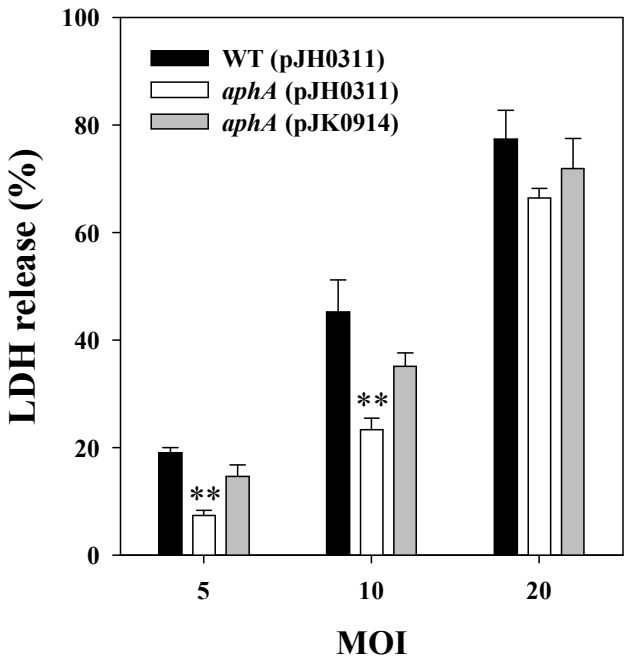

Figure III-7. Cytotoxicity of *V. vulnificus*. INT-407 cells were infected with the *V. vulnificus* strains at various MOI for 1.5 h. The cytotoxicity was determined by an LDH release assay, and expressed using the total LDH released from the cells completely lysed by 1% Triton-X 100 as 100%. Error bars represent the SEM. **, $P < 0.005$ relative to groups infected with the wild type at each MOI. WT (pJH0311), wild type; *aphA* (pJH0311), *aphA* mutant JK131; *aphA* (pJK0914), complemented strain.

In addition, the LD_{50}s in the iron-overloaded mice after intraperitoneal infection with the wild type and *aphA* mutant JK131 were measured. For six iron-treated mice in each inoculation group and with inoculations ranging from 10^0 to 10^8 CFU in 10-fold increments, the intraperitoneal LD_{50} the *aphA* mutant JK131 was 5.6×10^2 CFU, compared with an LD_{50} of an 4.8×10^0 CFU for the wild type. Therefore, for the mouse model of intraperitoneal infection, in which the *aphA* mutant exhibited a >2-log increase in the LD_{50} over that of the isogenic parental strain, the *aphA* mutant appeared to be less virulent than its parental wild type. The combined results clearly revealed that AphA is essential for virulence of *V. vulnificus* in tissue cultures and in mice.

III-4. Discussion

The present study identified *V. vulnificus* AphA, a homologue of the transcriptional regulator AphA in *V. cholerae*, *V. harveyi*, and *V. parahaemolyticus* (De silva *et al*., 2005; Rutherford *et al*., 2011; Sun *et al*., 2012). The amino acid sequence deduced from the *V. vulnificus* AphA protein exhibits a high level of identity (87-92%) with those in other *Vibrio* species (data not shown). Furthermore, *V. vulnificus* AphA contains an N-terminal winged helix DNA binding domain and C-terminal antiparallel coiled coil dimerization domain at positions corresponding to those of *V. cholerae* AphA (De Silva *et al*., 2005). These observations suggest that the properties of AphA as a transcriptional regulator may be highly conserved throughout the *Vibrio* species. AphA in *V. cholerae* initiates the virulence cascade by activating the transcription of *tcpPH* with another transcriptional regulator AphB (Kovacikova *et al*., 2004). However, a search of the genome sequences for *V. vulnificus* CMCP6, YJ016, and MO6-24/O to find any *tcpPH* gene homologues with a substantial level of identity was not successful (data not shown), suggesting that both *V. vulnificus* AphA and AphB may have different roles in gene regulation that contribute to virulence. Consistently, my group has reported that *V. vulnificus* AphB regulates many genes involved in the acquisition and metabolism of nutrients and growth and adaptation in the host (Jeong and Choi, 2008).

I have revealed that the Fe-S cluster regulator IscR play a role in survival and virulence of *V. vulnificus* by regulating the genes involved in motility and adhesion to host cells, hemolytic activity, and survival under oxidative stress (see chapter II). In the present results, AphA upregulates the expression of *iscR* (Fig. III-1) and the disruption of the functional *aphA* gene resulted in the reduced virulence toward the host cells (Fig. III-7) and in mice. Therefore, it is likely that the reduced level of IscR may be a reason, if not the sole reason, for the reduced virulence exhibited by the *aphA* mutant. It is noteworthy that the *iscR* expression is upregulated by AphA in exponential-phase cells, possibly LCD. I speculate that during the initial stage of infection in which the cell density is low, the LCD regulator AphA is highly expressed, leading to the IscR production. The elevated IscR, in turn, facilitates the initiation of *V. vulnificus* pathogenesis by upregulating the genes involved in survival and virulence. In fact, *V. cholerae* AphA is known to play a role in connecting the quorum sensing with virulence by sensing a low cell density and initiating the virulence cascade (Matson *et al*., 2007). Furthermore, IscR upregulated the expression of genes involved in transport, metabolism and energy production (Table 4 and 5). Therefore, it is not difficult to imagine that an increase of cellular IscR in LCD may enable *V. vulnificus* to adapt and multiply under adverse environments by enhancing the ability to acquire and metabolize nutrients.

The mechanism for the negative autoregulation of *iscR* transcription has already been studied extensively in *E. coli* (Schwartz *et al*., 2001; Giel *et al*., 2006; Giel *et al*., 2013). However, the nucleotide sequences of the *iscR* regulatory region in *V. vulnificus* were somewhat different from those in *E. coli* (Giel *et al*., 2006; Giel *et al*., 2013). DNase I protection analysis revealed that there are four IscR-binding sites in the regulatory region of *V. vulnificus iscR* (ISCRB1~ISCRB4 in Fig. III-2B). The ISCRB2 and ISCRB3 regions were completely conserved with the *E. coli* IscR-binding sites A and B, which are critical for negative autoregulation (Fig. III-2B; Giel *et al*., 2013). Consistently, *V. vulnificus* IscR also repressed its own expression by directly binding to the regulatory region of *iscR* (Fig. III-2B and 4A). Meanwhile, the ISCRB1 and ISCRB4 regions have not been previously reported in *E. coli*, although the position of ISCRB4 partially overlapped the *E. coli* IscR-binding site C, which has no effect on the P_{iscR} activity (Giel *et al*., 2013). The roles of ISCRB1 and ISCRB4 regions in the expression of *iscR* require further investigation.

The assigned sequences for APHAB (C<u>TATTCA</u>TAGGGA<u>TGAATA</u>C; *underline*, palindrome; Fig. III-2B) scored 80% similarity to a consensus sequence for AphA binding in *V. parahaemolyticus* (the ATATGCAN_6TGCATAT, see Ref. Sun *et al*.,

2012). This observation confirmed that AphA binds to the *iscR* regulatory region directly (Fig. III-3B and 5B). My results show that AphA positively controls the P_{iscR} activity by hindering the negative autoregulation of *iscR* (Fig. III-2B and 6). However, the APHAB region only overlapped with part of the ISCRB1 and ISCRB2 regions, not with the ISCRB3 and ISCRB4 regions. This implies that IscR could repress the P_{iscR} activity by only binding to the ISCRB3 or ISCRB4 region, even though AphA occupies the APHAB region. The mechanism may enable *V. vulnificus* to maintain the cellular Fe-S cluster homeostasis regardless of cell density.

I further inspected whether *E. coli* or other *Vibrio* species (*V. harveyi*, *V. cholerae*, and *V. parahaemolyticus*) also possess the conserved AphA-binding site at a position corresponding to the *V. vulnificus* APHAB region, but I could not find any putative AphA-binding site in them (data not shown). Consistently, no one has reported the *iscR* gene as an AphA regulon in the previous transcriptome analyses of *V. cholerae* and *V. harveyi* (Kovacikova *et al*., 2005; Rutherford *et al*., 2011; van Kessel *et al*., 2013). Therefore, AphA-mediated control of *iscR* expression is possibly an unusual feature of *V. vulnificus*. Overall, it is possible to suggest that *V. vulnificus* AphA may have been differentially evolved to control virulence gene expression according to the pathogenesis mechanism.

Chapter IV.

Evidence that a *Vibrio vulnificus* peroxiredoxin gene, required for survival under oxidative and nitrosative stress and virulence, is regulated by Fe-S cluster regulator IscR

IV-1. Introduction

Bacteria continually encounter toxic reactive oxygen species (ROS) such as superoxide anion (O_2^-), hydrogen peroxide (H_2O_2), and hydroxyl radical ($^{\bullet}OH$) in their growth environments. Nitric oxide ($NO^{\bullet}$) is also present in the environment, and is produced by bacteria, animals and plants. $NO^{\bullet}$ and its derivatives such as peroxynitrite, peroxynitrous acid, nitrite, nitrogen dioxide, and nitrate are collectively known as reactive nitrogen species (RNS) (Szabó C *et al*. 2007). Oxidative stress and nitrosative stress caused by increased levels of the ROS and RNS can lead to the damage of cellular components including protein, DNA, and membrane lipid. In addition, pathogenic bacteria are inevitably exposed to ROS and RNS that are crucial to host defense for the optimal microcidal activity of neutrophils and other phagocytes (Miller and Britigan, 1997; Fang, 2004). Therefore, pathogens have evolved sophisticated mechanisms to overcome oxidative and nitrosative stress during not only the growth in their environments but also host infection, and the mechanisms are closely linked to their virulence (Janssen *et al*., 2003; Fang, 2004).

Bacterial defense against ROS and RNS consists of evasion, suppression, enzymatic inactivation, scavenging, iron sequestration, stress responses and repair

mechanisms (Fang, 2004). Although the non-enzymatic defense mechanisms contribute to removing toxic ROS and RNS, more efficient and specific detoxification is performed by enzymes. Detoxification of ROS is performed by enzymes such as superoxide dismutase, catalase, and peroxidases (Miller and Britigan, 1997; Fang, 2004). Enzymes that are involved in the RNS detoxification includes microbial haemoglobins, $NO^{\bullet}$ reductase, S-nitrosoglutathione reductase, and peroxynitrite reductase (Fang, 2004). Among these, peroxiredoxins, a family of cysteine-based peroxidases, exhibit high reactivity with H_2O_2, organic hydroperoxide, and peroxynitrite and play a major role in peroxide defense (Poole *et al*., 2011).

Bacteria respond to ROS or RNS by using their redox-sensitive transcription regulators. OxyR and SoxRS of enteric bacteria respond to H_2O_2 an O_2^-, respectively (Christman *et al*., 1985; Greenberg *et al*., 1990) and also to RNS. OxyR undergoes reversible cysteine oxidation whereas SoxR undergoes oxidation of a [2Fe-2S] cluster in response to oxidative and nitrosative stress. Since both ROS and RNS can target thiols or Fe-S clusters, there is considerable overlap between antioxidant and antinitrosative defences (Fang, 2004). In addition NorR and Fur regulatory proteins are known to have a dominant role in response to nitrosative stress (Mukhopadhyay *et al*., 2004). Activation of these regulatory

proteins results in the coordinated expression of genes involved in defense against oxidative or nitrosative stress (Fang, 2004).

In the previous chapter II, a gene encoding a putative peroxiredoxin was identified as IscR regulon (Fig. II-2). The product of this gene was annotated as putative peroxiredoxin, a homologue of human peroxiredoxin 5 (PRDX5). In the present study, this protein was identified as *V. vulnificus* Prx3 and *prx3* mutant was constructed to further examine its role in survival and pathogenesis. In addition IscR-mediated regulatory mechanism of *prx3* was also uncovered. It appears that *V. vulnificus* Prx3 is essential for survival under oxidative and nitrosative stress and virulence in mice and is positively controlled by IscR in a cellular Fe-S cluster-dependent manner.

IV-2. Materials and Methods

IV-2-1. Bacterial strains, plasmids, and culture conditions.

The strains and plasmids used in this study are listed in Table 1. Unless noted otherwise, the *V. vulnificus* strains were grown in LB medium supplemented with 2.0% (wt/vol) NaCl (LBS) at 30°C.

IV-2-2. Generation of *prx3* mutant.

The *prx3* gene was inactivated *in vitro* by deletion of the *prx3* ORF (282-bp of 474-bp) using the PCR-mediated linker-scanning mutation method as described previously (Kim *et al*., 2011). Pairs of primers PRX001F and PRX001R (for amplification of the 5' amplicon) or PRX002F and PRX002R (for amplification of the 3' amplicon) were designed (Table 2). The 282-bp deleted *prx3* was amplified by PCR using the mixture of both amplicons as the template and PRX001F and PRX002R as primers. The resulting 1,195-bp DNA fragment containing the deleted *prx3* was ligated with SpeI-SphI-digested pDM4 (Milton *et al*., 1996) to generate pJK1127 (Table 1). The *E. coli* S17-1 λ *pir, tra* strain (containing pJK1127) (Simon *et al*., 1983) was used as a conjugal donor to *V. vulnificus* MO6-24/O to generate the *prx3* mutant JK134 (Table 1). The conjugation and isolation of the transconjugants were conducted as previously described (Kim *et al*., 2011).

IV-2-3. Site-specific mutagenesis of IscR.

The coding region of *iscR* was amplified by a PCR using a set of primers ISCR009F and ISCR009R (Table 2). The PCR product was subcloned into pGEM-T Easy vector (Promega) to result in pJK0915 (Table 1). Cysteines 92, 98, and 104 of IscR were replaced with alanine (IscR3CA) by use of a QuikChange site-directed mutagenesis kit (Stratagene) (Bang *et al*., 2012). The complementary mutagenic primers listed in Table 2 were used in conjunction with pJK0915 (as a template DNA) to create pJK0929 (Table 1). The mutations were confirmed by DNA sequencing. To substitute the constructed *iscR3CA* (encoding IscR3CA) for the *iscR* allele of *V. vulnificus* chromosome, the coding region of *iscR3CA,* amplified by a PCR using pJK0929 (as a template DNA) and a set of primers ISCR009F and ISCR009R, was subcloned into pDM4 to result in pJK1250 (Table 1). The *E. coli* S17-1 λ *pir, tra* strain (containing pJK1250) was used as a conjugal donor to *V. vulnificus* MO6-24/O. The chromosomal *iscR3CA* mutant confirmed by DNA sequencing was named JK128 (Table 1).

IV-2-4. Growth of *V. vulnificus* under oxidative and nitrosative stress.

Cultures of the *V. vulnificus* strains grown to log phase in LBS containing 0.02% (wt/vol) arabinose (Sigma) were challenged with 250 μM hydrogen peroxide (H_2O_2)

or 250 μM peroxynitrite ($ONOO^-$) (Millipore, Billerica, MA). The cultures were further incubated at 30°C with shaking and their growth was monitored by measuring the absorbance at 600 nm using spectrophotometer at 1 h intervals.

IV-2-5. Mouse mortality test.

Mouse mortalities of the wild type and *prx3* mutant JK134 were compared as described elsewhere (Hwang *et al*., 2013). Groups of (n = 10) 7-week-old ICR female mice (specific pathogen-free, Seoul National University) were starved without food and water for 12 h until infection. Then the mice, without iron-dextran pretreatment, were intragastrically administered with 50 μl of 8.5% (wt/vol) sodium bicarbonate solution, followed immediately with 50 μl of the inoculum, representing approximately 10^9 cells of either the wild type or *iscR* mutant. Mouse mortalities were recorded for 24 hr. All manipulations of mice were approved by the Animal Care and Use Committee at Seoul National University.

IV-2-6. Construction of a *prx3-luxCDABE* transcription fusion and measurement of cellular luminescence.

The regulatory region of *prx3* was amplified by a PCR using a set of primers PRX004F and PRX004R (Table 2) and the PCR product was subcloned into pBBR-*lux* carrying promoterless *luxCDABE* (Lenz *et al*., 2004). The resulting

prx3-luxCDABE fusion pJK0924 reporter (Table 1), as confirmed by DNA sequencing, was then transferred into the *V. vulnificus* wild type or *iscR* mutant JK093 by conjugation as described above. The luminescence in the exponential-phase cells was measured with an Infinite^{TM} M200 microplate reader (Tecan, Männedorf, Switzerland). The relative luminescence unit (RLU) was calculated by dividing the luminescence by the A_{600}, as described previously (Hwang *et al*., 2013). When necessary, the cells were exposed to various concentrations of 2,2'-dipyridyl (Sigma), an intracellular iron chelator, to establish the condition of iron starvation.

IV-2-7. *E. coli* dual plasmid system.

The coding region of *iscR* or *iscR3CA* was amplified from pJK0915 or pJK0929 (Table 1) by a PCR using a set of primers ISCR009F and ISCR009R (Table 2). Each PCR product was subcloned into the pBAD24 vector and under an arabinose-inducible promoter (Guzman *et al*., 1995) to result in pJK0920 (pBAD-*iscR*) and pJK1008 (pBAD-*iscR3CA*) (Table 1). *E. coli* DH5α strains were cotransformed with the pJK0924 reporter and one of either pJK0920 or pJK1008. The cells were grown at 37°C in LB media containing 100 μg/ml (wt/vol) ampicilin, 20 μg/ml (wt/vol) chloramphenicol, and 0.2% (wt/vol) arabinose and the cellular luminescence of the cultures was measured and calculated as describe above.

IV-2-8. RNA purification and analysis of *prx3* transcripts.

Total cellular RNAs were isolated from the wild type, the *iscR*, and *iscR3CA* mutants grown to log phase in LBS using an RNeasy® Mini Kit (Qiagen, Valencia, CA) (Kim *et al*., 2012). For quantitative real-time PCR (qRT-PCR), cDNA was synthesized using iScript™ cDNA Synthesis Kit (Bio-Rad, Hercules, CA), and real-time PCR amplification of the cDNA was performed by using the Chromo 4 real-time PCR detection system (Bio-Rad) with the specific primer pair for *prx3* gene (Table 2). Relative expression levels of the *prx3* transcript were calculated by using the 16 S rRNA expression level as the internal reference for normalization as described previously (Kim *et al*., 2012).

To determine the transcription start site of the *prx3*, a primer extension analysis was conducted as descried previously (Kim *et al*., 2011). An end-labeled 21-base primer PRX005R (Table 2) complementary to the coding region of *prx3* was added to the RNA and then extended with SuperScript II RNase H^- reverse transcriptase (Invitrogen, Carlsbad, CA). The cDNA products were purified and resolved on a sequencing gel alongside sequencing ladders generated from pJK0919 (Table 1) with the same primer used for the primer extension. The primer extension products were visualized using a phosphorimage analyzer (BAS1500, Fuji Photo Film Co.

Ltd., Tokyo, Japan).

IV-2-9. Western blot analysis.

The *V. vulnificus* wild type, the *iscR*, and *iscR3CA* mutants were grown to log phase in LBS and then harvested by centrifugation. The cells were lysed using complete lysis-B buffer (Roche, Mannheim, Germany) for 1 min, and residual cell debris was removed by centrifugation (Kim *et al*., 2012). Protein samples from the cell lysates, equivalent to 10 μg of total protein, were resolved by using SDS-PAGE and immunoblotted using the anti-IscR polyclonal antibodies as described previously (Kim *et al*., 2012).

IV-2-10. Overexpression and purification of *V. vulnificus* IscR3CA.

The coding region of *iscR3CA* was amplified by a PCR using pJK0929 (as a template DNA) and a set of primers ISCR003F and ISCR003R (Table 2). The PCR product was subcloned into a His_6 tag expression vector, pET22b(+) (Novagen, Madison, WI), to result in pJK1001 (Table 1). The His-tagged IscR3CA protein was then expressed in *E. coli* BL21(DE3), and purified by affinity chromatography according to the manufacturer's procedure (Qiagen).

IV-2-11. Electrophoretic mobility shift assay (EMSA) and DNase I protection

assay.

The 309-bp *prx3* regulatory region extending from residues −198 to +111 from the transcription start site of *prx3*, was amplified by a PCR using ^{32}P-labeled PRX005F and unlabeled PRX005R as the primers (Table 2). The labeled 309-bp DNA (5 nM) fragment was incubated with varying concentrations of purified His-tagged IscR3CA for 30 min at 30°C in a 20-μl reaction mixture containing 1× binding buffer (Giel *et al*., 2006) and 0.1μg of poly(dI-dC) (Sigma). Electrophoretic analyses of the DNA-protein complexes were performed as described previously (Kim *et al*., 2012).

The same 309-bp regulatory region was labeled by PCR amplification using a combination of ^{32}P-labeled and unlabeled primers, PRX005F and PRX005R, and used for DNase I protection assays. The binding of IscR3CA to the labeled DNA was performed as described above and DNase I digestion of the DNA-protein complexes followed the procedures previously described (Kim *et al*., 2011). After precipitation with ethanol, the digested DNA products were resolved on a sequencing gel alongside of sequencing ladders of pJK0919 generated using either PRX005F (for the coding strand) or PRX005R (for the noncoding strand) as the primer. The gels were visualized as described above for the primer extension analysis.

IV-3. Results

IV-3-1. Identification of *V. vulnificus prx3* gene.

In the previous transcriptome analysis, a gene encoding a putative peroxiredoxin was identified as IscR regulon (Fig. II-2). This gene and its product were named as *prx3* and Peroxiredoxin 3 (Prx3) respectively, since two peroxiredoxins of *V. vulnificus* (Prx1 and Prx2) were already reported (Bang *et al*., 2012). The amino acid sequence deduced from Prx3 composed of 157 amino acids with a theoretical molecular mass of 16,579 Da and a pI of 4.80. As shown in Fig. IV-1, Prx3 exhibited 52% identity with human peroxiredoxin 5, PRDX5 in amino acid sequence except the mitochondrial-targeting sequence of PRDX5 (Seo *et al*., 2000). Prx3 contained two cysteine residues (C48 and C73) which were conserved in PRDX5. Meanwhile, resolving cysteine of PRDX5 (C151) that is involved in the reduction of oxidized PRDX5 was not observed in Prx3 (Fig. IV-1). Furthermore, three residues (P41, T45, and R124) required for the stabilization of the catalytic site of PRDX5 were completely conserved in Prx3.

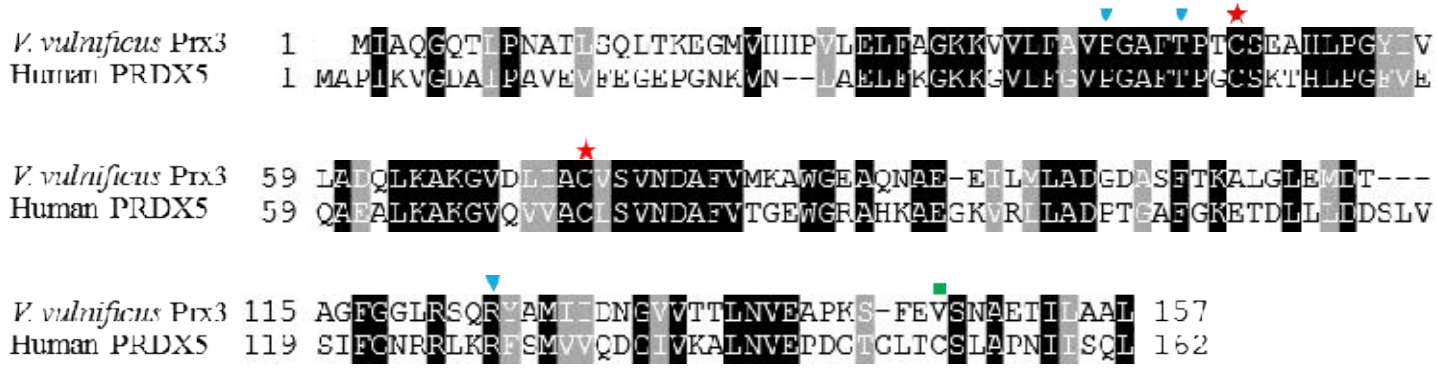

Figure IV-1. Amino acid sequence alignment of *V. vulnificus* Prx3 and human PRDX5. Identical and conservative residues are highlighted in *dark* and *light gray*, respectively. Dashed lines represent missing sequences. The positions of two-conserved cysteines are indicated by *stars*. The position of resolving cysteine of PRDX5 is indicated by a *square*. Residues involved in the stabilization of the catalytic site of PRDX5 are indicated by *inverted triangles* (Knoops *et al*., 2011). The NH_2-terminal mitochondrial targeting sequence of PRDX5 preprotein is not shown. Alignment is based on the amino acid sequences in the GenBank (NCBI) database and derived by the CLUSTALW alignment program. GenBank accession numbers for amino acid sequences are ADV89163 (for Prx3) and NM_012094 (for PRDX5).

IV-3-2. Effect of *prx3* mutation on the growth of *V. vulnificus* under oxidative and nitrosative stress.

Since it is known that peroxiredoxins play a major role in defense against oxidative and nitrosative stress (Poole *et al*., 2011), I compared growth rates of the wild type and *prx3* mutant JK134 under the conditions of H_2O_2-induced oxidative stress and peroxynitrite-induced nitrosative stress. It was obvious that growth of both strains were impaired with a longer exponential phase and lower growth rate when they were cultured with 250 μM H_2O_2 (Fig. IV-2B) or 250 μM peroxynitrite (Fig. IV-2C). In the LBS media without any challenge, the both strains did not show any difference in growth (Fig. IV-2A). However, the growth rate of the *prx3* mutant in the LBS supplemented with 250 μM H_2O_2 or 250 μM peroxynitrite was much lower than that of the wild type (Fig. IV-2B and C). I also compared the growth of both strains in the LBS supplemented with *tert*-butyl hydroperoxide (*t*-BOOH) or paraquat (a superoxide generator), but there were no significant differences in the growth between them (data not shown).

For the complementation of the *prx3* mutant, plasmid pJK1303 was constructed by subcloning the *prx3* amplified by a PCR using the primers PRX003F and PRX003R (Table 2) into the broad host-range vector pJK1113 and under an arabinose-inducible promoter (Table 1). Complementation of the *prx3* gene in

JK134 with a functional *prx3* gene (pJK1303) restored the growth rate to levels comparable to that of the wild type (Fig. IV-2B and C). Therefore, the decreased growth of the *prx3* mutant resulted from the inactivation of functional *prx3* rather than any polar effects on any gene downstream of *prx3*. Combined results suggest that Prx3 is responsible for growth and survival of *V. vulnificus* under oxidative and nitrosative stress which are induced by H_2O_2 and peroxynitrite.

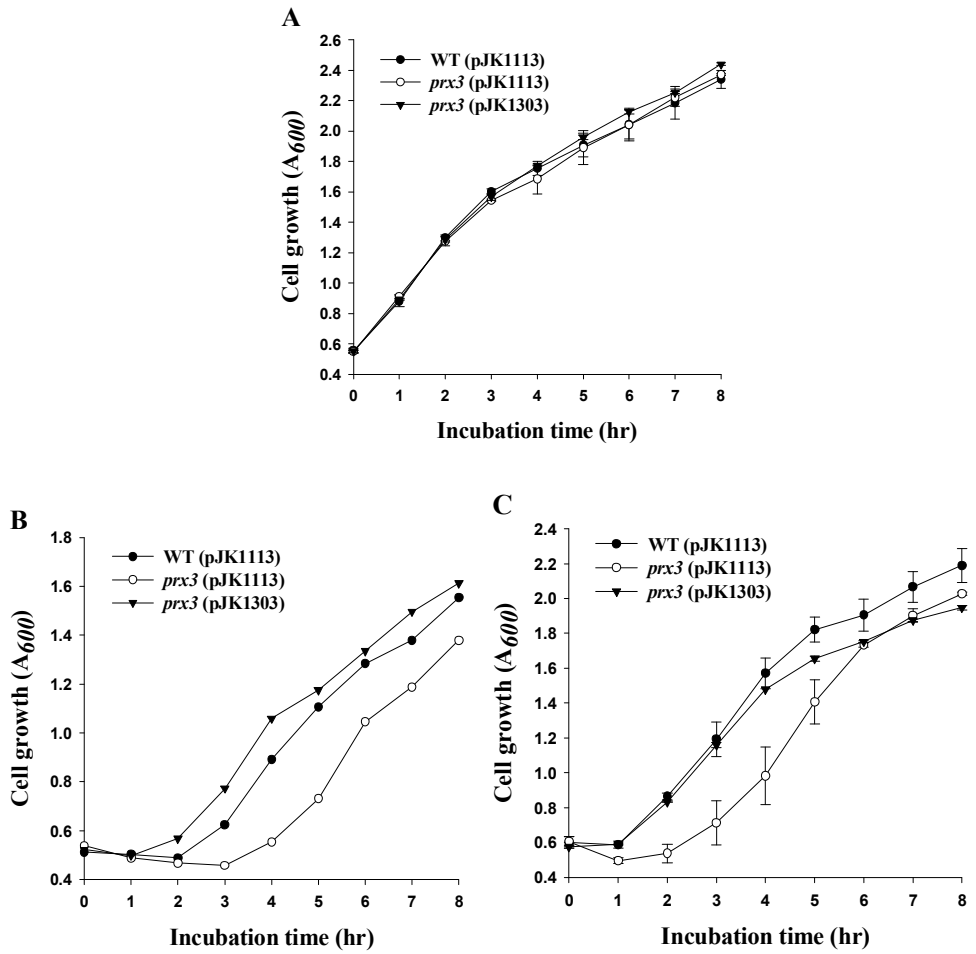

Figure IV-2. Growth of *V. vulnificus* under oxidative and nitrosative stress. The log phase cultures of *V. vulnificus* strains grown in LBS containing 0.02% arabinose were challenged without (A) or with 250 μM hydrogen peroxide (B) or 250 μM peroxynitrite (C), and then cell growth was monitored by measuring the absorbance at 600 nm (A_{600}) at 1 h intervals. WT (pJK1113), wild type; *prx3* (pJK1113), *prx3* mutant; *prx3* (pJK1303), complemented strain.

IV-3-3. Effect of *prx3* mutation on virulence of *V. vulnificus* in mice.

When the pathogen infect their host, they inevitably encounter the phagocyte-derived reactive oxygen species (ROS) and nitrogen species (RNS), leading to oxidative and nitrosative stress (Fang, 2004). In order to examine the effect of the *prx3* mutation on the virulence of *V. vulnificus*, mice were infected intragastrically with the wild type or *prx3* mutant and the numbers of dead mice were counted. As shown in Fig. IV-3, the death of mice infected with the *prx3* mutant was consistently delayed, compared to those of mice infected with the parental wild type. Totally, 60% of mice infected with the wild type were dead, while only 20% for mice infected the *prx3* mutant. This result suggested that Prx3 is essential for the virulence of *V. vulnificus* in mice.

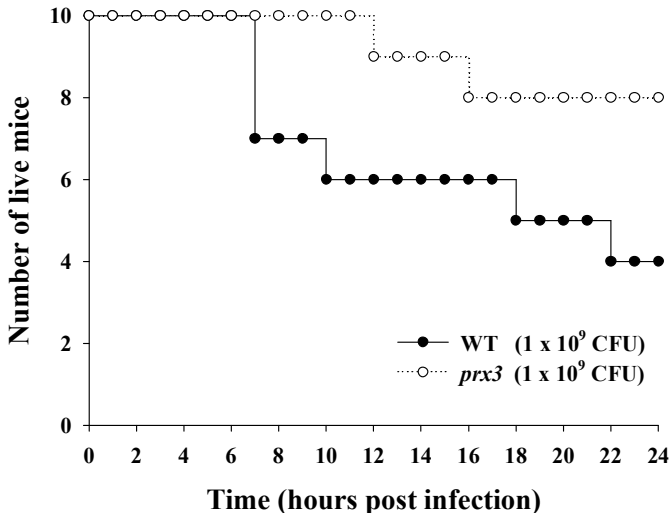

Figure IV-3. Effect of *prx3* mutation on mouse mortality. (A) Seven-week-old specific pathogen-free female ICR mice were intragastrically infected with the wild type (WT) or the *prx3* mutant at doses of 10^9 CFU. Mouse survival was monitored for 24 h.

IV-3-4. Transcription of *prx3* is controlled by IscR and iron.

I have shown that the expression of *prx3* is upregulated by IscR (Fig. II-2). Since IscR contains Fe-S cluster and the status of Fe-S cluster affect its DNA-binding property, the effects of *iscR* mutation and chelation of iron on the *prx3* transcription were evaluated using a *luxCDABE* reporter transcriptionally fused to *prx3* (pJK0924). As shown in Fig. IV-4, the transcription of *prx3-luxCDABE* in the *V. vulnificus* wild type was greater than that in the *iscR* mutant when grown in LBS, consistent with the previous transcript analysis (Fig. II-2). In the wild-type strain, *prx3* expression was increased in a dipyridyl (DP)-dependent manner, indicating iron depletion induces the *prx3* expression (Fig. IV-4). Meanwhile, the prx3 expression in the *iscR* mutant was not altered by the addition of DP, suggesting that the DP-dependent expression of *prx3* in the wild type was through IscR (Fig. IV-4). These results let me to hypothesize that IscR-dependent sensing of the cellular Fe-S cluster status involves the *prx3* transcription and Fe-S cluster of IscR may be dispensable for activation of *prx3* transcription.

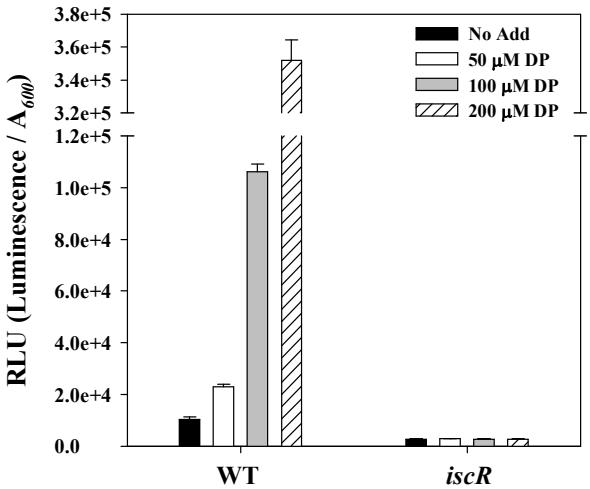

Figure IV-4. Iron- and IscR-dependent expression of *prx3-luxCDABE* transcription fusion. A PCR fragment carrying the upstream region of *prx3* was subcloned into pBBR*lux* to create pJK0924. *V. vulnificus* wild type (WT) and *iscR* mutant carrying pJK0924 were grown in LBS supplemented with chloramphenicol (2 μg/ml) and various concentrations of 2,2'-dipyridyl (DP), an intracellular iron chelator, as indicated. Cultures in the log phase of growth were used to measure the cellular luminescence. The relative luminescence unit (RLU) was calculated by dividing the luminescence by the A_{600} of each strain. Error bars represent the SEM.

IV-3-5. Transcription of *prx3* in the presence of functional IscR or IscR3CA.

The result of *lux* reporter assay (Fig. IV-4) suggested that Fe-S cluster-less IscR (apo-IscR) can activates the *prx3*transcription. To test this hypothesis, three cysteine residues C92, C98, and C104, which are required for the Fe-S cluster ligation of IscR were replaced with alanine (*iscR3CA*). The resulting *iscR3CA* gene encodes IscR3CA, an Fe-S cluster ligation-defective IscR namely, apo-IscR (Giel *et al*., 2013). Using the *E. coli* dual plasmid system assay with the *E. coli* DH5α strain cotransformed with the reporter pJK0924 and one of either IscR-expressing plasmid pJK0920 (pBAD-*iscR*) or IscR3CA-expressing plasmid pJK1008 (pBAD-*iscR3CA*), the effect of IscR or IscR3CA on the *prx3* transcription was determined. When IscR was induced by the addition of 0.2% (wt/vol) arabinose, the level of *prx3* transcription was almost 10-fold incrased (Fig. IV-5, *left* panel). Similarly, induction of IscR3CA resulted in the 20-fold increase in *prx3* transcription (Fig. IV-5, *right* panel). These results revealed that the *prx3* transcription is activated by IscR and IscR3CA, both. In addition, the result showed that the induction of IscR3CA more activates the *prx3* transcription (about 2-fold, Fig. IV-5). It has been reported that IscR represses its own expression only when it contains Fe-S cluster (Schwartz *et al*., 2001). Therefore, the result is possibly due to the difference of total cellular amount of IscR between the IscR- and IscR3CA-overexpressed strains since *V. vulnificus* IscR, induced from pBAD-*iscR*, can read to decrease in *E. coli*

IscR production. It is also possible to consider that IscR3CA protein has higher affinity with the *prx3* promoter than IscR.

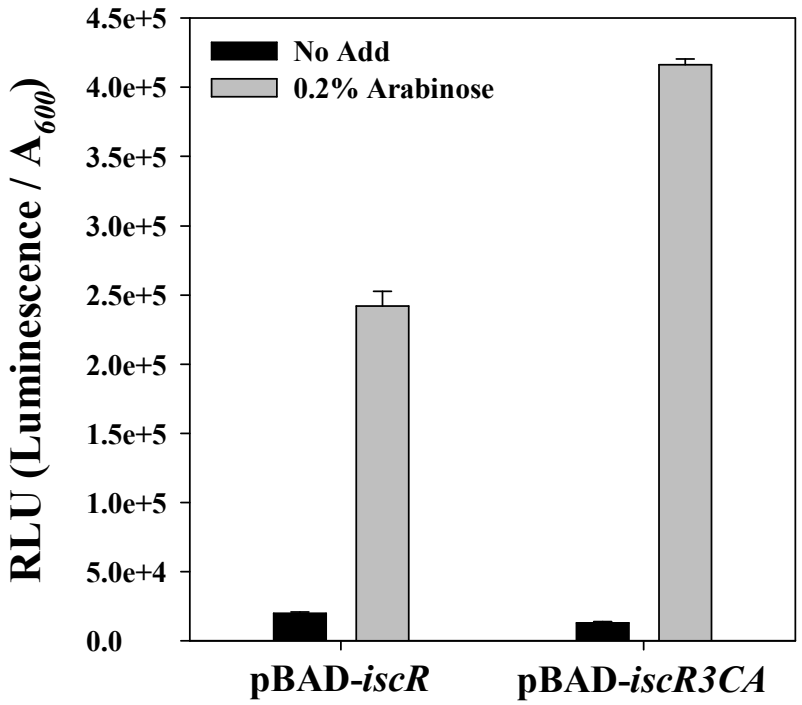

Figure IV-5. Expression of *prx3-luxCDABE* transcription fusion in the presence of IscR or IscR3CA. Expressions of *prx3-luxCDABE* were measured by using an *Escherichia coli* dual plasmid system assay in which cells were cotransformed with pJK0924 (Fig. 4) and pBAD-*iscR* (left panel) or pBAD-*iscR3CA* (encoding Fe-S cluster ligation-defective IscR) (right panel). Cultures were grown in LB supplemented with ampicilin (100 μg/ml) and chloramphenicol (20 μg/ml) at 37°C and 0.2% arabinose was used to induce IscR and IscR3CA. The relative luminescence unit (RLU) was determined as described in Fig. 4. Error bars represent the SEM.

IV-3-6. Effect of *iscR* or *iscR3CA* mutation on the expression of *prx3*.

To further confirm the result of *E. coli* dual plasmid system assay in *V. vulnificus*, the *iscR* allele on the *V. vulnificus* chromosome was substituted with the *iscR3CA* to generate *iscR3CA* mutant JK128 (Table 1). The *prx3* mRNA expression levels in the wild type, the *iscR*, and *iscR3CA* mutants were compared using a qRT-PCR. As shown in Fig. IV-6A, the *prx3* mRNA levels were significantly decreased in the *iscR* mutant and increased in the *iscR3CA* mutant when compared to that in the wild type. In addition, the activities of the *prx3* promoter were also compared using primer extension analysis. A single reverse transcript was identified from the RNAs isolated from the bacterial cells (Fig. IV-6B). The 5'-end of the *prx3* transcript, located 31-bp upstream of the translational initiation codon of the *prx3* gene, was subsequently designated +1 and the putative promoter constituting this transcription start site (TSS) was named P_{prx3} (See Fig. IV-8B). Based on the intensity of the reverse transcripts, P_{prx3} activity was significantly decreased in the *iscR* mutant and increased in the *iscR3CA* mutant when compared to that in the wild type (Fig. IV-6B), consistent with the qRT-PCR analysis (Fig. IV-6A). Combined results demonstrate that both IscR and IscR3CA activate the transcription of *prx3*. Furthermore, the levels of IscR or IscR3CA protein in the *V. vulnificus* strains were measured using a Western blot analysis. As expected, the level IscR3CA protein level in the *iscR3CA* mutant was clearly higher than the

level of IscR protein in the wild type (Fig. IV-6C). Therefore, it is possible to conclude that the increased *prx3* transcription in the *iscR3CA* mutant was resulted from the increase of the total cellular level of IscR.

Figure IV-6. Effect of *iscR* or *iscR3CA* mutation on the expression of *prx3*. Cultures of the *V. vulnificus* wild type (WT), *iscR* mutant, and *iscR3CA* mutant (a chromosomal mutant defective in Fe-S cluster ligation) were grown in LBS, and samples removed at A_{600} of 0.5 were used to isolate total cellular RNAs (A and B) or proteins (C). (A) The *prx3* mRNA levels were determined by qRT-PCR analyses and normalized to the 16 S rRNA expression. The *prx3* mRNA level of the wild type was presented as 1. Error bars represent the SEM. (B) The P_{prx3} activities were determined seperately by primer extension analyses. *Lanes G, A, T,* and *C* represent the nucleotide sequencing ladders of pJK0919 (pGEM-T Easy with the upstream region of *prx3*). An asterisk indicates the transcription start site of P_{prx3}. (C) Protein samples were resolved by SDS-PAGE, and the levels of IscR or IscR3CA were detected by Western blot analyses using a rabbit anti-IscR antiserum. The positions of protein size markers (in kDa, Bio-Rad) are shown on the right of the gel.

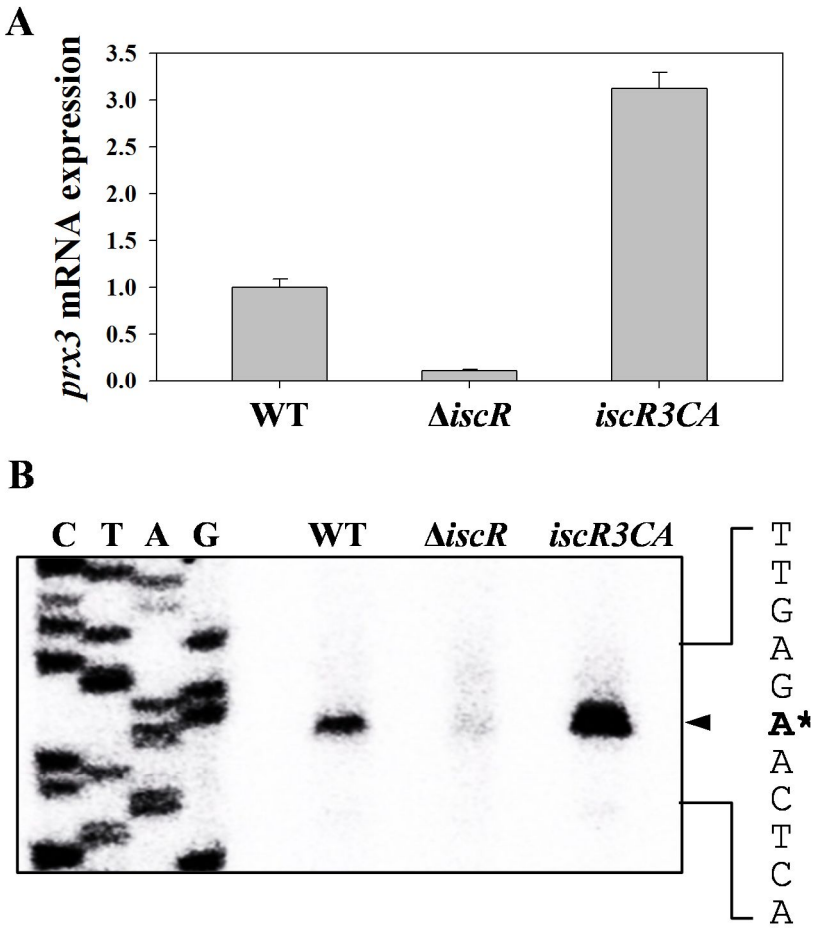
A
prx3 mRNA expression
3.5
3.0
2.5
2.0
1.5
1.0
0.5
0.0
WT
ΔiscR
iscR3CA
B
C T A G
WT
ΔiscR
iscR3CA
T
T
G
A
G
A*
A
C
T
C
A
C
WT
ΔiscR
iscR3CA
IscR or
IscR3CA
20
15

IV-3-7. IscR3CA binds specifically to the *prx3* regulatory region.

The 309-bp DNA fragment encompassing the *prx3* regulatory region was incubated with increasing amounts of IscR3CA (Fig. IV-7) and then subjected to electrophoresis. As shown in Fig. 7, the addition of IscR3CA at 5 nM resulted in a shift of the 309-bp DNA fragment with to a single band a slower mobility. The binding of IscR3CA was also specific, because assays were performed in the presence of 100 ng poly(dI-dC) as a nonspecific competitor. In a second EMSA, the same but unlabeled 309-bp DNA fragment was used as a self-competitor to confirm the specific binding of IscR. The unlabeled 309-bp DNA competed for the binding of IscR in a dose-dependent manner (Fig. IV-7, *lanes 6-9*), confirming that IscR3CA binds specifically to the *prx3* regulatory region.

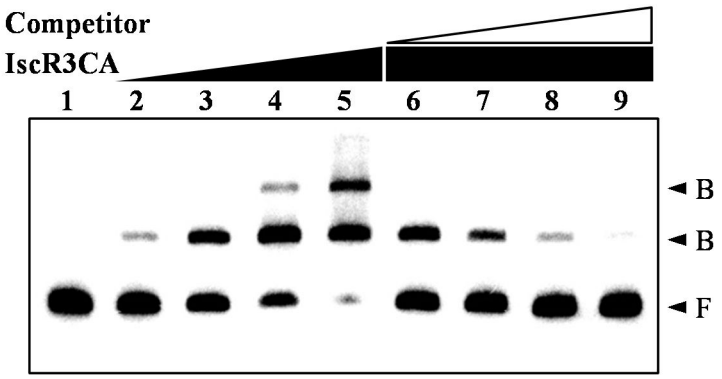

Figure IV-7. EMSA for binding of IscR3CA to the *prx3* regulatory region. A 309-bp DNA fragment of the upstream region of *prx3* was radioactively labeled and then used to as a DNA probe. The radiolabeled fragments (5 nM) were mixed with increasing amounts of IscR3CA (0, 5, 10, 20, and 30 nM in the *lanes 1-5*, respectively) and then resolved on a 5% polyacrylamide gel. For competition analysis, the same but unlabeled 309-bp DNA fragment was used as a self-competitor DNA. The labeled DNA probe was incubated with the self-competitor DNA (at 25, 75, 150, 300 nM, from *lanes 6* to *9*, respectively) prior to the addition of 30 nM IscR3CA. *B*, bound DNA; *F*, free DNA.

IV-3-8. Identification of the IscR3CA binding site using DNase I protection analysis.

To determine the precise location of the IscR3CA-binding site in the *prx3* regulatory region, a DNase I protection analysis was performed using the same 309-bp DNA fragment used for the EMSA. DNase I footprinting revealed a clear protection pattern in the upstream region of *prx3* between -59 and -29 (Fig. IV-8A). This IscR3CA binding site is centered 44 bp upstream of the TSS of P_{prx3}. The sequences for IscR3CA binding overlap with the -35 region (Fig. IV-8B), indicating IscR3CA bound to the binding site could recruit RNA polymerase to the promoter by interacting with domain 4 of the RNA polymerase σ subunit (Browning and Busby, 2004). This idea supported the earlier observation that IscR activates the transcription of *prx3* (Fig. IV-6A and B). Taken together, these results demonstrate that IscR3CA activates the *prx3* expression by directly binding to P_{prx3}.

Figure IV-8. Identification of IscR3CA binding site and sequence analysis of the *prx3* regulatory region. (A) The ^{32}P-labeled 309-bp DNA fragments were incubated with increaseing amounts of IscR3CA and then digested with DNase I. *Lanes 1* and *5*, no IscR added; *lanes 2-4*, IscR3CA at 50, 100, and 200 nM, respectively. *Lanes G, A, T,* and *C* represent nucleotide sequencing ladders of pJK0919. The regions protected by IscR3CA are indicated by the *open boxes* and the nucleotides showing enhanced cleavage are indicated by *black boxes*. (B) TSS of P_{prx3} is indicated by *bent arrow*, and the positions of putative -10 and -35 regions are *underlined*. The sequences proposed for the binding site of IscR are shown in a *shaded box*. The ATG translation initiation codon and the putative ribosome-binding site (AAGGA) are indicated in *boldface*. The type 2 IscR-binding consensus sequences from *E. coli* (Rajagopalan *et al*., 2013) are shown above the *V. vulnificus* DNA sequence in *capital letters*. *W*, A or T; *Y*, C or T; *R*, A or G; *N*, any base.

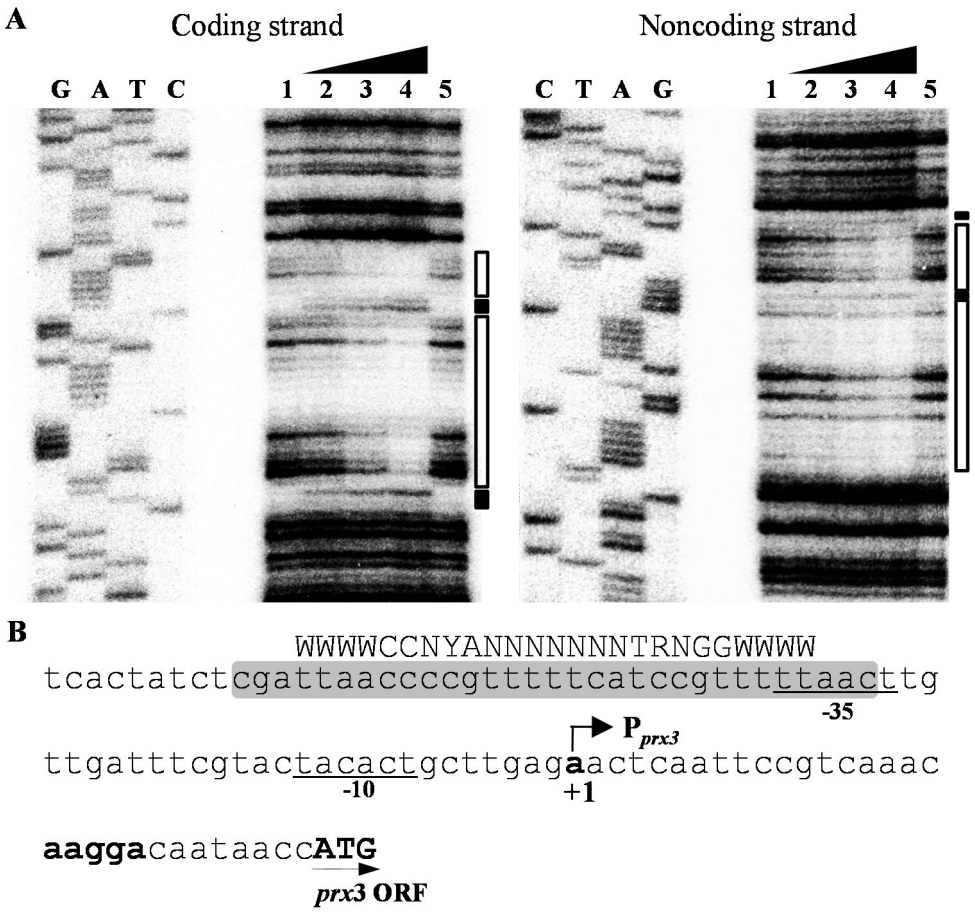
A
Coding strand
Noncoding strand
G A T C
1 2 3 4 5
C T A G
1 2 3 4 5
B
WWWWCCNYANNNNNNNTRNGGWWWW
tcactatctcgattaaccccgttttcatccgtttttaacttg
-35
P prx3
ttgatttcgtactacactgcttgagaactcaattccgtcaaac
-10
+1
aaggacaataaccATG
prx3 ORF

IV-4. Discussion

The present study showed that *V. vulnificus* Prx3 is two cysteine-containing peroxiredoxin and has a high level of identitiy with human PRDX5. As shown in Fig. IV-1, the peroxidatic cysteine of PRDX5 (C47) that is required for the peroxidase activity is conserved in *V. vulnificus* Prx3 (C48). C72 of PRDX5 is also conserved in Prx3 (C73) but its role in peroxidase reaction is insignificant (Seo *et al*., 2000). Rather, C73 of Prx3 is assumed to involve in its reduction step because resolving cysteine of PRDX5 (C151) is not observed in Prx3. Therefore, it is likely that *V. vulnificus prx3* may have somewhat different resolving system when compared to PRDX5, which forms an intramolecular disulfide as a reaction intermediate (Seo *et al*., 2000; Marlene *et al*., 2004). The exact catalytic and resolving mechanisms of Prx3 need additional work. PRDX5 is known to catalyze the reduction of H_2O_2 and peroxynitrite (Seo *et al*., 2000; Marlene *et al*., 2004). Consistently, present results revealed that *V. vulnificus* Prx3, a homologue of PRDX5, is essential for survival under H_2O_2-induced oxidative stress and peroxynitrite-induced nitrosative stress (Fig. IV-2). Meanwhile, the *prx3* mutant did not show any defect in survival against *t*-BOOH, an organic hydroperoxide or paraquat, a superoxide anion (data not shown), indicating Prx3 has higher reactivity to H_2O_2 and peroxynitrite.

The assigned sequences for the IscR3CA binding on the *prx3* promoter (TTAACCCCGTTTTTCATCCGTTTTT; Fig. IV-8B) scored 92% similar to a type 2 consensus sequence for IscR binding in *E. coli* (the WWWWCCNYAN$_7$TRNGGWWWW, see Ref. Rajagopalan *et al*., 2013). This implies that apo-IscR can bind to the promoter region since Fe-S cluster is dispensable when IscR binds to the type 2 IscR-binding site. At the same time, this observation reinforces that apo-IscR also activates the *prx3* expression (Fig. IV-5 and 6). The position of IscR binding site (centered at -44) overlapped with the -35 region of *prx3* promoter (Fig. IV-8B), suggesting IscR3CA bound to the binding site could recruit RNA polymerase to the promoter. This result is similar with the previous report in *E. coli*, in which *E. coli* IscR-binding sites on the *sufA* and *ydiU* promoter also overlap with the -35 region (Giel *et al*., 2006).

Pathogen is subject to face oxidative and nitrosative bursts upon infection of host cells, and induces a strong inflammatory response of the host cells, leading to generation of ROS and RNS (Battistoni *et al*., 2000; Janssen *et al*., 2003; Fang, 2004). Not only phagocytes but also endothelial cells and epithelial cells generate ROS and contribute to microbicidal activity (Battistoni *et al*., 2000; Kinnula *et al*., 1992). It is well known that infection with *V. vulnificus* induces ROS generation via

NADPH oxidase (Nox) in host cells (Chung *et al*., 2010) and iNOS expression that results in massive $NO^{\bullet}$ production (Kang *et al*., 2002). ROS and RNS are highly detrimental to maintain cellular Fe-S cluster (Fang, 2004). Therefore, it is reasonable to assume that *V. vulnificus* IscR is highly induced during infection of a host. Indeed, it was verified that expression of IscR increased significantly upon exposure to ROS generated by *V. vulnificus*-infected host epithelial cells (Fig. II-9). In turn, increased IscR may highly activate the expression of Prx3, which plays a role in defense against oxidative and nitrosative stress. Consistently, *V. vulnificus* Prx3 is important for the virulence in mice (Fig. IV-3). This novel regulatory mechanism may enable *V. vulnificus* to develop successful disease.

Chapter V. Conclusion

Vibrio vulnificus is a model pathogen for studying many other foodborne pathogens because it causes life-threatening septicemia and gastroenteritis with a case-fatality rate exceeding 50%. In an effort to screen for *V. vulnificus* virulence factors, an Fe-S cluster regulator was identified and the possible roles of the IscR protein during infection of *V. vulnificus* were explored. As a result, it was discovered that IscR is essential for the virulence of *V. vulnificus* in mice and in tissue culture. A transcriptome analysis newly identified several genes involved in motility and adhesion to host cells, hemolytic activity, and survival under oxidative stress as IscR regulon. Furthermore, IscR expression was found to be induced by exposure of the pathogen to host cells. Therefore, the results indicated that IscR is a global regulator and plays an essential role in bacterial pathogenesis, by being induced during infection. In an effort to examine the regulatory characteristics of *iscR*, I showed that IscR and AphA control negatively and positively the *iscR* transcription respectively by directly binding to the regulatory region of *iscR*. Mutational analysis revealed that AphA upregulates the *iscR* transcription only in the presence of functional IscR. The result was confirmed by a deletion analysis of the *iscR* promoter, suggesting that AphA may hinder the negative autoregulation of IscR. I extended my knowledge about the role of AphA by evaluating the effect of *aphA* mutation on virulence of *V. vulnificus*. It appeared that AphA plays a role in the pathogenesis of *V. vulnificus* possibly by upregulating the expression of IscR, the

global virulence regulator. Furthermore, functions and regulatory characteristics of *V. vulnificus prx3* which encodes a peroxiredoxin were examined. It appeared that *V. vulnificus* Prx3 is essential for survival under oxidative and nitrosative stress and virulence in mice and is positively controlled by IscR in a cellular Fe-S cluster-dependent manner. Taken together, it is possible to suggest a model for the regulation of virulence-related genes in *V. vulnificus* via IscR (Fig. V-1), and this novel mechanism may enable *V. vulnificus* to achieve successful pathogenesis.

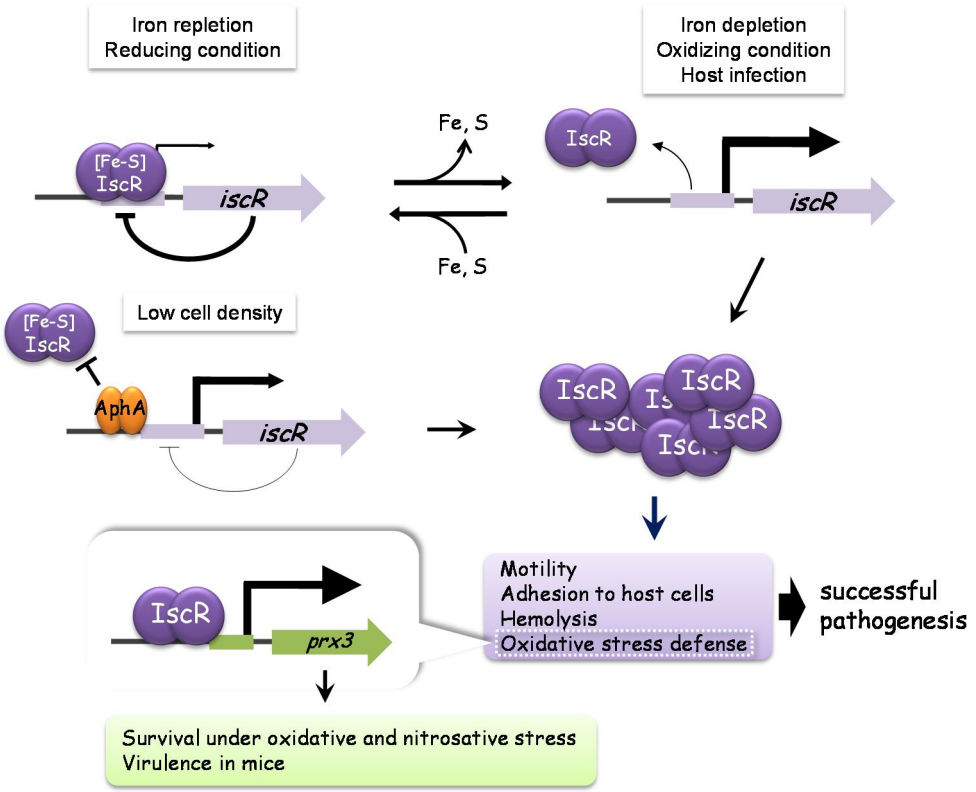

Figure V-1. A proposed model for the regulation of *V. vulnificus* pathogenesis via IscR.

References

Alice AF, Naka H, Crosa JH. 2008. Global gene expression as a function of the iron status of the bacterial cell: influence of differentially expressed genes in the virulence of the human pathogen *Vibrio vulnificus*. Infect. Immun. **76:**4019–4037.

Amaro C, Biosca EG. 1996. *Vibrio vulnificus* biotype 2, pathogenic for eels, is also an opportunistic pathogen for humans. Appl. Environ. Microbiol. **62:**1454-1457.

Aznar R, Ludwig W, Amann RI, Schleifer KH. 1994. Sequence determination of rRNA genes of pathogenic *Vibrio* species and whole cell identification of *Vibrio vulnificus* with rRNA targeted oligonucleotide. Int. J. Syst. Bacteriol. **44:**330-337.

Baek WK, Lee HS, Oh MH, Koh MJ, Kim KS, Choi SH. 2009. Identification of the *Vibrio vulnificus ahpC1* gene and its influence on survival under oxidative stress and virulence. J. Microbiol. **47:**624-632.

Baker MD, Wolanin PM, Stock JB. 2005. Signal transduction in bacterial chemotaxis. BioEssays **28:**9-22.

Bang YJ, Oh MH, Choi SH. 2012. Distinct characteristics of two 2-Cys peroxiredoxins of *Vibrio vulnificus* suggesting differential roles in detoxifying oxidative stress. J. Biol. Chem. **287:**42516-42524.

Bhowmick R, Ghosal A, Das B, Koley H, Saha DR, Ganguly S, Nandy RK,

Bhadra RK, Chatterjee NS. 2008. Intestinal adherence of *Vibrio cholerae* involves a coordinated interaction between colonization factor GbpA and mucin. Infect. Immun. **76:**4968-4977.

Bisharat N, Agmon V, Finkelstein R, Raz R, Ben-Dror G, Lerner L, Soboh S, Colodner R, Cameron DN, Wykstra DL, Swerdlow DL, Farmer JJ 3rd. 1999. Clinical, epidemiological, and microbiological features of *Vibrio vulnificus* biogroup 3 causing outbreaks of wound infection and bacteraemia in Israel. Lancet **354:**1421-1424.

Brown SA, Palmer KL, Whiteley M. 2008. Revisiting the host as a growth medium. Nat. Rev. Microbiol. **6:**657-666.

Browning DF, Busby SJ. 2004. The regulation of bacterial transcription initiation. Nat. Rev. Microbiol. **2:**57-65.

Butler SM, Camilli A. 2005. Going against the grain: chemotaxis and infection in *Vibrio cholerae*. Nat. Rev. Microbiol. **3:**611-620.

Cerdà-Cuéllar M, Jofre J, Blanch AR. 2000. A selective medium and a specific probe for detection of *Vibrio vulnificus*. Appl. Environ. Microbiol. **66:**855-859.

Chang AK, Kim HY, Park JE, Acharya P, Park IS, Yoon SM, You HJ, Hahm KS, Park JK, Lee JS. 2005. *Vibrio vulnificus* secretes a broad-specificity metalloprotease capable of interfering with blood homeostasis through prothrombin activation and fibrinolysis. J. Bacteriol. **187:**6909–6916.

Chatzidaki-Livanis M, Jones MK, Wright AC. 2006. Genetic variation in the *Vibrio vulnificus* group 1 capsular polysaccharide operon. J. Bacteriol.

188:1987–1998.

Choi HK, Park NY, Kim DI, Chung HJ, Ryu S, Choi SH. 2002. Promoter analysis and regulatory characteristics of *vvhBA* encoding cytolytic hemolysin of *Vibrio vulnificus*. J. Biol. Chem. **277:**47292-47299.

Christman MF, Morgan RW, Jacobson FS, Ames BN 1985. Positive control of a regulon for defenses against oxidative stress and some heat-shock proteins in *Salmonella typhimurium*. Cell **41:**753–762.

Chuang YC, Sheu HM, Ko WC, Chang TM, Chang MC, Huang KY. 1997. Mouse skin damage caused by a recombinant extracellular metalloprotease from *Vibrio vulnificus* and by *V. vulnificus* infection. J. Formos. Med. Assoc. **96:**677e84.

Chuang YC, Yuan CY, Liu CY, Lan CK, Huang AH. 1992. *Vibrio vulnificus* infection in Taiwan: report of 28 cases and review of clinical manifestations and treatment. Clin. Infect. Dis. **15:**271-176.

Chung KJ, Cho EJ, Kim MK, Kim YR, Kim SH, Yang HY, Chung KC, Lee SE, Rhee JH, Choy HE, Lee TH. 2010. RtxA1-induced expression of the small GTPase Rac2 plays a key role in the pathogenicity of *Vibrio vulnificus*. J. Infect. Dis. **201:**97-105.

Clatworthy AE, Pierson E, Hung DT. 2007. Targeting virulence: a new paradigm for antimicrobial therapy. Nature Chem. Biol. **3:**541-548.

Cotter PA, DiRita VJ. 2000. Bacterial virulence regulation: an evolutionary perspective. Annu. Rev. Microbiol. **54:**519-565.

De Silva RS, Kovacikova G, Lin W, Taylor RK, Skorupski K, Kull FJ. 2005.

Crystal structure of the virulence gene activator AphA from *Vibrio cholerae* reveals it is a novel member of the winged helix transcription factor superfamily. J. Biol. Chem. **280:**13779-13783.

Falkow S. 1988**.** Molecular Koch's postulates applied to microbial pathogenicity. Rev. Infect. Dis. **10 Suppl 2:**S274-276.

Fan JJ, Shao CP, Ho YC, Yu CK, Hor LI. 2001. Isolation and characterization of a *Vibrio vulnificus* mutant deficient in both extracellular metalloprotease and cytolysin. Infect. Immun. **69:**5943–5948.

Fang FC. 2004. Antimicrobial reactive oxygen and nitrogen species: concepts and controversies. Nat. Rev. Microbiol. **10:**820-832.

Fleischhacker AS, Stubna A, Hsueh KL, Guo Y, Teter SJ, Rose JC, Brunold TC, Markley JL, Münck E, Kiley PJ. 2012. Characterization of the [2Fe-2S] cluster of *Escherichia coli* transcription factor IscR. Biochemistry **51:**4453-4462.

Fontecave M. 2006. Iron-sulfur clusters: ever-expanding roles. Nat. Chem. Biol. **2:**171-174.

Giel JL, Nesbit AD, Mettert EL, Fleischhacker AS, Wanta BT, Kiley PJ. 2013. Regulation of iron-sulphur cluster homeostasis through transcriptional control of the Isc pathway by [2Fe-2S]-IscR in *Escherichia coli*. Mol. Microbiol. **87:**478-492.

Giel JL, Rodionov D, Liu M, Blattner FR, Kiley PJ. 2006. IscR-dependent gene expression links iron-sulphur cluster assembly to the control of O_2-regulated genes in *Escherichia coli*. Mol. Microbiol. **60:**1058-1075.

Goo SY, Lee HJ, Kim WH, Han KL, Park DK, Kim SM, Kim KS, Lee KH. Park SJ. 2006. Identification of OmpU of *Vibrio vulnificus* as a fibronectin binding protein and its role in bacterial pathogenesis. Infect. Immun. **74:**5586-5594.

Gray LD, Kreger AS. 1987. Mouse skin damage caused by cytolysin from *Vibrio vulnificus* and by *V. vulnificus* infection. J. Infect. Dis. **155:**236–241.

Greenberg JT, Monach P, Chou JH, Josephy PD, Demple B. 1990. Positive control of a global antioxidant defense regulon activated by superoxide-generating agents in *Escherichia coli*. Proc. Natl. Acad. Sci. U.S.A. **87:**6181–6185.

Gulig PA, Bourdage KL, Starks AM. 2005. Molecular pathogenesis of *Vibrio vulnificus*. J. Microbiol. **43:**118–131.

Guzman LM, Belin D, Carson MJ, Beckwith J. 1995. Tight regulation, modulation, and high-level expression by vectors containing the arabinose P_{BAD} promoter. J. Bacteriol. **177:**4121-4130.

Hlady WG, Klontz KC. 1996. The epidemiology of *Vibrio* infections in Florida, 1981-1993. J. Infect. Dis. **173:**1176-1183.

Hollis DG, Weaver RE, Baker CN, Thornsberry C. 1976. Halophilic *Vibrio* species isolated from blood cultures. J. Clin. Microbiol. **3:**425-431.

Hor LI, Chang YK, Chang CC, Lei HY, Ou JT. 2000. Mechanism of high susceptibility of iron-overloaded mouse to *Vibrio vulnificus* infection. Microbiol. Immunol. **44:**871–878.

Hor LI, Goo CT, Wan L. 1995. Isolation and characterization of *Vibrio vulnificus*

inhabiting the marine environment of the southwestern area of Taiwan. J. Biomed. Sci. **2:**384-389.

Horseman MA, Surani S. 2011. A comprehensive review of *Vibrio vulnificus*: an important cause of severe sepsis and skin and soft-tissue infection. Int. J. Infect. Dis. **15:**e157-166.

Howard R, Brennaman B, Lieb S. 1986. Soft tissue infections in Florida due to marine *Vibrio* bacteria. J. Fla. Med. Assoc. **73:**29–34.

Hwang J, Kim BS, Jang SY, Lim JG, You DJ, Jung HS, Oh TK, Lee JO, Choi SH, Kim MH. 2013. Structural insights into the regulation of sialic acid catabolism by the *Vibrio vulnificus* transcriptional repressor NanR. Proc. Natl. Acad. Sci. U. S. A. **110:**e2829-2837.

Imlay JA. 2006. Iron-sulphur clusters and the problem with oxygen. Mol. Microbiol. **59:**1073-1082.

Jeong HG, Choi SH. 2008. Evidence that AphB essential for the virulence of *Vibrio vulnificus* is a global regulator. J. Bacteriol. **190:**3768-3773.

Jeong HG, Oh MH, Kim BS, Lee MY, Han HJ, Choi SH. 2009. The capability of catabolic utilization of *N*-acetylneuraminic acid, a sialic acid, is essential for *Vibrio vulnificus* pathogenesis. Infect. Immun. **77:**3209-3217.

Jeong HG, Satchell KJ. 2012. Additive function of *Vibrio vulnificus* $MARTX_{Vv}$ and VvhA cytolysins promotes rapid growth and epithelial tissue necrosis during intestinal infection. PLoS Pathog. **8:**e1002581.

Jeong HS, Jeong KC, Choi HK, Park KJ, Lee KH, Rhee JH, Choi SH. 2001. Differential expression of *Vibrio vulnificus* elastase gene in a growth phase-

dependent manner by two different types of promoters. J. Biol. Chem. **276:**13875–13880.

Jeong HS, Lee MH, Lee KH, Park SJ, Choi SH. 2003. SmcR and cyclic AMP receptor protein coactivate *Vibrio vulnificus vvpE* encoding elastase through the RpoS-dependent promoter in a synergistic manner. J. Biol. Chem. **278:**45072–45081.

Jeong KC, Jeong HS, Rhee JH, Lee SE, Chung SS, Starks AM, Escudero GM, Gulig PA, Choi SH. 2000. Construction and phenotypic evaluation of a *Vibrio vulnificus vvpE* mutant for elastolytic protease. Infect. Immun. **68:**5096–5106.

Johnson DC, Dean DR, Smith AD, Johnson MK. 2005. Structure, function, and formation of biological Fe-S clusters. Annu. Rev. Biochem. **74:**247-281.

Jones MK, Oliver JD. 2009. Minireview *Vibrio vulnificus*: disease and pathogenesis. Infect. Immun. **77:**1723-1733.

Kang IH, Kim JS, Kim EJ, Lee JK. 2007a. Cadaverine protects *Vibrio vulnificus* from superoxide stress. J. Microbiol. Biotechnol. **17:**176–179.

Kang IH, Kim JS, Lee JK. 2007b. The virulence of *Vibrio vulnificus* is affected by the cellular level of superoxide dismutase activity. J. Microbiol. Biotechnol. **17:**1399–1402.

Kang MK, Jhee EC, Koo BS, Yang JY, Park BH, Kim JS, Rho HW, Kim HR, Park JW. 2002. Induction of nitric oxide synthase expression by *Vibrio vulnificus* cytolysin. Biochem. Biophys. Res. Commun. **290:**1090-1095.

Kaspar CW, Tamplin ML. 1993. Effect of temperature and salinity on the

survival of *Vibrio vulnificus* in seawater and shellfish. Appl. Environ. Microbiol. **59:**2425-2429.

Keen NT, Tamaki S, Kobayashi D, Trollinger D. 1988. Improved broad-host-range plasmids for DNA cloning in Gram-negative bacteria. Gene **70:**191-197.

Kim BS, and Kim JS. 2002. Cholesterol induces oligomerization of *Vibrio vulnificus* cytolysin specifically. Exp. Mol. Med. **34:**239–242.

Kim BS, Hwang J, Kim MH, Choi SH. 2011. Cooperative regulation of the *Vibrio vulnificus nan* gene cluster by NanR protein, cAMP receptor protein, and N-acetylmannosamine 6-phosphate. J. Biol. Chem. **286:**40889-40899.

Kim CM, Park RY, Park JH, Sun HY, Bai YH, Ryu PY, Kim SY, Rhee JH, Shin SH. 2006a. *Vibrio vulnificus* vulnibactin but not metalloprotease VvpE is essentially required for iron-uptake from human holotransferrin. Biol. Pharm. Bull. **29:**911–918.

Kim HR, Rho HW, Jeong MH, Park JW, Kim JS, Park BH, Kim UH, Park SD. 1993. Hemolytic mechanism of cytolysin produced from *Vibrio vulnificus*. Life Sci. **53:**571–577.

Kim HY, Chang AK, Park JE, Park IS, Yoon SM, Lee JS. 2007. Procaspase-3 activation by a metalloprotease secreted from *Vibrio vulnificus*. Int. J. Mol. Med. **20:**591–595.

Kim IH, Shim JI, Lee KE, Hwang W, Kim IJ, Choi SH, Kim KS. 2008a. Nonribosomal peptide synthetase is responsible for the biosynthesis of siderophore in *Vibrio vulnificus* MO6-24/O. J. Microbiol. Biotechnol. **18:**35–42.

Kim JS, Choi SH, Lee JK. 2006b. Lysine decarboxylase expression by *Vibrio vulnificus* is induced by SoxR in response to superoxide stress. J. Bacteriol. **188:**8586e92.

Kim JS, Sung MH, Kho DH, Lee JK. 2005a. Induction of manganese-containing superoxide dismutase is required for acid tolerance in *Vibrio vulnificus*. J. Bacteriol. **187:**5984–5995.

Kim SH, Lee BY, Lau GW, Cho YH. 2009. IscR modulates catalase A (KatA) activity, peroxide resistance and full virulence of *Pseudomonas aeruginosa* PA14. J. Microbiol. Biotechnol. **19:**1520-1526.

Kim SM, Lee DH, Choi SH. 2012. Evidence that the *Vibrio vulnificus* flagellar regulator FlhF is regulated by a quorum sensing master regulator SmcR. Microbiology **158:**2017-2025.

Kim SM, Park JH, Lee HS, Kim WB, Ryu JM, Han HJ, Choi SH. 2013. LuxR homologue SmcR is essential for *Vibrio vulnificus* pathogenesis and biofilm detachment, and its expression is induced by host cells. Infect. Immun. **81:**3721-3730.

Kim YR, Kim SY, Kim CM, Lee SE, Rhee JH. 2005b. Essential role of an adenylate cyclase in regulating *Vibrio vulnificus* virulence. FEMS Microbiol. Lett. **243**:497–503.

Kim YR, Lee SE, Kim CM, Kim SY, Shin EK, Shin DH, Chung SS, Choy HE, Progulske-Fox A, Hillman JD, Handfield M, Rhee JH. 2003. Characterization and pathogenic significance of *Vibrio vulnificus* antigens preferentially expressed in septicemic patients. Infect. Immun. **71:**5461-5471.

Kim YR, Lee SE, Kook H, Yeom JA, Na HS, Kim SY, Chung SS, Choy HE, Rhee JH. 2008b. *Vibrio vulnificus* RTX toxin kills host cells only after contact of the bacteria with host cells. Cell. Microbiol. **10:**848-862.

Kirn TJ, Jude BA, Taylor RK. 2005. A colonization factor links *Vibrio cholerae* environmental survival and human infection. Nature **438:**863–866.

Klontz KC, Lieb S, Schreiber M, Janowski HT, Baldy LM, Gunn RA. 1988. Syndromes of *Vibrio vulnificus* infections. Clinical and epidemiological features in Florida cases, 1981-1987. Ann. Intern. Med. **109:**318-323.

Knoops B, Loumaye E, Van Der Eecken V. 2007. Evolution of the peroxiredoxins: Taxonomy, homology and characterization, p 27-40. *In* Flohé L, Harris JR (ed), Peroxiredoxin systems, Springer, New York, NY.

Kothary MH, Kreger AS. 1987. Purification and characterization of an elastolytic protease of *Vibrio vulnificus*. J. Gen. Microbiol. **13:**1783–1791.

Kovacikova G, Lin W, Skorupski K. 2004. *Vibrio cholerae* AphA uses a novel mechanism for virulence gene activation that involves interaction with the LysR-type regulator AphB at the *tcpPH* promoter. Mol. Microbiol. **53:**129-142.

Kovacikova G, Lin W, Skorupski K. 2005. Dual regulation of genes involved in acetoin biosynthesis and motility/biofilm formation by the virulence activator AphA and the acetate-responsive LysR-type regulator AlsR in *Vibrio cholerae*. Mol. Micriobiol. **57:**420-433.

Kovacikova G, Skorupski K. 1999. A *Vibrio cholerae* LysR homolog, AphB, cooperates with AphA at the *tcpPH* promoter to activate expression of the

ToxR virulence cascade. J. Bacteriol. **181:**4250-4256.

Kovacikova G, Skorupski K. 2001. Overlapping binding sites for the virulence gene regulators AphA, AphB and cAMP-CRP at the *Vibrio cholerae tcpPH* promoter. Mol. Microbiol. **41:**393-407.

Kwon KB, Yang JY, Ryu DG, Rho HW, Kim JS, Park JW, Kim HR, Park BH. 2001. *Vibrio vulnificus* cytolysin induces superoxide anion-initiated apoptotic signaling pathway in human ECV304 cells. J. Biol. Chem. **276:**47518–47523.

Larsen RA, Wilson MM, Guss AM, Metcalf WW. 2002. Genetic analysis of pigment biosynthesis in *Xanthobacter autotrophicus* Py2 using a new, highly efficient transposon mutagenesis system that is functional in a wide variety of bacteria. Arch. Microbiol. **178:**193-201.

Lee BC, Kim SH, Choi SH, Kim TS. 2005. Induction of interleukin-8 production via nuclear factor-kappaB activation in human intestinal epithelial cells with *Vibrio vulnificus*. Immunology **115:**506–515.

Lee BC, Lee JH, Kim MW, Kim BS, Oh MH, Kim KS, Kim TS, Choi SH. 2008b. *Vibrio vulnificus rtxE* is important for virulence, and its expression is induced by exposure to host cells. Infect. Immun. **76:**1509-1517.

Lee CT, Amaro C, Wu KM, Valiente E, Chang YF, Tsai SF, Chang CH, Hor LI. 2008a. A common virulence plasmid in biotype 2 *Vibrio vulnificus* and its dissemination aided by a conjugal plasmid. J. Bacteriol. **190:**1638-1648.

Lee HJ, Kim JA, Lee MA, Park SJ, Lee KH. 2013a. Regulation of haemolysin (VvhA) production by ferric uptake regulator (Fur) in *Vibrio vulnificus*: repression of *vvhA* transcription by Fur and proteolysis of VvhA by Fur-

repressive exoproteases. Mol. Microbiol. **88:**813-826.

Lee JH, Kim MW, Kim BS, Kim SM, Lee BC, Kim TS, Choi SH. 2007. Identification and characterization of the *Vibrio vulnificus rtxA* essential for cytotoxicity in vitro and virulence in mice. J. Microbiol. **45:**146–152.

Lee JH, Rho JB, Park KJ, Kim CB, Han YS, Choi SH, Lee KH, Park SJ. 2004. Role of flagellum and motility in pathogenesis of *Vibrio vulnificus*. Infect. Immun. **72:**4905-4910.

Lee KJ, Kim JA, Hwang W, Park SJ, Lee KH. 2013b. Role of capsular polysaccharide (CPS) in biofilm formation and regulation of CPS production by quorum-sensing in *Vibrio vulnificus*. Mol. Microbiol. **90:**841-857.

Lenz DH, Mok KC, Lilley BN, Kulkarni RV, Wingreen NS, Bassler BL. 2004 The small RNA chaperone Hfq and multiple small RNAs control quorum sensing in *Vibrio harveyi* and *Vibrio cholerae*. Cell **118:**69-82.

Linkous DA, Oliver JD. 1999. Pathogenesis of *Vibrio vulnificus*. FEMS Microbiol. Lett. **174:**207-214.

Litwin CM, Byrne BL. 1998. Cloning and characterization of an outer membrane protein of *Vibrio vulnificus* required for heme utilization: regulation of expression and determination of the gene sequence. Infect. Immun. **66:**3134–3141.

Liu M, Alice AF, Naka H, Crosa JH. 2007. The HlyU protein is a positive regulator of *rtxA1*, a gene responsible for cytotoxicity and virulence in the human pathogen *Vibrio vulnificus*. Infect. Immun. **75:**3282–3289.

Liu M, Naka H, Crosa JH. 2009. HlyU acts as H-NS antirepressor in the regulation of the RTX toxin gene essential for the virulence of the human pathogen *Vibrio vulnificus* CMCP6. Mol. Microbiol. **72:**491-505.

Matson JS, Withey JH, DiRita VJ. 2007. Regulatory networks controlling *Vibrio cholerae* virulence gene expression. Infect. Immun. **75:**5542-5549.

Miller RA, Britigan BE. 1997. Role of oxidants in microbial pathophysiology. Clin. Microbiol. Rev. **10:**1-18.

Milton DL, O'Toole R, Horstedt P, Wolf-Watz H. 1996. Flagellin A is essential for the virulence of *Vibrio anguillarum*. J. Bacteriol. **178:**1310-1319.

Miyoshi N, Miyoshi S, Sugiyama K, Suzuki Y, Furuta H, Shinoda S. 1987. Activation of the plasma kallikrein-kinin system by *Vibrio vulnificus* protease. Infect. Immun. **55:**1936–1939.

Miyoshi S, Shinoda S. 1988. Role of the protease in the permeability enhancement by *Vibrio vulnificus*. Microbiol. Immunol. **32:**1025–1032.

Miyoshi S. 2006. *Vibrio vulnificus* infection and metalloprotease. J. Dermatol. **33:**589-595.

Mueller RS, McDougald D, Cusumano D, Sodhi N, Kjelleberg S, Azam F, Bartlett DH. 2007. *Vibrio cholerae* Strains Possess Multiple Strategies for Abiotic and Biotic Surface colonization. J. Bacteriol. **189:**5348-5360.

Mukhopadhyay P, Zheng M, Bedzyk LA, LaRossa RA, Storz G. 2004. Prominent roles of the NorR and Fur regulators in the *Escherichia coli* transcriptional response to reactive nitrogen species. Proc. Natl. Acad. Sci. U.S.A. **101:**745–750.

Nesbit AD, Giel JL, Rose JC, Kiley PJ. 2009. Sequence-specific binding to a subset of IscR-regulated promoters does not require IscR Fe-S cluster ligation. J. Mol. Biol. **387:**28-41.

O'Toole R, Milton DL, Wolf-Watz H. 1996. Chemotactic motility is required for invasion of the host by the fish pathogen *Vibrio anguillarum*. Mol. Microbiol. **19:**625-637.

Oh MH, Lee SM, Lee DH, Choi SH. 2009. Regulation of the *Vibrio vulnificus hupA* gene by temperature alteration and cyclic AMP receptor protein and evaluation of its role in virulence. Infect. Immun. **77:**1208-1215.

Oliver JD. 2005. Wound infections caused by *Vibrio vulnificus* and other marine bacteria. Epidemiol. Infect. **133:**383–391.

Oliver JD. 2006. *Vibrio vulnificus*, p. 349-366 *In* F. L. Thompson, B. Austin, and J. Swing (eds.), Biology of *Vibrios*. ASM Press, Washington, D.C.

Osaka K, Komatsuzaki M, Takahashi H, Sakano S, Okabe N. 2004. *Vibrio vulnificus* septicemia in Japan: an estimated number of infections and physicians' knowledge of the syndrome. Epidemiol. Infect. **132:**993-996.

Ottemann KM, Miller JF. 1997. Role for motility in bacterial-host interactions. Mol. Microbiol. **24:**1109-1117.

Outten FW, Djaman O, Storz G. 2004. A *suf* operon requirement for Fe-S cluster assembly during iron starvation in *Escherichia coli*. Mol. Microbiol. **52:**861-872.

Paranjpye RN, Strom MS. 2005. A *Vibrio vulnificus* type IV pilin contributes to biofilm formation, adherence to epithelial cells, and virulence. Infect. Immun. **73:**1411-1422.

Park J, Kim SM, Jeong HG, Choi SH. 2012. Regulatory characteristics of the *Vibrio vulnificus rtxHCA* operon encoding a MARTX toxin. J. Microbiol. **50:**878-881.

Park NY, Lee JH, Kim MW, Jeong HG, Lee BC, Kim TS, Choi SH. 2006. Identification of the *Vibrio vulnificus wbpP* gene and evaluation of its role in virulence. Infect. Immun. **74:**721–728.

Poole LB, Hall A, Nelson KJ. 2011. Overview of peroxiredoxins in oxidant defense and redox regulation. Curr. Protoc. Toxicol. **49:**7.9.1-7.9.15.

Py B, Barras F. 2010. Building Fe-S proteins: bacterial strategies. Nat. Rev. Microbiol. **8:**436-446.

Py B, Moreau PL, Barras F. 2011. Fe-S clusters, fragile sentinels of the cell. Curr. Opin. Microbiol. **14:**218-223.

Rajagopalan S, Teter SJ, Zwart PH, Brennan RG, Phillips KJ, Kiley PJ. 2013. Studies of IscR reveal a unique mechanism for metal-dependent regulation of DNA binding specificity. Nat. Struct. Mol. Biol. **20:**740-747.

Reed LJ, Muench H. 1938. A simple method of estimating fifty percent endpoints. Am. J. Hyg. **27:**493-497.

Rhee JE, Jeong HG, Lee JH, Choi SH. 2006. AphB influences acid tolerance of *Vibrio vulnificus* by activating expression of the positive regulator CadC. J. Bacteriol. **188:**6490–6497.

Rhee JE, Kim KS, Choi SH. 2005. CadC activates pH-dependent expression of the *Vibrio vulnificus cadBA* operon at a distance through direct binding to an upstream region. J. Bacteriol. **187:**7870–7875.

Rhee JE, Rhee JH, Ryu PY, Choi SH. 2002. Identification of the *cadBA* operon from *Vibrio vulnificus* and its influence on survival to acid stress. FEMS Microbiol. Lett. **208:**245–251.

Rincon-Enriquez G, Crété P, Barras F, Py B. 2008. Biogenesis of Fe/S proteins and pathogenicity: IscR plays a key role in allowing *Erwinia chrysanthemi* to adapt to hostile conditions. Mol. Microbiol. **67:**1257-1273.

Runyen-Janecky L, Daugherty A, Lloyd B, Wellington C, Eskandarian H, Sagransky M. 2008. Role and regulation of iron-sulfur cluster biosynthesis genes in *Shigella flexneri* virulence. Infect. Immun. **76:**1083-1092.

Rutherford ST, van Kessel JC, Shao Y, Bassler BL. 2011. AphA and LuxR/HapR reciprocally control quorum sensing in vibrios. Genes. Dev. **25:**397-408.

Schwartz CJ, Giel JL, Patschkowski T, Luther C, Ruzicka FJ, Beinert H, Kiley PJ. 2001. IscR, an Fe-S cluster-containing transcription factor, represses expression of *Escherichia coli* genes encoding Fe-S cluster assembly proteins. Proc. Natl. Acad. Sci. U. S. A. **98:**14895-14900.

Senoh M, Okita Y, Shinoda S, Miyoshi S. 2008. The crucial amino acid residue related to inactivation of *Vibrio vulnificus* hemolysin. Microb. Pathog. **44:**78-83.

Sepp A, Binns RM, Lechler RI. 1996. Improved protocol for colorimetric detection of complement-mediated cytotoxicity based on the measurement of cytoplasmic lactate dehydrogenase activity. J. Immunol. Methods **196:**175-180.

Shao CP, Hor LI. 2000. Metalloprotease is not essential for *Vibrio vulnificus* virulence in mice. Infect. Immun. **68:**3569–3573.

Shinoda S, Kobayashi M, Yamada H, Yoshida S, Ogawa M, Mizuguchi Y. 1987. Inhibitory effect of capsular antigen of *Vibrio vulnificus* on bactericidal activity of human serum. Microbiol. Immunol. **31:**393-401.

Simon R, Priefer U, Pühler A. 1983. A broad host range mobilization system for *in vivo* genetic engineering transposon mutagenesis in gram negative bacteria. Nat. Biotechnol. **1:**784-791.

Simpson LM, Oliver JD. 1983. Siderophore production by *Vibrio vulnificus*. Infect. Immun. **41:**644–649.

Simpson LM, Oliver JD. 1987. Ability of *Vibrio vulnificus* to obtain iron from transferrin and other iron-binding compounds. Curr. Microbiol. **15:**155–158.

Smith AB, Siebeling RJ. 2003. Identification of genetic loci required for capsular expression in *Vibrio vulnificus*. Infect. Immun. **71:**1091–1097.

Starks AM, Bourdage KL, Thiaville PC, Gulig PA. 2006. Use of a marker plasmid to examine differential rates of growth and death between clinical and environmental strains of *Vibrio vulnificus* in experimentally infected mice. Mol. Microbiol. **61:**310–323.

Stelma GN, Reyes AL Jr, Peter JT, Johnson CH, Spaulding PL. 1992. Virulence characteristics of clinical and environmental isolates of *Vibrio vulnificus*. Appl. Environ. Microbiol. **58:**2776–2782.

Strom MS, Paranjpye RN. 2000. Epidemiology and pathogenesis of *Vibrio vulnificus*. Microbes Infect. **2:**177–188.

Sun F, Zhang Y, Wang L, Yan X, Tan Y, Guo Z, Qiu J, Yang R, Xia P, Zhou D. 2012. Molecular characterization of direct target genes and cis-acting consensus recognized by quorum-sensing regulator AphA in *Vibrio parahaemolyticus*. PLoS One **7:**e44210.

Szabó C, Ischiropoulos H, Radi R. 2007, Peroxynitrite: biochemistry, pathophysiology and development of therapeutics. Nat. Rev. Drug. Discov. **6:**662-680.

Tison DL, Nishibuchi M, Greenwood JD, Seidler RJ. 1982. *Vibrio vulnificus* biogroup 2: new biogroup pathogenic for eels. Appl. Environ. Microbiol**.** **44:**640–646.

van Kessel JC, Rutherford ST, Shao Y, Utria AF, Bassler BL. 2013. Individual and combined roles of the master regulators AphA and LuxR in control of the *Vibrio harveyi* quorum-sensing regulon. J. Bacteriol. **195:**436-443.

Vimr ER, Kalivoda KA, Deszo EL, Steenbergen SM. 2004. Diversity of microbial sialic acid metabolism. Microbiol. Mol. Biol. Rev. **68:**132-153.

Vlamis-Gardikas A, Potamitou A, Zarivach R, Hochman A, Holmgren A. 2002. Characterization of *Escherichia coli* null mutants for glutaredoxin 2. J. Biol. Chem. **277:**10861-10868.

Wang L, Ling Y, Jiang H, Qiu Y, Qiu J, Chen H, Yang R, Zhou D. 2013. AphA is required for biofilm formation, motility, and virulence in pandemic *Vibrio parahaemolyticus*. Int. J. Food Microbiol. **160:**245-251.

Webster ACD, Litwin CM. 2000. Cloning and characterization of *vuuA*, a gene encoding the *Vibrio vulnificus* ferric vulnibactin receptor. Infect. Immun. **68:**526–534.

Weinberg ED. 1978. Iron and infection. Microbiol. Rev. **42:**45–66.

Wen Y, Kim IH, Son JS, Lee BH, Kim KS. 2012. Iron and quorum sensing coordinately regulate the expression of vulnibactin biosynthesis in *Vibrio vulnificus*. J. Biol. Chem. **287:**26727-26739.

Wilks A, Burkhard KA. 2007. Heme and virulence: how bacterial pathogens regulate, transport and utilize heme. Nat. Prod. Rep. **24:**511-522.

Wright AC, Hill RT, Johnson JA, Roghman MC, Colwell RR, Morris JG Jr. 1996. Distribution of *Vibrio vulnificus* in the Chesapeake Bay. Appl. Environ. Microbiol. **62:**717-724.

Wright AC, Morris JG Jr. 1991. The extracellular cytolysin of *Vibrio vulnificus*: inactivation and relationship to virulence in mice. Infect. Immun. **59:**192–197.

Wright AC, Powell JL, Kaper JB, Morris JG Jr. 2001. Identification of a group 1-like capsular polysaccharide operon in *Vibrio vulnificus*. Infect. Immun. **69:**6893–6901.

Wright AC, Powell JL, Tanner MK, Ensor LA, Karpas AB, Morris JG Jr, Sztein MB. 1999. Differential expression of *Vibrio vulnificus* capsular polysaccharide. Infect. Immun. **67:**2250-2257.

Wright AC, Simpson LM, Oliver JD. 1981. Role of iron in the pathogenesis of *Vibrio vulnificus* infections. Infect. Immun. **34:**503–507.

Wu Y, Outten FW. 2009. IscR controls iron-dependent biofilm formation in *Escherichia coli* by regulating type I fimbria expression. J. Bacteriol. **191:**1248-1257.

Yamamoto K, Wright AC, Kaper JB, Morris JG Jr. 1990. The cytolysin gene of *Vibrio vulnificus*: sequence and relationship to the *Vibrio cholerae* E1 Tor hemolysin gene. Infect. Immun. **58:**2706-2709.

Yang M, Frey EM, Liu Z, Bishar R, Zhu J. 2010. The virulence transcriptional activator AphA enhances biofilm formation by *Vibrio cholerae* by activating expression of the biofilm regulator VpsT. Infect. Immun. **78:**697-703.

Yeo WS, Lee JH, Lee KC, Roe JH. 2006. IscR acts as an activator in response to oxidative stress for the *suf* operon encoding Fe-S assembly proteins. Mol. Microbiol. **61:**206-218.

Yoshida S, Ogawa M, Mizuguchi Y. 1985. Relation of capsular materials and colony opacity to virulence of *Vibrio vulnificus*. Infect. Immun. **47:**446-451.

Zaidenstein R, Sadik C, Lerner L, Valinsky L, Kopelowitz J, Yishai R, Agmon V, Parsons M, Bopp C, Weinberger M. 2008. Clinical characteristics and molecular subtyping of *Vibrio vulnificus* illnesses, Israel. Emerg. Infect. Dis. **14:**1875-1882.

Zheng M, Wang X, Templeton LJ, Smulski DR, LaRossa RA, Storz G. 2001. DNA microarray-mediated transcriptional profiling of the *Escherichia coli* response to hydrogen peroxide. J. Bacteriol. **183:**4562-4570.

국문초록

병원성 미생물은 발병 과정 동안 다양한 독성 인자들이 총체적으로 발현되고 작용할 수 있도록 하는 조절 기전을 발달시켜왔다. 패혈증 비브리오균은 이러한 독성 인자 조절 기전을 통해 인간의 생명을 위협하는 패혈증을 일으키므로 다른 식품유래 병원균 연구에 모델 병원균으로서 사용되어 왔다. 본 연구는 철-황 클러스터 ([Fe-S])를 가지는 전사 조절자 IscR을 동정하고 IscR의 기능과 조절 특성을 밝혀내었다.

숙주의 장 상피세포를 이용한 비 생체 조건과 쥐를 이용한 생체 조건 모두에서 *iscR* 돌연변이 균주의 병원성은 야생형과 비교하였을 때 현저히 감소함을 알 수 있었다. Microarray를 이용한 전사체 분석을 통해 IscR 단백질이 조절하는 타겟 유전자들을 동정하였고, 그 결과 IscR은 52개 유전자들의 발현을 증가시키고 동시에 15개 유전자들의 발현을 감소시킴을 알 수 있었다. IscR의 타겟 유전자들 중에서 패혈증 비브리오균의 발병에 중요한 역할을 할 것이라고 판단되는 12개의 유전자를 선별하였고, real-time PCR (qRT-PCR) 기법을 통해 이들 12개의 유전자가 IscR에 의해서 조절됨을 재확인하였다. 12개의 유전자는 패혈증 비브리오균의 운동성, 부착성, 용혈성, 그리고 산화적 스트레스 상황에서의 생존에 중요하다고 보고되었거나 판단되는 것들이었다. 이와 일치하게, *iscR* 유전자를 불활성화 시켰을 때 패혈증 비브리오균의 운동성, 숙주 장 상피 세포에 대한

부착성, 적혈구에 대한 용혈성, 활성 산소 종에 대한 저항성이 현저히 감소하였다. 나아가 숙주의 장 상피 세포에 패혈증 비브리오균이 노출되었을 때 *iscR* 유전자의 발현이 증가하며 이는 감염 진행 동안 상피 세포에서 발생하는 활성 산소 종에 의한 것임을 밝혀내었다.

더불어 본 연구는 *iscR* 유전자의 발현을 조절하는 기전을 연구하였다. IscR의 발현을 스스로 억제하는 피드백 조절기전 (negative autoregulation)은 여러 미생물 종에서 이미 알려져 있었으나, 본 연구는 패혈증 비브리오균의 지수증식기에서 *iscR*의 발현이 또 다른 전사 조절자 AphA 단백질에 의해 증가함을 보여주었다. 이는 패혈증 비브리오균의 세포 농도가 낮을 때 *iscR*이 높은 수준으로 발현됨을 의미한다. 또한 Primer extension 실험을 통하여 *iscR*의 프로모터 (promoter) 활성은 AphA에 의해 증가, IscR에 의해 각각 감소함을 확인하였다. 전기영동이동성 변화 실험 (electrophoretic mobility shift assay; EMSA)과 DNase I protection 실험 결과를 통해 AphA와 IscR 단백질 모두 *iscR* promoter 디엔에이 (DNA)에 결합하며, AphA 결합 부분이 IscR 결합 부분과 겹침을 알 수 있었다. 따라서 AphA는 *iscR* promoter 부위에 결합함으로써 IscR의 negative autoregulation을 저해하고 결과적으로 *iscR*의 발현을 증가시킬 것이라는 가설을 세울 수 있었다. 이를 확인하고자, *aphA iscR* 유전자가 모두 불활성화 된 돌연변이 균주를 제작하였고, qRT-PCR 분석을 통해서 AphA는 세포 내에

IscR이 존재할 때에만 *iscR* 발현에 영향을 미침을 확인하였다. 또한 Promoter deletion 실험을 통해 AphA와 AphA 결합 부위가 *iscR* promoter의 활성을 증가시키는 데에 중요함을 재확인하였다. 나아가, 숙주의 장 상피 세포를 이용한 비 생체 조건과 쥐를 이용한 생체 조건 모두에서 *aphA* 돌연변이 균주의 병원성이 야생형과 비교하였을 때 현저히 감소함을 확인하였다. 따라서 AphA는 IscR의 생산을 촉진시킴으로써 패혈증 비브리오균의 발병에 중요한 역할을 한다고 결론 지을 수 있었다.

IscR의 타겟 유전자를 찾기 위한 전사체 분석 결과로부터 IscR이 항산화효소인 peroxiredoxin을 encoding하는 유전자의 발현을 증가시킴을 알 수 있었다. 본 연구는 이 유전자를 *prx3*라 명명하고 그 기능을 밝혀내고자 *prx3* 돌연변이 균주를 제작하였다. *prx3* 돌연변이 균주는 야생형 균주와 비교하였을 때 과산화수소 (H_2O_2) 및 퍼옥시니트리트 (peroxynitrite)에 의해 발생한 산화적 스트레스 및 질산화적 스트레스에 의해 그 생장이 현저히 감소하였다. 쥐를 이용한 병원성 실험 결과 *prx3*는 패혈증 비브리오균의 발병에도 관여함을 알 수 있었다. *prx3*의 발현은 철 결핍 조건에서 증가하였고 이는 *prx3*의 조절자인 IscR에 의존적이었다. 대장균을 이용한 프로모토 활성 실험 결과 IscR이 *prx3*의 발현을 증가시키는 데에 있어 IscR의 [Fe-S]는 필요하지 않음을 알 수 있었다. 패혈증 비브리오균 내에서 IscR이 항상 apo- 형태로 만들어지도록 한 돌연변이 균주

(*iscR3CA* 돌연변이 균주)를 제작하여 *prx3*의 발현량을 qRT-PCR 및 primer extension 실험으로 확인한 결과, *iscR3CA* 돌연변이 균주에서의 *prx3* 발현량이 야생형 균주에 비해서 현저히 높았고 이는 두 균주 내의 IscR 단백질 양의 차이에서 기인함을 Western blot 실험을 통해 알 수 있었다. 나아가 apo-IscR과 *prx3* promoter DNA의 직접적인 결합을 EMSA 와 DNase I protection 실험으로 확인하였고, 이를 통해 IscR이 *prx3*의 발현을 직접적으로 활성화시킴을 재확인할 수 있었다.

종합해 보자면, IscR은 패혈증 비브리오균의 독성 인자들의 발현을 증가시킴으로써 병원성에 기여하였다. 이러한 IscR 자체의 발현은 숙주 세포 감염 과정에서 발생한 활성 산소 종과 전사 조절자 AphA에 의해 매개되는 세포 밀도 인식에 의해 조절되었다. 또한 IscR은 패혈증 비브리오균의 산화적 또는 질산화적 스트레스 상황에서의 생존과 병원성에 있어 중요한 역할을 하는 Prx3의 발현을 증가시켰다. 결론적으로, 본 연구를 통하여 전사 조절자 IscR을 중심으로 한 패혈증 비브리오균의 발병 기전을 밝혀낼 수 있었다.

주요어 : 패혈증 비브리오균, 철-황 클러스터 (Fe-S cluster), IscR, AphA, Peroxiredoxin

학 번 : 2008 – 21377